—journal of
physics

April 1998
pp. 271–280

Correlation between zeroes and poles of *S* matrix for complex potentials

I JAMIR, E F P LYNGDOH and C S SHASTRY
Department of Physics, North Eastern Hill University, Shillong 793 022, India

MS received 6 October 1997; revised 13 March 1998

Abstract. Using several illustrative examples, the nature of resonance poles and the corresponding zeroes of the s-wave *S* matrix is examined for several potentials having an absorptive pocket followed by a barrier. It is shown that even though the presence of absorption practically suppresses the manifestation of resonance in the elastic scattering cross section, the effect of the resonances generated by the absorptive pocket is more clearly manifested in the absorption cross section provided the barrier width is not too large. We further find that the signature of barrier top resonances are also more clearly manifested in the absorption cross section rather than in the elastic scattering cross section. These results have been interpreted in terms of complex resonance poles and corresponding zeroes of the *S* matrix. This implies that in complex potential scattering like heavy ion collisions, the reaction channel cross section peak is a more reliable signature of resonance phenomenon than the variation of the elastic channel cross section with energy.

Keywords. S-matrix; resonance.

PACS Nos 24.90; 03.65

1. Introduction

The analytic properties of the *S* matrix for real well-behaved potentials, their applications in scattering theory and the interpretation of physical states of quantal systems, are well-established subjects [1–3]. However, in nuclear scattering, the effective potential between the interacting systems is complex and detailed investigations and applications of the analytic properties of the *S* matrix for complex nuclear potentials have been studied only to a limited extent [4–7]. Recently, there has been some renewed interest in the nature of the singularities of the *S* matrix for complex potentials and its applications to nuclear physics [8–11]. It may be noted that in complex potential scattering, the primary observables of interest are the scattering cross section σ_s and the absorption cross section σ_{ab}. It is desirable to study to what extent both of these quantities can be correlated with the analytic features and poles of the *S* matrix.

We use the convention $2m = \hbar = 1$ and energy $E = k^2$. In numerical calculations, we express energy in fm^{-2} unit and length in fm. The Jost functions $f(\pm k)$ are defined as the Wronskian $W[\phi(k,r),\ f(\pm k,r)] = f(\pm k)$ where $\phi(k,r)$ is the regular solution of the modified radial Schrödinger equation with potential $U(r)$,

$$\frac{\mathrm{d}^2\phi(r)}{\mathrm{d}r^2} + [k^2 - U(r)]\phi(r) = 0 \tag{1}$$

having the behaviour $\phi(r) \simeq r$ near the origin and the Jost solutions $f(\pm k, r)$ of eq. (1) behave as $\mathrm{Lt}_{r\to\infty} \exp(\pm ikr) f(\pm k, r) = 1$. Some authors, as a matter of convention use the symbol $f(-k)$ for $f(k)$ and vice versa (for example, see refs [1] and [8]).

For real potentials, the Jost functions satisfy the symmetry relations $f^*(k) = f(-k^*)$ which means that for real k, $f^*(k) = f(-k)$. We denote any typical pole position in the k-plane by k_P and the corresponding zero by k_Z. The analytic properties of $f(k)$ ensures that if $k_P = \mathrm{Re}(k_P) - i\ \mathrm{Im}(k_P)$ is a zero of $f(-k)$, then the corresponding zero of $f(k)$ is $k_Z = k_P^*$. This makes the distribution of the poles and corresponding zeroes of the S matrix symmetric with respect to the real k axis. For potentials with a pocket, resonance states occur inside the pocket which can decay by tunneling through the barrier between the outer region and the pocket. For large barrier parameters, the imaginary part of the resonance poles become exceedingly small and this can lead to very sharp and narrow resonances implying that extremely high resolution is needed to resolve them. However, when an absorptive complex potential

$$U(r) = U_0 g(r) \tag{2}$$

with U_0 complex having $\mathrm{Im}(U_0) < 0$ and form factor $g(r)$ is used, the symmetry relation of the Jost function changes [4] to $f^*(k, U_0) = f(-k^*, U_0^*)$. As a result, the zeroes and poles of the S matrix are no longer symmetrically distributed with respect to the real k axis. Hence, we cannot conclude that there is a zero of the S matrix at $k = k_P^*$ corresponding to a pole at $k = k_P$. Further, resonance states inside the pocket can have larger widths of the order of $\mathrm{Im}\,(U_0)$ or larger and hence can give significantly broader resonances. It is therefore important to see to what extent such resonances get manifested in σ_{s} and σ_{ab} as a function of energy. In the case of complex potential scattering, the zeroes of the S matrix have additional significance due to the fact that σ_{ab} is governed by the factor $(1 - |S(k)|^2)$. This means that one can expect σ_{ab} to have a maximum when $|S(k)|$ is a minimum. This minimum can be expected to occur in the vicinity of the complex zero of the S matrix. Thus peaks in σ_{ab} are related in this sense to the zeroes of the S matrix.

This raises the question as to whether the resonance poles which should get manifested in σ_{s} (which gets suppressed due to the large $\mathrm{Im}\,(k_P)$) can be related to the peaks in σ_{ab} which occur due to the zeroes of the S matrix. Such a clear correlation can come only when $\mathrm{Re}\,(k_P)$ and the corresponding $\mathrm{Re}\,(k_Z)$ are same or very close to each other. In this paper, we examine this problem using several examples and demonstrate that even though the peaks in σ_{s} get suppressed due to the presence of the complex potential, the presence of these states are manifested in σ_{ab} at about the same energies when the imaginary part because the real part of the resonance poles and the corresponding zeroes are found to be very close to each other in the energy plane. This means that it is appropriate to look forward to the nature of the resonance states by studying the peaks of the absorption cross section as a function of energy. In § 2, we describe the details of our calculation and § 3 gives the discussion and conclusion.

2. Resonance poles and zeroes of S matrix for complex potentials

In this section we calculate the zeroes and poles of the s-wave S matrix for three different absorptive potentials having a barrier in the outer region. Such potentials can generate resonance states of comparatively large widths inside the potential pocket. We then examine the variation of σ_s and σ_{ab} as a function of E and interpret them in terms of the poles and zeroes of the S matrix.

2.1 *Rectangular barrier with absorptive pocket*

We first study the poles and zeroes of the S matrix of the potential

$$\begin{aligned} U(r) &= -iW, \quad r < a \\ &= U_B, \quad a \le r \le b \\ &= 0, \quad r > b \end{aligned} \tag{3}$$

with $U_B = 8\,\text{fm}^{-2}$, $W = 0.2\,\text{fm}^{-2}$, $a = 5\,\text{fm}$, $b = 5.5\,\text{fm}$. This gives an absorptive pocket in the region $r < a$, followed by a barrier of height U_B and width $(b - a)$. The s-wave S matrix is obtained analytically by solving the radial Schrödinger equation which is straightforward and we omit the algebraic details. The poles and zeroes of the S-matrix are calculated using Newton–Raphson iterative procedure. In figure 1a, we show the variation of σ_s and σ_{ab} for s-wave as a function of energy. Curve B indicates σ_s obtained with $W = 0$, i.e. curves C and B indicate the scattering cross section in the presence and absence of absorption inside the potential pocket. The minima of σ_s are very small but non-zero. The minima in σ_s are due to the variation of the hard core type phase shift present in the S matrix and are not intimately correlated with resonance. Figure 1b shows the resonance poles and corresponding zeroes in the E-plane. Table 1 lists the location of the same poles and zeroes in the k-plane. The points in the upper (lower) half k^2-plane in figure 1b should be understood to belong to the first (second) Riemann sheet. Same observation holds for figure 2b and figure 3b described later.

It is clear that the introduction of the imaginary part in the potential practically eliminates the sharp resonances of curve B from curve C. It should be understood that the broad peaks in σ_s are not the state resonances but arise as shape resonances. We also note that the location of the peaks in curve A are practically at the position of the peaks in curve B. The corresponding peaks in curve C are unable to manifest itself due to the large width arising from the complex potential.

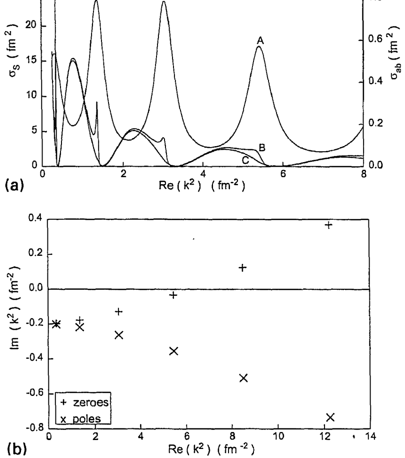

Figure 1. (**a**) Variation of σ_s and σ_{ab} with energy for the rectangular barrier of eq. (3) with $U_B = 8\,\mathrm{fm}^{-2}$, $W = 0.2\,\mathrm{fm}^{-2}$, $a = 5\,\mathrm{fm}$ and $b = 5.5\,\mathrm{fm}$. Curve A is the plot of σ_{ab} and curves C and B correspond to σ_s with and without absorption respectively. (**b**) Position of poles and zeroes corresponding to curves A and C in the k^2 plane. When poles and zeroes lie very close to each other, the marker resembles an asterisk.

Table 1. Poles and zeroes of the S matrix in k plane for the rectangular barrier of eq. (3).

$U_B = 8$ fm^{-2}, $a = 5$ fm, $b = 5.5$ fm

Poles		Zeroes	
$W = 0$	$W = 0.2$ fm^{-2}	$W = 0$	$W = 0.2$ fm^{-2}
$0.582\text{–}2.100 \times 10^{-3}i$	$0.605\text{–}0.167i$	$0.582 + 2.100 \times 10^{-3}i$	$0.605\text{–}0.163i$
$1.642\text{–}8.461 \times 10^{-3}i$	$1.671\text{–}9.332 \times 10^{-2}i$	$1.642 + 8.461 \times 10^{-3}i$	$1.675\text{–}7.641 \times 10^{-2}i$
$1.747\text{–}1.922 \times 10^{-2}i$	$1.747\text{–}7.535 \times 10^{-2}i$	$1.747 + 1.922 \times 10^{-2}i$	$1.748\text{–}3.691 \times 10^{-2}i$
$2.330\text{–}3.452 \times 10^{-2}i$	$2.329\text{–}7.614 \times 10^{-2}i$	$2.330 + 3.451 \times 10^{-2}i$	$2.331\text{–}7.119 \times 10^{-3}i$
$2.915\text{–}5.444 \times 10^{-2}i$	$2.914\text{–}8.735 \times 10^{-2}i$	$2.915 + 5.444 \times 10^{-2}i$	$2.916 + 2.151 \times 10^{-2}i$
$3.500\text{–}7.908 \times 10^{-2}i$	$3.499\text{–}0.106i$	$3.500 + 7.908 \times 10^{-2}i$	$3.501 + 5.197 \times 10^{-2}i$

bottom of the pocket, the S matrix pole and zero are located very close to each other and they gradually diverge as far as the imaginary part is concerned, as the real part of the poles and zeroes in the energy plane increases. Thus, one can state that peaks in σ_{ab}

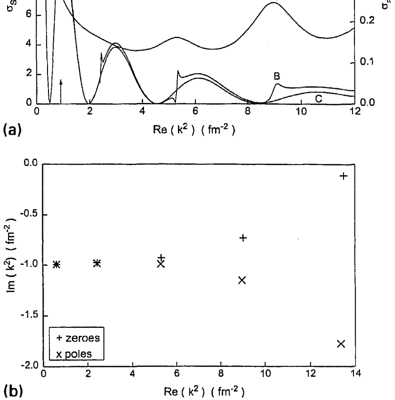

Figure 2. (**a**) Variation of σ_s and σ_{ab} with energy for the Gaussian barrier of eq. (4) with $U_B = 10\,\mathrm{fm}^{-2}$, $W = 1\,\mathrm{fm}^{-2}$, $a = 0.5\,\mathrm{fm}$, $a_I = 0.3\,\mathrm{fm}$, $R_G = 4.25\,\mathrm{fm}$ and $R = 4.25\,\mathrm{fm}$. Curve A is the plot of σ_{ab} and curves C and B correspond to σ_s with and without absorption respectively. The arrow mark indicate the position of the first extremely narrow peak in curve B which have not been reproduced due to the finite step size of the energy intervals. (**b**) Same as figure 1b for the potential of eq. (4).

indicate the presence of resonance states generated by the complex potential. The conclusion is, non-elastic or reaction channels provide a much clearer signature of resonance than the corresponding elastic channel. Figure 1a also indicates that the width of the σ_s resonance peaks in curve B gradually increases as the real part of the energy becomes large as it should since $\Gamma \propto \mathrm{Im}\,(E_R)$. Physically speaking, this means that a resonance state with higher energy can decay more easily by tunneling across the barrier as compared to the states with lower energy. The conclusion from figures 1a and 1b is that peaks in σ_{ab} arise from the zeroes of the S matrix but at the same time indicate resonance state positions because the real part of zeroes and poles for these cases are practically the same as indicated in figure 1b. The first peak in σ_{ab} at $k^2 \simeq 0.6\,\mathrm{fm}^{-2}$ is less prominent because in this case, the S matrix pole and zero having appreciable imaginary parts are very close to each other thus making $|S(k) \simeq 1|$. This point will be elaborated later.

Poles		Zeroes	
$W = 0\,\mathrm{fm}^{-2}$	$W = 1\,\mathrm{fm}^{-2}$	$W = 0\,\mathrm{fm}^{-2}$	$W = 1\,\mathrm{fm}^{-2}$
$0.787–0.416 \times 10^{-4}i$	$0.946–0.525i$	$0.788 + 1.416 \times 10^{-4}i$	$0.946–0.525i$
$1.561–1.128 \times 10^{-3}i$	$1.591–0.309i$	$1.561 + 1.128 \times 10^{-3}i$	$1.591–0.307i$
$2.303–6.975 \times 10^{-3}i$	$2.312–0.214i$	$2.303 + 6.975 \times 10^{-3}i$	$2.314–0.201i$
$3.001–3.520 \times 10^{-2}i$	$3.001–0.191i$	$3.001 + 3.520 \times 10^{-2}i$	$3.008–0.121i$
$3.668–0.113i$	$3.664–0.242i$	$3.668 + 0.113i$	$3.676–1.510 \times 10^{-2}i$

2.2 *Gaussian barrier with absorptive pocket*

Now, we examine the same problem for a smoother potential having a Gaussian barrier with an absorptive Woods–Saxon pocket

$$U(r) = U_B \exp\left[-\left(\frac{r-R_G}{a}\right)^2\right] - iW\left[1+\exp\left(\frac{r-R}{a_I}\right)\right]^{-1} \tag{4}$$

with $U_B = 10\,\mathrm{fm}^{-2}$, $W = 1\,\mathrm{fm}^{-2}$, $R_G = 4.25\,\mathrm{fm}$, $R = 4.25\,\mathrm{fm}$, $a = 0.5\,\mathrm{fm}$, $a_I = 0.3\,\mathrm{fm}$. In this example, the barrier is comparatively broader. We have solved the Schrödinger equation using the Runge–Kutta method and the results of the calculation are summarized in figures 2a, b and table 2. We see that this potential essentially reproduces results that corroborate those of the previous potential, given by (3) leading to similar conclusions. We note that the sharp resonance peaks in σ_s in curve B for $W = 0$ gradually gets narrower ($\simeq 10^{-4}\,\mathrm{fm}^{-2}$) until they are too narrow to be observed due to the finite size of the energy steps used for the calculation. The arrow in figure 2a indicates the position of the sharpest resonance of curve B. But as in the previous example, the locations of these extremely sharp peaks match with the positions of the corresponding absorption peaks for the higher lying states. This point is explained in § 3. Compared with the former case, this potential has a larger imaginary part and width and the absorption cross section shows less structure as compared with that in figure 1a. Numerically speaking, this is due to the fact that poles and zeroes of the S matrix for this complex potential are much closer to each other than the corresponding case depicted in figure 1b. In this case, barrier tunneling is reduced due to the larger width and higher barrier. As expected, in the present case the resonance peaks in σ_s for $W = 0$ are sharper than the previous case studied.

2.3 *Woods–Saxon type barrier with absorptive pocket*

As the last example, we analyse the potential having a still larger barrier with a Woods–Saxon shape and an absorptive pocket of the same shape [11]. This potential is given by

$$U(r) = U_B\left[1+\exp\left(\frac{R_0-c_1-r}{a_1}\right)\right]^{-1} - iW\left[1+\exp\left(\frac{r-R_0+c_W}{a_W}\right)\right]^{-1}, \quad r < R_0 \tag{5}$$

The parameters used for this potential are $U_B = 10\,\text{fm}^{-2}$, $W = 1\,\text{fm}^{-2}$, $R_0 = 4.5\,\text{fm}$, $a_1 = 0.12\,\text{fm}$, $a_2 = 0.25\,\text{fm}$, $a_W = 0.05\,\text{fm}$, $c_1 = 1.5\,\text{fm}$, $c_2 = 2\,\text{fm}$, $c_W = 1.5\,\text{fm}$. The scattering and absorption cross sections as well as the positions of the poles and zeroes given in figures 3a, b and table 3 at first glance, do not seem to be similar to our previous two potentials of (3) and (4). The large barrier width effectively suppresses tunneling though the barrier and the corresponding resonances in curve B with $W = 0$ have extremely narrow widths. These peaks in curve B have not been reproduced in the graph due to the finite step size of the energy interval but we have indicated them by arrow marks. We have verified that these fine peaks in σ_s are reproduced with discernible width

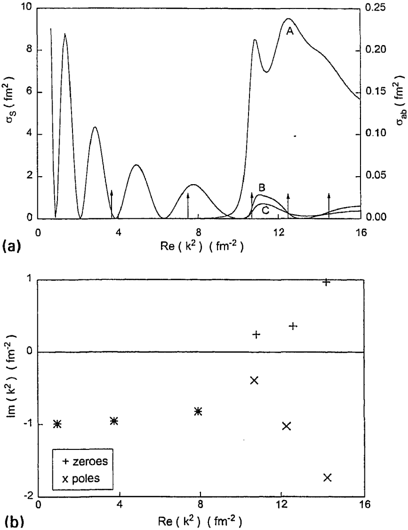

Figure 3. **(a)** Variation of σ_s and σ_{ab} with energy for the Woods–Saxon shaped barrier of eq. (5) with $U_B = 10\,\text{fm}^{-2}$, $W = 1\,\text{fm}^{-2}$, $a_1 = 0.12\,\text{fm}$, $a_2 = 0.25\,\text{fm}$, $a_W = 0.05\,\text{fm}$, $c_1 = 1.5\,\text{fm}$, $c_2 = 2\,\text{fm}$, $c_W = 1.5\,\text{fm}$, $R_0 = 4.5\,\text{fm}$. Curve A is the plot of σ_{ab} and curves C and B correspond to σ_s with and without absorption respectively. The arrow marks indicate the positions of the extremely narrow peaks in curve B which have not been reproduced due to the finite step size of the energy intervals. Below $E = 10\,\text{fm}^{-2}$, curves B and C practically merge into one. **(b)** Same as figure 1b

$c_2 = 2.0\,\text{fm}$, $c_W = 1.5\,\text{fm}$

Poles		Zeroes	
$W = 0\,\text{fm}^{-2}$	$W = 1\,\text{fm}^{-2}$	$W = 0\,\text{fm}^{-2}$	$W = 1\,\text{fm}^{-2}$
$0.978 - 3.244 \times 10^{-11}i$	$1.081 - 0.459i$	$0.978 + 3.286 \times 10^{-11}i$	$1.081 - 0.459i$
$1.928 - 7.743 \times 10^{-9}i$	$1.945 - 0.246i$	$1.928 + 7.743 \times 10^{-9}i$	$1.945 - 0.246i$
$2.808 - 2.274 \times 10^{-5}i$	$2.815 - 0.146i$	$2.808 + 2.274 \times 10^{-5}i$	$2.815 - 0.146i$
$3.275 - 4.774 \times 10^{-2}i$	$3.267 - 5.976 \times 10^{-2}i$	$3.275 + 4.774 \times 10^{-2}i$	$3.283 + 3.719 \times 10^{-2}i$
$3.518 - 9.981 \times 10^{-2}i$	$3.504 - 0.147i$	$3.518 + 9.981 \times 10^{-2}i$	$3.545 + 5.013 \times 10^{-2}i$
$3.779 - 0.180i$	$3.779 - 0.229i$	$3.779 + 0.180i$	$3.771 + 0.128i$

if the width of the barrier is decreased. More importantly, the display of the zeroes and poles of the S matrix does not show the symmetry in the E-plane which was present in the earlier two examples. This indicates that the symmetry in figures 1b and 2b should not be considered as the general feature of the zeroes and poles of the S matrix for complex potentials. However, one feature which may be noted is that as far as the deeper lying resonances are concerned, both the zeroes and poles practically coincide with each other. In such cases, peaks in σ_{ab} also are not observed. The nature of variation of poles and zeroes in figure 3b shows the dramatic difference between below barrier absorptive pocket resonances and above barrier resonances. The above barrier resonances in this case are very clearly manifested in σ_{ab} but not in σ_{s}. It may be mentioned here that the resonances in heavy ion scattering which have highly absorptive pocket followed by large Coulomb barrier are often associated with barrier region orbiting resonance states.

3. Discussion and conclusions

We further analyse our results as follows. In the case of real potential we have $\text{Re}(k_P) = \text{Re}(k_Z)$ and in the examples studied, we find that the same relation is valid to a good degree of accuracy for complex absorptive potentials. Since the poles are observed to occur lower down in the k-plane as compared to the corresponding zeroes, the following relations also hold for complex potentials.

$$\text{Im}(k_Z) > \text{Im}(k_P) \quad \text{and} \quad |\text{Im}(k_P)| > |\text{Im}(k_Z)|.$$

For the s-wave scattering case, we have

$$\sigma_{\text{s}} = \frac{\pi}{k^2}|1 - S(k)|^2,$$
$$\sigma_{\text{ab}} = \frac{\pi}{k^2}(1 - |S(k)|^2).$$

Near a pole or zero, we can write the S matrix as

$$S(k) = g(k)\frac{k - k_Z}{k - k_P},$$

$$\frac{\mathrm{d}}{\mathrm{d}k}|S(k)|^2 = 0 \quad \text{and} \quad \frac{\mathrm{d}^2}{\mathrm{d}k^2}|S(k)|^2 > 0 \text{ at } k = \mathrm{Re}\,(k_P)$$

and hence $S(k)$ has a minimum at $k = \mathrm{Re}\,(k_P)$. This will give rise to a maximum in the absorption cross section at the same energy. However, the corresponding rise in the scattering cross section is suppressed by the imaginary part of the potential due to the fact that in this case,

$$|1 - S(k)|^2 = \left(1 - \frac{\mathrm{Im}\,(k_Z)}{\mathrm{Im}\,(k_P)}\right)^2$$

and for all cases, either $\mathrm{Im}\,(k_Z) \simeq \mathrm{Im}\,(k_P)$ or $|\,\mathrm{Im}\,(k_Z)| < |\,\mathrm{Im}\,(k_P)|$. Hence $|1 - S(k)|^2$ becomes much smaller than the maximum possible value 4. On the other hand, in the case of real potentials, $|1 - S(k)|^2 = 4$ near a resonance. Thus the lack of mirror symmetry with respect to the real k axis and the nature of the poles and zeroes for complex potentials suppresses the resonance peaks in σ_s which the corresponding real potential can manifest when proper resolution is taken.

The width ΔE of the absorption peak of $(1 - |S(k)|^2)$ can be shown to be $\Delta E \simeq 4|\,\mathrm{Re}\,(k_P)\,\mathrm{Im}\,(k_P)|$. Even though a similar relation is valid for the peak in σ_s, due to the drastic suppression of the peak height as explained above, these are suppressed in σ_s.

As seen earlier in the case of the potential given by eq. (5), there are no peaks in σ_ab observed at lower energies because in this region, the complex zeroes and poles having significant imaginary parts are practically same leading to $|S(k)| \simeq 1$ for $E = E_R$. This can also be interpreted in terms of the inhibition posed by the large barrier to generate absorption in the pocket at lower energies. Thus in general, the variation of σ_ab provides a better indicator of the *effective* resonances in complex potentials as compared to σ_s.

To summarize, we have examined the poles and zeroes of the S matrix for three typical complex potentials having absorptive pocket followed by a barrier. We find that in general, the real parts of the low lying zeroes and the corresponding poles of $S(k)$ are practically the same and the imaginary parts are significantly different either in sign or magnitude or both. Such a statement is also substantially true for higher poles and zeroes. Due to this, $|1 - S(k)|^2$ gets greatly suppressed as compared with its peak value $(= 4)$ and hence elastic channel resonance peaks are not manifested appreciably. On the other hand, the zeroes of the S matrix corresponding to a pole enhance the absorption cross section factor $(1 - |S(k)|^2)$ in the vicinity of resonance energies. This enhancement prominently occurs when $|\,\mathrm{Im}\,(k_P)|$ is significantly larger than $|\,\mathrm{Im}\,(k_Z)|$ but when $\mathrm{Im}\,(k_P)$ is quite close to $\mathrm{Im}(k_Z)$, even in σ_ab the peaks get eliminated. As a result, peaks in σ_ab can be correlated with the resonances generated by the complex potential. This is consistent with the fact that in the analysis of resonances in nucleus-nucleus collisions, one of the important criteria for identifying resonance is that resonance structure should appear correlated in energy in several exit i.e., reaction channels. [12] The peaks in the absorption cross section also gets suppressed if the width of the barrier is quite large and in such cases, peaks in σ_ab occur due to the barrier top states. These observations mean that in be comparatively weaker.

References

[1] R G Newton, in *Scattering Theory of Waves and Particles* (McGraw-Hill, New York, 1966) p. 339

[2] V de Alfaro and T Regge, in *Potential Scattering* (North-Holland, Amsterdam, 1975) p. 34

[3] C J Jochain, in *Quantum Collision Theory* (North-Holland, Amsterdam, 1965) p. 243

[4] S Mukherjee and C S Shastry, *Nucl. Phys.* **A128**, 256 (1969)

[5] S Joffily, *Nucl. Phys.* **A215**, 301 (1973)

[6] L P Kok and H van Haeringa, *Ann. Phys. (NY)* **131**, 426 (1981)

[7] W Cassing, M Stingl and A Weiguny, *Phys. Rev.* **C26**, 22 (1982)

[8] J Dabrowski, *Phys. Rev.* **C53**, 2004 (1996)

[9] A Gal, G Toker and Y Alexander, *Ann. Phys. (NY)* **137**, 341 (1981)

[10] E Oset, P F de Córdoba, L L Salcedo and R Brockman, *Phys. Rep.* **188**, 79 (1990)

[11] P Susan, B Sahu, B M Jyrwa and C S Shastry, *J. Phys.* **G20**, 1243 (1994)

[12] R Singh in *Nuclear Reactions* edited by R Singh and S N Mukherjee (New Age International Limited 1996) p. 206

Universal inaccessibility principle

ANIL A BHALEKAR
Department of Chemistry, Nagpur University, Amravati Road, Nagpur 440 010, India
Departamento de Física, Universidad Autónoma Metropolitana-Iztapalapa, Apdo. Postal 55-534, México, D.F. 09340, México

MS received 26 July 1996

Abstract. The universal inaccessibility principle (UIP) which was previously used in developing the generalized phenomenological irreversible thermodynamic theory (GPITT) is discussed at length. UIP provides both the thermodynamic temperature and the corresponding entropy function for a local nonequilibrium state without involving any physical device. The Carathéodory principle is obtained as a particular case of the equilibrium part of UIP. The system with negative temperatures are also covered by UIP. It is revealed that the use of UIP is implied in the De Donderian thermodynamic description of irreversibility due to chemical reactions and also in the classical irreversible thermodynamic description of Onsager–Prigogine–Meixner–de Groot. The reversible adiabatic paths of a chemically reactive closed system remain perfectly isentropic even if concomitantly a chemical conversion takes place within the system.

Keywords. Thermodynamics; irreversible thermodynamics; thermodynamic processes; thermodynamic properties and entropy.

PACS Nos 05.70; 44.60; 65.50

1. Introduction

A new irreversible thermodynamic formalism, viz. the generalized phenomenological irreversible thermodynamic theory (GPITT) [1–6] has been developed. This theory reveals that every irreversible thermodynamic formalism is necessarily governed by the validity of Gibbs–Duhem equation (GDE). Hence, according to GPITT all nonequilibrium thermodynamic situations belong to GDE-regulated regime. The breakdown of GDE means the crumbling down of irreversible thermodynamics itself. For example, GPITT derives (does not assume) the traditional local level version of the Gibbs relation, namely:

$$\frac{\mathrm{d}s}{\mathrm{d}t} = T^{-1}\frac{\mathrm{d}u}{\mathrm{d}t} + pT^{-1}\frac{\mathrm{d}v}{\mathrm{d}t} - T^{-1}\sum_k \mu_k \frac{\mathrm{d}c_k}{\mathrm{d}t} \tag{1.1}$$

under the condition that its corresponding GDE, namely

$$s\,\frac{\mathrm{d}T}{\mathrm{d}t} - v\frac{\mathrm{d}p}{\mathrm{d}t} + \sum_k c_k \frac{\mathrm{d}\mu_k}{\mathrm{d}t} = 0 \tag{1.2}$$

---

density, μ_k is the chemical potential per unit mass of the component k, c_k is the mass fraction of the component k and t is time. In GPITT one also derives an extended Gibbs relation,

$$\frac{\mathrm{d}s}{\mathrm{d}t} = T^{-1}\frac{\mathrm{d}u}{\mathrm{d}t} + pT^{-1}\frac{\mathrm{d}v}{\mathrm{d}t} - T^{-1}\sum_k \mu_k \frac{\mathrm{d}c_k}{\mathrm{d}t} + T^{-1}\sum_j \beta_j \odot \frac{\mathrm{d}\alpha_j}{\mathrm{d}t} \qquad (1.3)$$

which is valid provided its GDE, namely:

$$s\frac{\mathrm{d}T}{\mathrm{d}t} - v\frac{\mathrm{d}p}{\mathrm{d}t} + \sum_k c_k \frac{\mathrm{d}\mu_k}{\mathrm{d}t} - \sum_j \alpha_j \odot \frac{\mathrm{d}\beta_j}{\mathrm{d}t} = 0 \qquad (1.4)$$

also holds true, where α_j and β_j are the extensive and intensive parameters respectively and are identified in GPITT as the additional irreversibility parameters. They originate from the additional nonequilibrium interactions [3–5] other than the thermal, mechanical (both long and short range ones) and chemical. Unfortunately, at present no physical basis for these so-called additional nonequilibrium interactions is in sight.

Thus the classical irreversible thermodynamics (CIT) of Onsager–Prigogine–Meixner–de Groot [7–11] is reproduced in GPITT (c.f. eq. (1.1)) but with a difference that it stresses the fundamental rôle of the GDE, eq. (1.2) and one is not at all required to invoke the local equilibrium assumption for the derivation of eq. (1.1). On the other hand the derived (not proposed) extended Gibbs relation, eq. (1.3), of GPITT has specific requirements and those do not seem to be fulfilled by the existing other irreversible thermodynamic theories, for example extended irreversible thermodynamics (EIT) [12–15].

The strength of the GPITT lies in its simple but overall picture about the thermodynamics of irreversible processes, though at times a nonequilibrium situation may be a highly complex one from many points of views. Amongst the vital tenets of GPITT is the recognition of an universal inaccessibility principle (UIP), which reads as:

> "*In every neighbourhood of every equilibrium and nonequilibrium state of a system there exist states (both equilibrium and nonequilibrium ones) which remain unattainable by reversible or spontaneous paths.*"

This principle guarantees the existence of an integrating denominator to the concept of thermodynamic heat also identified and defined so in GPITT. This then leads us to the corresponding entropy function and the thermodynamic temperature for nonequilibrium states. Indeed, while presenting our development of GPITT [1] we had simply stated the UIP and used it without elaborating its essential contents. However, recently we have demonstrated [3] that UIP serves as a local level analogue of Clausius' inequality. Thus, we take this opportunity to elaborate on its essential contents.

The next section describes reversibility and spontaneity. In § 3 some relevant concepts of GPITT are presented, in § 4 and § 5, how the use of UIP is involved in the De Donderian thermodynamic description of chemical reactions at finite rates and in the CIT, is demonstrated. Section 6 contains remarks on the inclusion of the situations with negative temperatures in the fold of UIP and § 7 contains concluding remarks.

In thermodynamics of equilibrium states, a prescribed path through the succession of equilibrium states is said to be reversible because the same succession of equilibrium states can be traversed in the reverse order. These paths in principle can only be traversed infinitely slowly and hence they are also termed as quasi-static paths. Recently, the reversible paths through the succession of nonequilibrium stationary states (NSS) have also been recognized. Keizer has developed a generalized fluctuation-dissipation principle, a statistical kinetic theory description, and one of its results is the prescription of reversible paths through NSS [16–20], which too by prescription can only be traversed infinitely slowly, meeting the requirement of quasi-staticity. Therefore, in this presentation reversibility implies the passages through the succession of either equilibrium states or NSS. However, along every reversible path through a succession of equilibrium states a set of corresponding time independent differential conditions, $G_j(y_i)$s are followed, namely:

$$F = F(G_j(y_i)), \tag{2.1}$$

where y_is are the corresponding variables. Whereas for the reversible paths through NSS there exist similar equations,

$$f(\mathbf{r}) = f(g_j(x_i(\mathbf{r}))). \tag{2.2}$$

To distinguish between equilibrium and nonequilibrium we have used x_is in eq. (2.2) instead of y_is and changed to a local level description. However, for the present purpose it is not required to know the exact expressions for the above functions. It is only sufficient to know that there exist the constitutive equations, $g_j(x_i(\mathbf{r}))$s and $G_j(y_i)$s.

In the true sense of the word 'spontaneous' there are no processes which occur without intervention. But still one describes the so called spontaneous processes. These are the processes which cannot be arrested if the constraints on the system are not appropriately altered. The constraints on the system may be time invariant or time dependent. In UIP and GPITT the evolution of a system under the given constraints is described as spontaneous one. Let us make it a specific mathematical idea. Consider a closed system in an equilibrium. Now if the system is instantly brought into a nonequilibrium condition by a suitable manipulation it will follow an irreversible adiabatic path if the adiabaticity is adhered throughout. Depending upon the initial time invariant conditions to which the closed adiabatic system is subjected to, a final equilibrium state is reached. To reach different final equilibrium states adiabatically, the initial conditions need to be changed accordingly. This behaviour is well documented and is easy to visualize [21, 22]. Thus for different irreversible adiabatic transitions, even if all of them originate from the same initial equilibrium state by suitable manipulations, the end equilibrium states are different. That is, along a given irreversible adiabatic transition of a system it passes through an unique succession of local nonequilibrium conditions (within the system) or in other words with a given set of dynamical conditions there is one and only one real trajectory for an irreversible adiabatic transition.

However, to ascertain which trajectory is followed during an irreversible adiabatic where g_js are the dynamical differential conditions or constitutive equations whose variables are the $x_i(\mathbf{r}, t)$s and $\mathbf{r}$ is the position vector. Thus the knowledge of all the $g_j(x_i(\mathbf{r}, t))$s along with the initial conditions identifies an irreversible adiabatic. However, every spontaneous transition whether it is an adiabatic or a nonadiabatic one possesses the same characteristics, that is, the passage is determined by $g_j(x_i(\mathbf{r}, t))$s. Therefore, eq. (2.3) contains a set of constitutive equations of spontaneous paths. The existence of the constitutive equations g_js in terms of $x_i(\mathbf{r}, t)$s amounts to the recognition of the *transitory local conditions* as *local nonequilibrium states*. If a process is much *faster* than the time required to experimentally register $x_i(\mathbf{r}, t)$s then no g_js can be prescribed. Some of the examples of $x_i(\mathbf{r}, t)$ are temperature, pressure, concentrations, internal energy, volume, physical fluxes, gradients of intensive quantities etc. Recall that even in nonequilibrium situations one measures at the local level temperature, pressure (or stresses) and concentrations with ease and also the physical fluxes. For example, temperature can be measured within the time period approaching nanoseconds and *in situ* measurements of concentrations require a time period much shorter than a picosecond (for example the spectrophotometric absorption and emission measurements). Thus with the recognition of the constitutive equations a *notion* of nonequilibrium states gets *informally* incorporated in our description and irreversible thermodynamics makes it a *formal* concept. From the above discussion it is clear that by definition the local nonequilibrium states exist for exceedingly short but *finite* duration depending upon the fastness of the process. Further, it is not necessary that all the $x_i(t)$s would become independent thermodynamic variables. The latter are determined by the laws of thermodynamics and not by a constitutive theory [3, 5]. In nutshell $g_j(x_i(\mathbf{r}, t))$s and $x_i(\mathbf{r}, t) = x_i(\mathbf{r}, 0)$ determine which spontaneous path is being followed by the system. These we know say from fluid dynamics. However, in connection with the application of UIP we will see in the following that all g_js are not required to construct the corresponding condition, namely $f(\mathbf{r}, t)$. Also notice that eqs (2.1) to (2.3) are the constitutive theory.

To cite the illustrative examples of the above deductions in terms of processes we may recall that under a given condition a chemical reaction proceeds through a corresponding given succession of nonequilibrium states. If this were not true then it could not have been possible to obtain the reproducible values of rate constants on repeating the experiment. Recall from the literature on chemical reaction rates that even in the case of diffusion controlled reactions the experimentally measured accurate values of rate constants are available. Yet another simple example is that of the rigid body heat conduction. When a heat conducting bar is placed between two heat reservoirs at different temperatures and if the temperature at a position z along the length of the bar is measured with time then the same temperature-time profile is obtained on repeating the experiment. A good example of this is the experimental recording of temperature waves [23]. To this list one can add numerous examples for there is no dearth of them.

Further, recall that in the case of irreversibility the end equilibrium states are mutually inaccessible; the accessibility is in one direction only. For example, from an equilibrium local nonequilibrium states cannot be traversed in the reverse direction. In contrast Muschik [21] describes that any two equilibrium states of a closed system are attainable by more than one irreversible adiabatic paths but then it demands at least one additional equilibrium state to be reached in between [21]. Therefore, the contents of UIP should not be confused with such situations. Yet another example, if sufficient care is taken, it can mislead to that of a reversible chemical reaction. Such reactions can be made to proceed in forward as well as in reverse directions so that the chemical composition of the system is changed exactly in the mutually reverse order in the two situations. But if the chemical conversion is not carried under the reversible conditions then one needs to adequately change say T and/or p to effect the chemical reaction at a finite rate in the reverse direction and hence although the chemical composition changes exactly in reverse order it is under a different thermodynamic condition, that is the system traverses a different succession of nonequilibrium states. Thus the above elaboration makes it precise what is implied by the terms spontaneity and reversibility in UIP and hence in GPITT.

Moreover, all the heat differentials used in global and local level descriptions, in the following sections, are the inexact differentials but they have not been distinguished so in their notation compared to the other thermodynamic exact differentials. Hence the former should not be read as a differentiation of a function. Further, in order to appreciate UIP and its application we felt that it is advantageous to describe first the appropriate concepts of GPITT in adequate details which is the subject matter of the next section.

3. Some relevant concepts of GPITT and application of UIP

To meet the requirements of self-sufficiency and brevity we are describing below the *thermodynamic heat* as defined in GPITT [1–5] considering only a simplest situation. Let the following fluid-dynamical internal energy balance equation (which does have sufficient element of generality) be a total description of a situation in hand:

$$\rho \frac{\mathrm{d}u}{\mathrm{d}t} = -\operatorname{div}\mathbf{q} + \mathbf{T}\colon \operatorname{grad}\mathbf{u}. \tag{3.1}$$

In eq. (3.1) $\mathbf{q}$ is the so-called heat flux density, $\mathbf{T}$ is the stress tensor and $\mathbf{u}$ is the barycentric velocity.

In the first step the stress tensor is split into two parts,

$$\mathbf{T} = -p\mathbf{1} + \Pi, \tag{3.2}$$

such that the first term on the right hand side of the following equation,

$$\mathbf{T}\colon \operatorname{grad}\mathbf{u} = -p\rho \frac{\mathrm{d}v}{\mathrm{d}t} + \Pi\colon \operatorname{grad}\mathbf{u} \tag{3.3}$$

completely quantifies the nondissipative part of the work due to the contact forces. Therefore, the second term on the right hand side of eq. (3.3) measures the total are designated as *Born's heat*,

$$\rho \frac{\mathrm{d}q_{\mathrm{B}}}{\mathrm{d}t} = -\operatorname{div}\mathbf{q} + \Pi\colon \operatorname{grad}\mathbf{u}. \tag{3.4}$$

Note that according to GPITT eq. (3.4) is the definition of Born's heat corresponding to the internal energy balance equation of eq. (3.1).

Since even in CIT [7–11] the terms on the right hand side of eq. (3.4) taken together are *not adequate enough* to describe the total change in entropy of the system we must search for a new heat concept. For a general nonequilibrium situation GPITT defines the thermodynamic heat as

$$\frac{\mathrm{d}q}{\mathrm{d}t} = \frac{\mathrm{d}q_{\mathrm{B}}}{\mathrm{d}t} + \frac{\mathrm{d}q_{\mathrm{nc}}}{\mathrm{d}t}. \tag{3.5}$$

Note that the nonconventional (nc) heat is not the one designated in the literature as Clausius' uncompensated heat, though through the former one can arrive at the corresponding expression for the latter [3]. Notice that the nonconventional heat is also recognized for the first time in GPITT [1–5]. In support of the above statement it can be shown that in the thermodynamics of equilibrium states of open systems the equilibrium Gibbs relation follows elegantly by using the nonconventional heat [24].

With the combination of eqs (3.1) and (3.4) and the standard definition of enthalpy, h (per unit mass),

$$h = u + pv \tag{3.6}$$

one gets the following expression for Born's heat:

$$\frac{\mathrm{d}q_{\mathrm{B}}}{\mathrm{d}t} = \frac{\mathrm{d}h}{\mathrm{d}t} - \rho^{-1}\frac{\mathrm{d}p}{\mathrm{d}t} \tag{3.7}$$

which resembles with the corresponding equation in the thermodynamics of equilibrium states and hence the first law of thermodynamics in the local form, eq. (3.1), is obeyed by Born's heat only.

Now we are in a position to use the UIP. From the discussion of § 2 above, it follows that with the restriction of spontaneity, that is by a given equation of a spontaneous path,

$$\frac{\mathrm{d}q}{\mathrm{d}t}(\mathbf{r},t) \equiv f(\mathbf{r},t) \tag{3.8}$$

there remain numerous nonequilibrium and equilibrium states of the system unattainable. This is what UIP precisely describes. Notice that only relevant dynamical conditions $g_j(x_i(\mathbf{r},t))$s need to be incorporated to construct $f(\mathbf{r},t)$ of eq. (3.8). Therefore, from the inaccessibility described on following (3.8) it immediately follows that $\mathrm{d}q$ has an integrating denominator and thus we obtain the entropy (s) and the local thermodynamic temperature (T) in a nonequilibrium situation as

$$\frac{\mathrm{d}s}{\mathrm{d}t} = \frac{1}{T}\frac{\mathrm{d}q}{\mathrm{d}t}. \tag{3.9}$$

Once an integrating denominator to $\mathrm{d}q$ is established one is free to coincide it with the

the name entropy for the function s in contrast to the practice in other irreversible thermodynamical theories where one encounters the terms like generalized entropy, calortropy and an entropy like function [12–14]. The remaining parts of the details wherein the traditional Gibbs relation, eq. (1.1) and the extended Gibbs relation of GPITT, eq. (1.3) are arrived at are to be found in our earlier discussions [1–5].

On the other hand, on following the restriction of reversibility (for closed systems), that is the condition of eq. (2.1),

$$\mathrm{d}Q_c \equiv F, \tag{3.10}$$

where $\mathrm{d}Q_c$ is the reversible differential element of heat and the subscript c stresses the conduction mode of energy exchange, no nonequilibrium state is attainable from any one of the equilibrium states of the system. Thus we conclude that all equilibrium states of a system are mutually accessible. This is the equilibrium part of UIP. In this case the form of the function F is none else than the first law of thermodynamics which in the simplest case reads as $F \equiv \mathrm{d}U + p\mathrm{d}V$. Moreover, on using $F = 0$, the differential condition, in eq. (3.10) (that is on imposing the condition of adiabaticity) the Carathéodory principle is obtained which describes that not only no nonequilibrium states are attainable but numerous other equilibrium states too remain unattainable on following a reversible adiabatic path. Notice that traditionally while applying Carathéodory's principle no nonequilibrium states are under consideration the unattainability of the latter category of states is neither of any consequence nor is required in thermodynamics of equilibrium states. The case of reversible paths through NSS is considered in one of the following sections. In order to make it further clear that UIP is not an offbeat statement the next two sections demonstrate the implied involvement of UIP in the already existing irreversible thermodynamic descriptions. For this purpose some relevant stepwise details of the two chosen irreversible thermodynamic descriptions are described in the next two sections in such a way that a connection with the various concepts of heat of GPITT is established.

4. The derivation of a variance of UIP from the De Donderian thermodynamic description of chemical reactions at finite rates

Though the Belgian group [7,24] does not seem to claim it emphatically, the De Donderian thermodynamic description of chemical reactions within a closed system does constitute one of the first irreversible thermodynamic descriptions. Prigogine and Defay in their classic monograph on chemical thermodynamics [25] describe it very elegantly. They start with a closed system having irreversibility within it only due to the occurence of a chemical reaction. Since the system considered is a closed one, the following form of Clausius' inequality is used:

$$\mathrm{d}S > \frac{\mathrm{d}Q_c}{T}, \tag{4.1}$$

where $\mathrm{d}Q_c$ appears in the corresponding first law expression, namely:

$$\mathrm{d}U = \mathrm{d}Q_c - p\mathrm{d}V \tag{4.2}$$

energy and V is the volume of the system. Since no irreversibility is assumed in heat and volume exchanges the temperature T, and pressure p, are those of the system itself. In the next step eq. (4.1) is converted into an equality by identifying a quantity of heat $\mathrm{d}Q'$, termed as the Clausius *uncompensated heat* having the property,

$$\mathrm{d}Q' > 0, \tag{4.3}$$

which vanishes in equilibrium and hence in the limit of reversibility through the succession of equilibrium states. Indeed, barring a sole example [26], hardly one finds the latter assertion in the literature. In view of eq. (4.3) the Clausius inequality, eq. (4.1), produces the following equation for the entropy change:

$$\mathrm{d}S = \frac{\mathrm{d}Q_c + \mathrm{d}Q'}{T}. \tag{4.4}$$

Since, the uncompensated heat measures the irreversibility on account of the occurence of a chemical reaction, it is then quantified as

$$\mathrm{d}Q' = \mathcal{A}\mathrm{d}\xi \geq 0, \tag{4.5}$$

where $\mathcal{A}$ is identified as the chemical affinity and ξ is the extent of chemical reaction. Next eqs (4.2), (4.4) and (4.5) are combined to give

$$\mathrm{d}U = T\mathrm{d}S - p\mathrm{d}V - \mathcal{A}\mathrm{d}\xi. \tag{4.6}$$

We notice that an irreversibility due to a chemical reaction can arise only when it occurs at a finite rate, this is what the Belgian school failed to stress. Since by definition $\mathcal{A}$ vanishes at equilibrium it needs to behave in identically the same way along a reversible path even if during a reversible transition $\mathrm{d}\xi \neq 0$. From which it immediately follows in the view of the definitions of eqs (4.4) and (4.5) that along a reversible adiabatic of a closed system even if chemical composition within it changes on account of accompanied internal chemical conversion the reversible adiabatic remains perfectly isentropic. We have demonstrated this in one of the previous discussions by using the flux-force relationships for chemical reactions [5]. It is, therefore, surprising to learn that this simple looking deduction failed to catch an attention in thermodynamic literature so far.

We stress that eq. (4.6) is, indeed in the Pfaffian exact differential form but it is at the same time a nonequilibrium thermodynamic description too. In other words, the above descriptions should involve the time parameter, so that eq. (4.6) reads as

$$\frac{\mathrm{d}U}{\mathrm{d}t} = T\frac{\mathrm{d}S}{\mathrm{d}t} - p\frac{\mathrm{d}V}{\mathrm{d}t} - \mathcal{A}\frac{\mathrm{d}\xi}{\mathrm{d}t}. \tag{4.7}$$

That is we have

$$U=U(t),\ S=S(t),\ V=V(t),\ \xi=\xi(t),\ T=T(t),\ p=p(t),\ \mathcal{A}=\mathcal{A}(t). \tag{4.8}$$

For the same reason eq. (4.4) should read as

$$\frac{\mathrm{d}S}{\mathrm{d}t} = \frac{1}{T}\left[\frac{\mathrm{d}Q_c}{\mathrm{d}t} + \frac{\mathrm{d}Q'}{\mathrm{d}t}\right]. \tag{4.9}$$

Clausius uncompensated heat, because the calorific quantity $\mathrm{d}Q_c$ of eq. (4.2) is inadequate to define the total change of entropy. Of course, $\mathrm{d}Q'$ quantifies the amount of non-retrievable damage caused by a chemical reaction at a finite rate.

Now let us view the above equations in terms of the concepts contained in GPITT. For this purpose we denote by $\mathrm{d}Q$, the sum

$$\mathrm{d}Q = \mathrm{d}Q_c + \mathrm{d}Q' \tag{4.10}$$

and call it the *thermodynamic heat*. The general definition of thermodynamic heat is given in GPITT [1–5] as in eq. (3.5) above. The name thermodynamic heat stems from the fact that it directly leads us to thermodynamic thermal parameters S and T. Thus eq. (4.9) is compactly expressed as

$$\frac{\mathrm{d}S}{\mathrm{d}t} = \frac{1}{T}\frac{\mathrm{d}Q}{\mathrm{d}t}. \tag{4.11}$$

The acceptance of the definition contained in eq. (4.11) implies that in this nonequilibrium situation the thermodynamic temperature has been identified in T and it has been assigned as an integrating denominator to the heat differential $\mathrm{d}Q$. Indeed, T so obtained is a temperature corresponding to the nonequilibrium state of the entire chemically reacting system, because the system is assumed to be thermally homogeneous. Hence, S so obtained, is the entropy in a nonequilibrium state originating due to a chemical reaction at a finite rate.

From Carathéodory's theorem [22, 27] we know that the existence of an integrating factor for an inexact differential implies the existence of a differential equation, in terms of the same inexact differential, describing the corresponding unattainability. In the view of this and eq. (4.11) the following statement immediately follows:

> "$\mathrm{d}Q$ *is an inexact differential but is integrable, that is it possesses an integrating factor, which implies that there exist states which remain unattainable by the paths given by* $\mathrm{d}Q/\mathrm{d}t \equiv F(t)$."

The function $F(t)$ is defined on the lines of eq. (2.3) and on keeping in mind that there is no spatial inhomogenieties within the system under consideration. Thus on using the above condition,

$$\frac{\mathrm{d}Q}{\mathrm{d}t} \equiv F(t) \tag{4.12}$$

in eq. (4.11) we have

$$\mathrm{d}S = \frac{1}{T}\,F(t)\mathrm{d}t \tag{4.13}$$

whose solution (in view of eq. (4.7) and in general T will be time dependent) reads as

$$S = S(U(t), V(t), \xi(t)) \tag{4.14}$$

subject to an additive constant.

$$\mathrm{d}Q/\mathrm{d}t \equiv F(t)$$

where $\mathrm{d}Q$ is the thermodynamic heat defined in equation (4.10).

Thus UIP-I is nothing else than the UIP applied to a global nonequilibrium system having thermal and mechanical homogeneity. Notice that in this case we have $F(t) \equiv \mathrm{d}U/\mathrm{d}t + p\mathrm{d}V/\mathrm{d}t + \mathrm{d}Q'/\mathrm{d}t$. Moreover, on making the dynamical condition $F(t)$ of eq. (4.12) as a time independent constant, the entropy varies linearly with time and on using $F(t) = 0$ in eq. (4.12) the system gets relegated to the corresponding NSS. But both the cases cannot be realized in a real situation for a chemically reacting closed system. Hence the case of $F(t) = 0$ means the attainment of chemical equilibrium and $F(t)$ equal to a time independent constant is devoid of a physical significance in the present case.

Note that if there exist irreversibilities for example due to the thermal and mechanical inhomogeneities within the system the above global inaccessibility principle, UIP-I, cannot be applied as such. For such situations a local level consideration is demanded. This we describe in the following section.

5. UIP from CIT

In this and in the following sections all the per unit mass time derivatives are in fact the substantial time derivatives at a given value of the position vector, $\mathbf{r}$. We assume that the illustrative system at hand is adequately described by the internal energy balance eq. (3.1). Note that in eq. (3.1) we have $u(\mathbf{r},t), \rho(\mathbf{r},t), \mathbf{q}(\mathbf{r},t), \mathbf{T}(\mathbf{r},t)$ and $\mathbf{u}(\mathbf{r},t)$. However, if the $\mathbf{r}$ and t dependence has not been depicted for the quantities in the following expressions of this paper it is implied as usual. In the development adopted in CIT [7–11] the stress tensor is splitted as

$$\mathbf{T} = -p\mathbf{1} - \mathbf{P}, \tag{5.1}$$

where $\mathbf{1}$ is the unit tensor, $\mathbf{P}$ is the viscous pressure tensor and p is understood as the hydrostatic pressure or more precisely $-(1/3)\mathrm{Tr}\,\mathbf{T}$. Next the validity of the traditional Gibbs relation, eq. (1.1), is taken as a thermodynamic condition of the existence of the *local equilibrium* within the system. Then (3.1), (5.1) and (1.1) are combined to give the following expression for the rate of change of the local entropy,

$$\rho\,\frac{\mathrm{d}s}{\mathrm{d}t} = -\mathrm{div}\left[\frac{1}{T}\left(\mathbf{q} - \sum_k \mu_k\,\mathbf{J}_k\right)\right] + \mathbf{q}\cdot\nabla\left(\frac{1}{T}\right) - \sum_k \mathbf{J}_k\cdot\nabla\left(\frac{\mu_k}{T}\right)$$
$$-\frac{1}{T}\,\mathbf{P}\colon\nabla\mathbf{u} + \frac{\mathcal{A}}{T}\,\rho\,\frac{\mathrm{d}\xi}{\mathrm{d}t}. \tag{5.2}$$

In arriving at eq. (5.2) the following standard fluid-dynamical equation is used:

$$\rho\,\frac{\mathrm{d}c_k}{\mathrm{d}t} = -\mathrm{div}\,\mathbf{J}_k + \rho m_k, \tag{5.3}$$

where $\mathbf{J}_k$ are the diffusion fluxes, m_k are the rates of mass fraction changes on account of chemical reaction, ξ is the corresponding extent of chemical reaction and the chemical where M_k is the mass per mole of the component k and ν_ks are the stoichiometric numbers.

Now we proceed to establish a connection between the above CIT description with the concepts contained in GPITT as follows. Recall from GPITT the definition of *Born's heat*, $\mathrm{d}q_{\mathrm{B}}$, which in the present case is quantified as

$$\rho \frac{\mathrm{d}q_{\mathrm{B}}}{\mathrm{d}t} = -\mathrm{div}\,\mathbf{q} - \mathbf{P}\colon \nabla\mathbf{u} \tag{5.5}$$

and recast eq. (5.2) as

$$\rho T \frac{\mathrm{d}s}{\mathrm{d}t} = -\mathrm{div}\,\mathbf{q} - \mathbf{P}\colon \nabla\mathbf{u} + \sum_k \mu_k \,\mathrm{div}\,\mathbf{J}_k + \mathcal{A}\frac{\mathrm{d}\xi}{\mathrm{d}t}. \tag{5.6}$$

Thus the first two terms on the right hand side of eq. (5.6) constitute Born's heat (c.f. eq. (5.5)) and are provided by the internal energy balance equation, eq. (3.1) hence they are calorific in nature. On the other hand, the last two terms of eq. (5.6) are the *additional* ones which are required for defining entropy rate and in GPITT are termed as *nonconventional* (nc) *heat* terms [3]. Therefore, in the present case we have:

$$\rho \frac{\mathrm{d}q_{\mathrm{nc}}}{\mathrm{d}t} = \sum_k \mu_k \,\mathrm{div}\mathbf{J}_k + \mathcal{A}\rho\frac{\mathrm{d}\xi}{\mathrm{d}t}. \tag{5.7}$$

Thus in terms of Born's and nonconventional heats eq. (5.2) gives

$$\frac{\mathrm{d}s}{\mathrm{d}t} = \frac{1}{T}\left[\frac{\mathrm{d}q_{\mathrm{B}}}{\mathrm{d}t} + \frac{\mathrm{d}q_{\mathrm{nc}}}{\mathrm{d}t}\right]. \tag{5.8}$$

The *thermodynamic heat*, $\mathrm{d}q$, in this case (c.f. eq. (3.5)) is given by

$$\mathrm{d}q = \mathrm{d}q_{\mathrm{B}} + \mathrm{d}q_{\mathrm{nc}}. \tag{5.9}$$

Therefore, eq. (5.8) reads as

$$\frac{\mathrm{d}s}{\mathrm{d}t} = \frac{1}{T}\frac{\mathrm{d}q}{\mathrm{d}t}. \tag{5.10}$$

Thus we see that the adoption of the traditional Gibbs relation, eq. (1.1) and the definitions of $\mathrm{d}q_{\mathrm{B}}$ and $\mathrm{d}q_{\mathrm{nc}}$ tantamounts to prescribing the definition contained in eq. (5.10) for the entropy rate. Therefore, it immediately follows that T should be identified as the local thermodynamic temperature in a nonequilibrium state and taken as the integrating denominator to $\mathrm{d}q$, the thermodynamic heat element. Since the validity of eq. (5.2) is beyond doubt, the adoption of eq. (5.10) is implied therein.

The assertions from eq. (5.10) are similar to those that follow after eq. (4.11) in the preceding section. The first statement from the above delineation is obtained as

> "$\mathrm{d}q$ *is an inexact differential but is integrable, that is it possesses an integrating factor, which implies that there exist states which remain unattainable by the paths*

$$\frac{\quad}{\mathrm{d}t}(\mathbf{r},t) \equiv f(\mathbf{r},t) \tag{5.11}$$

in combination with eq. (5.10) gives

$$\frac{\mathrm{d}s}{\mathrm{d}t}(\mathbf{r},t) = \frac{1}{T}\, f(\mathbf{r},t) \quad \text{and} \quad s = s(\mathbf{r},t). \tag{5.12}$$

In this case, the local level inaccessibility principle is obtained from the above considerations as

> *UIP-II*: *"In every neighbourhood of every local nonequilibrium state of a system there exist local states which remain unattainable on following the equation* $(\mathrm{d}q/\mathrm{d}t)(\mathbf{r},t) \equiv f(\mathbf{r},t)$"

where $\mathrm{d}q$ is the thermodynamic heat defined in eq. (5.9).

The discussion of § 4 and § 5 clearly surface out the operation of the corresponding inaccessibility principles viz. UIP-I and UIP-II. This has never been realized before. Recall that $\mathrm{d}Q/\mathrm{d}t = F(t)$ and $\mathrm{d}q/\mathrm{d}t = f(\mathbf{r},t)$ are the mathematical statements of spontaneity as defined earlier in § 2 and hence UIP-I and UIP-II are nothing else than the UIP stated in § 1 above. We see that the form of $f(\mathbf{r},t)$ in eq. (5.11) is $f(\mathbf{r},t) \equiv \mathrm{d}u/\mathrm{d}t + p\mathrm{d}v/\mathrm{d}t + \mathrm{d}q_{\mathrm{nc}}/\mathrm{d}t$. Further, on using the restriction $f(\mathbf{r},t) = 0$ in eq. (5.11) we relegate the system to NSS and thus UIP generates the *reversible paths* through the succession of NSS and thereby confirms the earlier proposal of Keizer [16–20] on a generalized thermodynamic footing. The use of $f(\mathbf{r},t)$ equal to a time independent constant in eq. (5.11) means entropy varies linearly with time. Such situations could be realized in practice by appropriate manipulations of a system. However, it would be curious to know whether such situations are encountered or not in industrial processes and in biological systems.

6. UIP and negative temperatures

The general statement of UIP reproduced in the introductory section of this paper is to be understood only in terms of reversibility and spontaneity described in § 2 of this paper. Thus the inaccessible states, under the restrictions of reversibility, are the nonequilibrium ones (from equilibrium states). While for the nonequilibrium states there are numerous nonequilibrium and equilibrium states in their vicinity which remain inaccessible by a given restriction describing the spontaneous path. Basically the nonequilibrium part of the UIP is indeed, a local level assertion and from which the corresponding global level assertions follow.

In the preceding sections we have seen that UIP is adequate enough to arrive at the thermodynamic local temperature and the corresponding entropy function for a system in nonequilibrium. It is now our choice to coincide the temperature given by UIP with the Kelvin temperature and in this way we make entropy S or s so obtained a physical quantity exactly on the same lines as one does in the case of equilibrium. The physical reality of the thermometric temperature for nonequilibrium states has been described temperature is the identically same physical entity irrespective of whether the system is in an equilibrium or in a nonequilibrium state.

The negative temperatures are associated to the population inverted states and hence these states basically constitute the extreme levels of nonequilibrium. Note that, since no restrictions were placed on the system while defining the thermodynamic heat function and neither UIP involves any such restriction, hence the nonequilibrium states with negative temperatures also find themselves into the fold of UIP and its application. Note that UIP provides the function T and not a particular sign to it. Hence, it is for us to conform the T function so obtained, that is from UIP, to the conventions we follow for the temperature function. Thus the concern spelled out by Muschik [28] that the traditional inaccessibility principle of Carathéodory does not cover the states with negative temperatures is non-existent with UIP.

7. Concluding remarks

This presentation was aimed at the elucidation of UIP and to surface out the hidden use of it, which exists in the appropriate versions in various irreversible thermodynamic descriptions. It was felt advantageous to present this discussion in the manner of a gradual development of UIP and its application tracing the same right from the earliest nonequilibrium thermodynamic descriptions up to the present level. However, we have restricted ourselves only to the De Donderian thermodynamic description of chemical reactions at finite rates and CIT and we found that it is adequate enough to reveal the basis and the essential contents of UIP. In doing so we have proposed that the UIP based local thermodynamic temperature at ease can be coincided with the experimentally measured local temperature, of a nonequilibrium system, on the Kelvin scale and thereby the corresponding entropy function is obtained with the same footing as the equilibrium based entropy function albeit the former pertains to a nonequilibrium state. In passing we deduced that the reversible adiabatic transitions of chemically reactive closed systems remain perfectly isentropic even if the chemical composition within the system changes on account of concomitant internal chemical conversion. Further, it also gets revealed that the UIP does cover in its fold the nonequilibrium states of negative temperatures. Moreover, through UIP we also arrive at the reversible paths through the succession of NSS and thus confirm the earlier proposal of Keizer [16–20] in a most general setting.

We have shown above that the Carathéodory principle is indeed a particular case of UIP which demonstrates the self-consistency of the latter. However, details of the correspondence between the two and related discussion is the subject matter of one of our forthcoming communications. Of course, Carathéodory's principle is the most economic statement of the second law of thermodynamics and in this respect nothing can surpass it but then it is also true that it is not capable of revealing all the details of the nonequilibrium behaviour of thermodynamic systems nor the entropy function for a nonequilibrium state can be generated through it. Thus the sacrificing of the said

The author is indebted to L S García-Colín for his constructive and valuable criticism during the entire period of this work which also helped in improving its presentation. The financial support from CONACyT is gratefuly acknowledged.

References

[1] A A Bhalekar, *J. Math. Chem.* **5**, 187 (1990)

[2] A A Bhalekar, Proc. International Symposium ECOS'92, *Am. Soc. Mech. Eng.* 121 (1992)

[3] A A Bhalekar, Clausius' Inequality Basis of Generalized Phenomenological Irreversible Thermodynamic Theory (GPITT), *J. Non-Equilib. Thermodyn.* (submitted)

[4] A A Bhalekar, Does Clausius' Inequality Analogue Exist for Open Systems?. *J. Non-Equilib. Thermodyn.* **21**, 330 (1996)

[5] L S García-Colín and A A Bhalekar, Recent Trends in Irreversible Thermodynamics, *Proc. Pakistan Acad. Sci.* (in press)

[6] A A Bhalekar and L S García-Colín, On the Construction of an Extended Thermodynamic Framework for Irreversible Processes, *Pramana–J. Phys.* **50**, 295 (1998)

[7] I Prigogine, *Introduction to Thermodynamics of Irreversible Processes* (Wiley-Interscience, New York, 1967)

[8] S R de Groot and P Mazur, *Non-Equilibrium Thermodynamics* (North-Holland, Amsterdam, 1962)

[9] D D Fitts, *Non-Equilibrium Thermodynamics* (McGraw-Hill, New York, 1962)

[10] I Gyarmati, *Non-Equilibrium Thermodynamics* (Springer-Verlag, Berlin, 1970)

[11] R Hasse, *Thermodynamics of Irreversible Processes* (Addison-Wesley, Reading, Ma., 1969)

[12] D Jou, J Casas-Vázquez and G Lebon, *Extended Irreversible Thermodynamics* (Springer-Verlag, Berlin, 1993; 1996)

[13] B C Eu, *Kinetic Theory and Irreversible Thermodynamics* (John Wiley, New York, 1992)

[14] I Müller and T Ruggeri, *Extended Thermodynamics* (Springer-Verlag, Berlin, 1993)

[15] P Salamon and S Sieniutycz (eds), *Extended Thermodynamic Systems* (Taylor and Francis, New York, 1992)

[16] J Keizer, *Statistical Thermodynamics of Nonequilibrium Processes* (Springer-Verlag, Berlin, 1987)

[17] J Keizer, *J. Chem. Phys.* **65**, 4431 (1976)

[18] J Keizer, *Phys. Rev.* **A30**, 1115 (1984)

[19] J Keizer, *J. Chem. Phys.* **82**, 2751 (1985)

[20] J Keizer, *Acc. Chem. Res.* **12**, 243 (1979)

[21] W Muschik, *Aspects of Non-Equilibrium Thermodynamics* (World Scientific, London, 1990)

[22] S M Blinder, *Advanced Physical Chemistry* (Macmillan, Toronto, 1969)

[23] D D Joseph and L Preziosi, *Rev. Mod. Phys.* **61**, 41 (1989); **62**, 375 (1990)

[24] A A Bhalekar (unpublished result)

[25] I Prigogine and R Defay, *Chemical Thermodynamics* (Longman Green, London, 1954) D H Everett (transl.)

[26] L S García-Colín, in *Recent Developments in Non-Equilibrium Thermodynamics* edited by G Lebon, D Jou and J Casas-Vázquez, *Lecture Notes in Physics*, No. 199 (Springer-Verlag, Berlin, 1984) p. 144

[27] C Carathéodory, *Math. Ann.* **67**, 355 (1909)

[28] W Muschik, *J. Phys. Chem. Solids* **49**, 709 (1988)

On the construction of an extended thermodynamic framework for irreversible processes

ANIL A BHALEKAR*,† and LEOPOLDO S GARCÍA-COLÍN†,§
* Department of Chemistry, Nagpur University, Amravati Road, Nagpur 440010, India
† Departamento de Física, Universidad Autónoma Metropolitana-Iztapalapa, Apdo. Postal 55-534, México D.F. 09340, México
§ Aslo at El Colegio Nacional, Luis González Obregón No. 23, México D.F. 06020, México

MS received 26 July 1996

Abstract. It is shown that the practice in extended irreversible thermodynamics of raising the physical fluxes, such as **q**, the heat flux density, etc. to the status of independent thermodynamic variables does not meet the basic thermodynamic requirements nor in a real situation by keeping them constant one can vary the other thermodynamic independent variables. To elucidate this point the phenomena of rigid body heat conduction is used as an illustrative example. It is argued that the thermometric temperature of systems whether in equilibrium or in nonequilibrium is the same physical entity.

Keywords. Irreversible thermodynamics; heat conduction; thermodynamics; thermodynamic processes; thermodynamic properties and entropy.

PACS Nos 05.70; 44.10; 44.60; 65.50

1. Introduction

The recent decades have witnessed the evolution of extended irreversible thermodynamics (EIT) [1–7]. It is claimed by the proponents of EIT that the classical irreversible thermodynamics (CIT) of Onsager–Prigogine–Meixner–de Groot [8–13] is not adequate enough to encompass all nonequilibrium thermodynamic situations. From the monographs and review articles on EIT [1–7] one gathers a long list of phenomena suggested as not falling within the fold of CIT. A preliminary as well as a striking example quoted is that of temperature waves. A simple mathematical description of the wave propagation of heat is the Maxwell–Cattaneo–Vernotte (MCV) equation [14], namely

$$\mathbf{q} = -\tau \frac{\partial \mathbf{q}}{\partial t} - \lambda \nabla T, \tag{1}$$

where **q** is the heat flux density, τ is the relaxation time, λ is the coefficient of thermal conduction, T is the temperature and t is time. Notice that the MCV equation is a constitutive equation and not a thermodynamic one. However, in EIT a thermodynamic derivation of it is presented and then it is claimed as a justification of the used thermodynamic framework. This approach of EIT shakes its very thermodynamic basis.

equilibrium or nonequilibrium states and corresponding processes. Indeed, it is not at all a business of thermodynamics to derive a constitutive equation [15–17], it simply takes the latter as it is given and presents the corresponding thermodynamic deductions. For example, thermodynamics cannot derive the ideal gas and van der Waal equations, they are taken in thermodynamics as they read. Yet another question one needs to ask is can a given constitutive equation lead us in constructing a suitable thermodynamic framework? The answer is yes and no. Yes, if the corresponding constitutive theory unambiguously establishes some additional fundamental interactions otherwise the answer is a clear no. In spite of this, for example for the phenomena of heat conduction EIT projects a picture that the MCV equation demands an extended thermodynamic framework whereas the Fourier law, namely

$$\mathbf{q} = -\lambda \nabla T \tag{2}$$

is consistent with CIT. The latter is also referred to as linear irreversible thermodynamics (LIT) because it is believed that the linear relationships between fluxes and forces such as eq. (2) are implied therein. This projection of EIT is an unfortunate situation in which thermodynamics remains guided by the individual constitutive equations and hence thermodynamics looses its fragrance of generality.

Therefore, in this presentation we clarify this fundamental thermodynamic aspect by first considering some of the relevant features of the rigid body heat conduction followed by a generalized discussion using the framework of generalized phenomenological irreversible thermodynamic theory (GPITT) [18–22] which is a recent addition to the thermodynamic literature. The reason for the choice of the GPITT framework lies in the fact that in GPITT an extended Gibbs relation is derived (not proposed) using the laws of thermodynamics and hence it has specific thermodynamic requirements [20, 21]. In view of this it is now expedient to analyse if the physical fluxes such as heat flux density etc. are taken as additional independent thermodynamic variables, as is the practice in EIT, whether the resultant thermodynamic structure would meet the thermodynamic requirements or not. Earlier García–Colín *et al* [23] on the basis of kinetic theory concluded that the physical fluxes are irrelevant for constructing an extended thermodynamic framework. This presentation also deduce the same albeit on a generalized footing. Then, we proceed to describe some of the existing inconsistencies in most of the versions of EIT in order to shed some light on the existing mix-ups in them. Finally, we clarify that the experimentally measured temperature of a system in nonequilibrium is not a different physical entity than that of an equilibrium system. This presentation at its certain parts takes up some elementary level discussions too but for the sake of maintaining a clarity of thoughts.

2. Some relevant features of rigid body heat conduction

Consider a single component heat conducting rigid bar of uniform cross-section placed between two heat reservoirs of temperature $T_{\mathrm{l}}(t)$ and $T_{\mathrm{r}}(t)$. The subscripts l and r stands for left and right respectively. Let us assume that $T_{\mathrm{l}}(t) > T_{\mathrm{r}}(t)$. In this case we have the ere u is the internal energy and ρ is the mass density. Now $T_\mathrm{l}(t)$ and $T_\mathrm{r}(t)$ are mani-ated in such a way that at every position x of the bar the div$\mathbf{q}$ is time independent that we have,

$$-\operatorname{div}\mathbf{q} = \text{const.} \tag{4}$$

:ice that $\mathbf{q}$ will be position and time dependent and const. in general will be position endent along the length of the bar. However, in view of (4), eq. (3) gives the following ily of solutions,

$$\Delta u = \text{ const. } \Delta t. \tag{5}$$

: value of the const. of eq. (5) at a given position will of course depend also on the ditions imposed by the heat reservoirs.

rom eq. (5) we see that at a given position the same lapses of time bring about the ne amount of change in internal energy irrespective of the change in the value of $\mathbf{q}$ at : position with time. Thus the existence of a heat flux does not influence the internal rgy but its divergence does. It is understandable because the divergence quantifies the rejection or retention of energy.

f const. $= 0$ then the bar attains a steady state condition. $\mathbf{q}$ becomes position and time ependent and u becomes time independent but remains position dependent. Again the ue of u is obtained as position dependent in spite of the same value of $\mathbf{q}$ at all positions. his condition too the mere existence of $\mathbf{q}$ does not influence u. However, the stationary es can be achieved for a series of different values of $\mathbf{q}$ by suitably manipulating T_l and Accordingly, at a given position the value of u will be different for different values of hrough $\operatorname{div}\mathbf{q} = 0$ in different set-ups.

Thus on the one hand we see that $\mathbf{q}$ does not determine the value of u and on the other id by keeping say $\mathbf{q}$ constant u cannot be varied at a given position neither in a steady e nor when $\operatorname{div}\mathbf{q} \neq 0$. Moreover, when $\mathbf{q}$ is allowed to relax to a value of zero or to a ady state value u does not remain constant. Thus even in this extremely fast process : relaxation time, $\tau \sim 10^{-12}$ s [1]) u and $\mathbf{q}$ do not vary independent of each other. This icates that the mere presence of $\mathbf{q}$ cannot be taken as influencing the thermodynamic :e of a system.

General considerations based on GPITT

ITT constructs its framework by using zeroth, first and second laws of rmodynamics and hence it has a sound thermodynamic basis [20, 21]. In contrast h EIT, GPITT is not aimed at the augmentation of LIT. GPITT yields a most general cription and from which LIT is obtained as a limiting case. One of the important elations of GPITT is that the Gibbs relation or an extended Gibbs relation becomes a rmodynamic description only by the virtue of the validity of the corresponding Gibbs–hem equations (GDE). That is, the crucial rôle of GDE is to confine our description ll within the thermodynamic domain.

$$\frac{\mathrm{d}s}{\mathrm{d}t} = \frac{1}{T}\frac{\mathrm{d}u}{\mathrm{d}t} + \frac{p}{T}\frac{\mathrm{d}v}{\mathrm{d}t} - \sum_k \frac{\mu_k}{T}\frac{\mathrm{d}c_k}{\mathrm{d}t} + \frac{1}{T}\sum_j \beta_j \odot \frac{\mathrm{d}\alpha_j}{\mathrm{d}t}, \tag{6}$$

where s is the per unit mass entropy, T is the local thermometric temperature, u is the per unit mass internal energy, p is local pressure, v is the specific volume, μ_k is the chemical potential per unit mass of the component k, c_k is the mass fraction of the component k, β_j and α_j are the additional irreversibility parameters intensive and extensive respectively and $\odot$ denotes the general scalar product. All the thermodynamic functions of the above equation are position ($\mathbf{r}$) and time (t) dependent and for the sake of brevity we are not showing this dependence in the major part of this presentation. The derivation of eq. (6) involves the following standard fluid-dynamical equations, namely:

$$\rho\frac{\mathrm{d}u}{\mathrm{d}t} = -\operatorname{div}\mathbf{q} - p\rho\frac{\mathrm{d}v}{\mathrm{d}t} + \Pi : \nabla\mathbf{u}, \tag{7}$$

$$\rho\frac{\mathrm{d}c_k}{\mathrm{d}t} = -\operatorname{div}\mathbf{J}_k + \rho M_k \nu_k \frac{\mathrm{d}\xi}{\mathrm{d}t}, \tag{8}$$

where $\mathbf{q}$ is the so-called heat flux density, $\mathbf{J}_k$ is the matter diffusion flux density of the component k, Π is the dissipative stress tensor, $\mathbf{u}$ is the barycentric velocity vector, M_k is the molar mass number, ρ is the mass density and ξ is the extent of chemical reaction.

When u, v and c_k become time independent then according to eqs (7) and (8) $\mathbf{q}$, Π, $\nabla\mathbf{u}$, $\mathbf{J}_k$, ξ and p too become time independent and hence with respect to the three fundamental interactions, namely thermal, mechanical and those causing the changes in chemical composition, the system gets relegated to a stationary state. However, in this situation eq. (6) reads as

$$\frac{\mathrm{d}s}{\mathrm{d}t} = \frac{1}{T}\sum_j \beta_j \odot \frac{\mathrm{d}\alpha_j}{\mathrm{d}t}. \tag{9}$$

Equation (9) describes that in the stationary state as determinable through eqs (7) and (8) the entropy of the system may still vary provided $\alpha_j s(\beta_j s)$ remain time dependent. But the constancy of the above stated three fundamental interactions in a stationary state described through eqs (7) and (8) implies that α_j and β_j parameters must describe other than these three fundamental interactions which in GPITT are termed as *additional nonequilibrium interactions* [20–22]. This explains why in GPITT α_j and β_j parameters are termed as additional irreversibility parameters. However, at present nothing is known about the so-called additional nonequilibrium interactions. In view of the above neither the physical fluxes, namely $\mathbf{q}$, Π, $\mathbf{J}_k$ etc. nor the physical forces, namely ∇T, $\nabla\mathbf{u}$, $\nabla(\mu_k/T)$, etc. can be taken as α_j and/or β_j variables. This assertion we further elaborate below by taking the case of rigid body heat conduction.

Now again consider a single component heat conducting rigid bar of uniform cross-section. For the time being pretend that the heat conduction process can generate the so-called additional nonequilibrium interactions and for this purpose at least one pair of α and β parameters would be required. In this case eq. (6) reduces to

$$\mathrm{d}s \quad T^{-1}\,\mathrm{d}u \quad T^{-1}\beta\odot\,\mathrm{d}\alpha$$

$$s = s(u, \alpha) = s(u(x,t), \alpha(x,t)) \tag{11}$$

and hence

$$u = u(s, \alpha) = u(s(x,t), \alpha(x,t)), \tag{12}$$

where x is the position coordinate along the length of the bar. We can as usual replace s by T in eq. (12) which gives

$$u = u(T, \alpha) = u(T(x,t), \alpha(x,t)). \tag{13}$$

In view of eq. (13) the total differential of u reads as

$$\frac{\mathrm{d}u}{\mathrm{d}t} = c_v \frac{\mathrm{d}T}{\mathrm{d}t} + \frac{\partial u}{\partial \alpha} \odot \frac{\mathrm{d}\alpha}{\mathrm{d}t}, \tag{14}$$

where c_v is the so-called heat capacity defined in this extended thermodynamic framework as

$$c_v = \left(\frac{\partial u}{\partial T}\right)_{v,\alpha}. \tag{15}$$

According to eq. (3) in the case of a steady state heat conduction, that is $\mathbf{q}$ time independent and $\operatorname{div} \mathbf{q} = 0, u$ too becomes time independent. However, in the case of steady state heat conduction our observations tell that $T(x)$ also remain time independent and hence eq. (14) makes $\alpha(x)$ too a time independent parameter. Thus we conclude that T and α *cannot* be taken as mutually independent variables if these two parameters are considered as concerned with the phenomenon of heat conduction. Hence in the case of a rigid body heat conduction α and β variables are redundant. The necessity of α and β variables could be felt only when we also have other than the heat conduction process. This then clearly establishes that the heat flux $\mathbf{q}$ *cannot* serve as α variable in eqs (10) and (14). Therefore, for the case under consideration the appropriate equations, instead of eqs (10) and (14) are

$$\frac{\mathrm{d}s}{\mathrm{d}t} = T^{-1} \frac{\mathrm{d}u}{\mathrm{d}t}, \tag{16}$$

$$\frac{\mathrm{d}u}{\mathrm{d}t} = c_v \frac{\mathrm{d}T}{\mathrm{d}t}. \tag{17}$$

Now c_v of eq. (17) has the standard definition, namely,

$$c_v = \left(\frac{\partial u}{\partial T}\right)_v \tag{18}$$

instead of the definition of eq. (15). Thus in general eq. (I7) rigorously gives

$$u = u(T) = u(T(x,t)) \tag{19}$$

and hence from eq. (16) we have,

parameter, namely, the local temperature T, which is none else than the local thermometric temperature.

4. Some of the incoherencies in EIT

We point out herein two inconsistencies existing in EIT while it describes the phenomena of rigid body heat conduction. The first inconsistency is as follows. The EIT expression in the present case is [1–7]

$$\mathrm{d}\eta = \theta^{-1}\mathrm{d}u - \theta^{-1}\alpha \cdot \mathrm{d}\mathbf{q}, \tag{21}$$

where η is said to be the nonequilibrium entropy, θ is the nonequilibrium thermodynamic temperature and is claimed to be different than the experimentally measured temperature T in the same nonequilibrium situation [1–4] and α is a parameter conjugate to the variable $\mathbf{q}$. Equation (21) gives

$$\eta = \eta(u, \mathbf{q}), \tag{22}$$

that is η is considered as dependent on two independent variables. This then implies that u too becomes dependent on two independent variables say as $u = u(\eta, \mathbf{q})$ which may be expressed as $u = u(T, \mathbf{q})$. Hence, the total differential of u should read as

$$\frac{\mathrm{d}u}{\mathrm{d}t} = \frac{\partial u}{\partial T}\frac{\mathrm{d}T}{\mathrm{d}t} + \frac{\partial u}{\partial \mathbf{q}} \cdot \frac{\mathrm{d}\mathbf{q}}{\mathrm{d}t}. \tag{23}$$

But in this connection in EIT eq. (3) is manipulated as [1–7]

$$\rho c_v \frac{\mathrm{d}T}{\mathrm{d}t} = -\operatorname{div}\mathbf{q}. \tag{24}$$

This means the function u and hence eq. (3) is not treated in the extended thermodynamic framework but for the η function eq. (21) is used. Thus what one is leading to is a mixture of unconnected mathematical descriptions which is not of a hybrid type though the latter if obtained cannot be termed as thermodynamic one. Strictly speaking one should use $u = u(\theta, \mathbf{q})$ instead of $u = u(T, \mathbf{q})$ but then eq. (24) would not be a direct result apart from the missing term corresponding to the variable $\mathbf{q}$. However, this does not lead us any where.

Secondly, there prevails another incoherence in the use of eq. (3) in EIT [1–7]. It is rightly argued that u, the internal energy, can remain time independent provided $\operatorname{div}\mathbf{q}$ is maintained effectively equal to zero. But it is not at all true that in general for a given set of different values of $\mathbf{q}$ there could be identically same constant value of u in the event of $\operatorname{div}\mathbf{q} = 0$. Equation $\rho\mathrm{d}u/\mathrm{d}t = \operatorname{div}\mathbf{q} = 0$ gives a family of solutions of constant internal energy, namely,

$$u = u(T) = u(T(x)) = \text{const.} \tag{25}$$

and not a single solution of constant internal energy. Let us elaborate it a little further.

Once again consider a single component rigid bar of uniform cross section placed

$$U = \int_0^L u(x)\mathrm{d}x = \int_{T_\mathrm{l}}^{T_\mathrm{r}} u(x(T))\,\frac{\partial x}{\partial T}\,\mathrm{d}T, \tag{26}$$

where $u(x)$ is the internal energy per unit length of the bar at the position x. Now let us change T_l and T_r to T'_l and T'_r ($T'_\mathrm{l} > T'_\mathrm{r}$). In this new situation and under the corresponding condition of steady state heat conduction we have

$$U' = \int_0^L u'(x)\mathrm{d}x = \int_{T'_\mathrm{l}}^{T'_\mathrm{r}} u'(x(T'))\,\frac{\partial x}{\partial T'}\,\mathrm{d}T'. \tag{27}$$

Obviously the temperature profile along the length of the bar will not be identically same in the two cases and hence $U \neq U'$ implying $u(x) \neq u'(x)$. Notice that in both the situations we rigorously have $\operatorname{div}\mathbf{q} = 0 = \operatorname{div}\mathbf{q}$ at all the positions along the length of the bar but in general $\mathbf{q}' \neq \mathbf{q}$. This remains true even if the respective Ts are infinitesimally away from T's. In this latter limit eqs (26) and (27) gives

$$\delta U = U' - U = \int_0^L [u'(x) - u(x)]\mathrm{d}x = \int_0^L \delta u(x)\mathrm{d}x, \tag{28}$$

where $\delta u(x)$ and δU represent the corresponding differences between the values of internal energy for the two set-ups. It is easy to realize that δU and $\delta u(x)$ can only be zero when,

$$u'(x(T')) = u(x(T)) \tag{29}$$

which can be true only if $T(x) = T'(x)$. Alternatively, if c_v of the bar is assumed as fairly constant then eq. (28) reads as

$$\delta U = c_v \int_0^L \delta T(x)\mathrm{d}x, \tag{30}$$

where $\delta T(x) = T'(x) - T(x)$. Equation (30) clearly shows that δU becomes zero only when $T'(x) = T(x)$.

Moreover, the preceding deductions remain true irrespective of $\nabla T' = T'_\mathrm{r} - T'_\mathrm{l} = T_\mathrm{l} - T_\mathrm{r} = \nabla T$ or not. In the case of $\nabla T \neq \nabla T'$ in general we have unequal values of the steady heat flux. Since in the case of a steady heat conduction $\mathbf{q}$ becomes position independent (that is throughout the length of the bar we have the same value of $\mathbf{q}$) but since T remains position dependent makes u too a position dependent quantity. The above discussion clearly demonstrates that u is determined only by T and not by $\mathbf{q}$. The latter quantity influences u via $\operatorname{div}\mathbf{q}$, that is by the net retention or rejection of energy. In the case of a finite but rapid change of Ts to T's and before a new steady state is reached we have $T(x,t)$, $\nabla T(x,t)$ and $\mathbf{q}(x,t)$. During this spontaneous attainment of the corresponding new steady state we still have $u(x,t) = u(T(x,t))$ and $(\mathrm{d}u/\mathrm{d}t)(x,t)$ is determined by the instantaneous value of $-\operatorname{div}\mathbf{q}(x,t)$ according to eq. (3) even if $\mathbf{q}(x,t)$ might be determined by say MCV equation, eq. (1). When MCV equation operates there are two

$$\rho\,\frac{\partial u}{\partial t}=\tau\frac{\partial}{\partial \mathbf{x}}\cdot\frac{\partial \mathbf{q}}{\partial t}+\lambda\,\frac{\partial^2 T}{\partial x^2}\,. \tag{31}$$

Notice that for the sake of simplicity τ and λ have been assumed constant of the operator $\partial/\partial\mathbf{x}$. Further, on once more using eq. (3), eq. (31) gives

$$\tau\rho\,\frac{\partial^2 u}{\partial t^2}+\rho\frac{\partial u}{\partial t}-\lambda\,\frac{\partial^2 T}{\partial x^2}=0. \tag{32}$$

Notice that eq. (32) clearly shows the T dependence of u. Of course, on substituting (17) into (32) produces the well known hyperbolic equation of the telegraphist type, namely,

$$\tau\,\frac{\partial^2 T}{\partial t^2}+\frac{\partial T}{\partial t}-\chi\nabla^2 T=0, \tag{33}$$

where $\chi=\lambda/\rho c_v$ is the thermal diffusivity. This derivation of eq. (33) uses (17) in the last step and hence in this respect this derivation is different than the one generally followed in the literature in which eq. (32) gets skipped over. Recall that in deriving eq. (33) one uses (17) which is a companion to the Gibbs relation, eq. (16), and not to the extended Gibbs relation, eq. (10). That is eq. (33) is a description within the traditional Gibbs relation domain and not in the domain of an extended Gibbs relation. Hence we conclude that eq. (33) is not connected at all with the proposed extended Gibbs relation, eq. (21) of EIT.

5. Systems in nonequilibrium and temperature

This discussion will be incomplete if we do not clarify that what one is describing by T when a system is not in equilibrium. In EIT [1–7] in particular and in thermodynamic discussions [17,24,25] in general, there exist conflicting claims about the concept of temperature for systems in nonequilibrium states. The views expressed are based on both macroscopic and microscopic considerations. However, herein we are restricting ourselves to the macroscopic considerations only because thermodynamics operates at this level. As said above θ of eq. (21) is not believed in EIT as the same physical entity as T for an equilibrium case. For example from eq. (21) a so-called thermodynamic definition of nonequilibrium temperature follows as $\theta^{-1}=(\partial\eta/\partial u)_{\mathbf{q},v}$. At other places the symbol Θ is used and is referred to as the contact temperature [24–27] and is described as the temperature of that heat reservoir which when brought in contact with the local nonequilibrium tiny system does not produce a heat flux. In view of these two divergent stands it becomes expedient to reexamine and understand the very basis of the experimentally measured temperatures.

Recall that when one measures temperature it is required in principle that this act should not significantly alter the state of the system (or precisely that of the local pocket of the system in contact with the measuring device). For example, when a thermometer is inserted in a system in equilibrium the immediate reaction is that a finite heat flux is generated across the boundary of the thermometer in case the temperature of the latter

The quantity of energy utilized by the thermometer is insignificantly small so that the state of the system remains practically unaltered. Now carefully scrutinize this experiment and enquire when a steady reading on the thermometer scale will be registered. The answer is when the thermometric fluid stops the net acceptance (or rejection) of the energy from its immediate surroundings. That is when the internal energy of the thermometric fluid becomes steady. From eq. (3) the sufficient and necessary requirement for this is that the divergence of the heat flux within the thermometric fluid vanishes. Notice that the vanishing of the divergence of the heat flux does not demand the vanishing of the heat flux itself. However, it is the consequence of the equilibrium state of the system, which had no heat flux before the insertion of the thermometer, that simultaneously the heat flux within the thermometric fluid dies out.

Now consider a system in nonequilibrium which at a given time and position has a finite value of heat flux. In this case too when a thermometer is inserted at a given position of the system the value of the heat flux at that position gets immediately altered by a significant amount. But after the passage of a very short period of time the thermometer shows a steady reading and the said position of the system practically regains its initial state. This happens due to the vanishing of the divergence of the heat flux within the thermometric fluid and not because of the dying out of the heat flux itself. If the latter would have been the case it would be at the expense of altering the state of the system. Thus we conclude that the *primary* requirement which is fulfilled by the temperature measurements is the vanishing of the divergence of the heat flux within the thermometric fluid. Hence, whether a system is in equilibrium or not the temperature measurements give us the identically same physical entity. Therefore, there is no such thing like nonequilibrium temperature (the adjective nonequilibrium applies only to a system and not to its state parameters) neither one is required to evoke a concept of contact temperature with the help of a hypothetical set of heat reservoirs. Since the definition of the contact temperature involves the condition of no heat flux then this cannot be achieved without altering the internal energy at the given nonequilibrium position of a system. Thus the contact temperature so obtained corresponds to a different state of the system and hence it is no wonder that this so-called contact temperature is obtained as independent of the internal energy of the tiny pocket under investigation [24, 26]. That is, the contact temperature is not related at all to the given state of the system and hence is a hypothetical entity irrelavant for thermodynamic descriptions. It may be useful for a constitutive theory and hence for dynamics but this fact, in any way, should not dictate thermodynamics and its basic framework which is governed solely by the laws of thermodynamics.

From the above discussion we establish that there is no distinction between the physical meaning of the temperature of an equilibrium and that of a nonequilibrium state of a system because the mechanism of registering temperature does not differ in the two cases. Indeed in a nonequilibrium state of a system there is a spatial temperature field while in the case of equilibrium the temperature is uniform throughout. The next obvious query is about the shortness of the time required for the dying out of the divergence of the heat flux within the thermometric fluid. This is determined by the corresponding of the above deductions we need to note that in practice one invariably measures temperatures in a wide variety of nonequilibrium situations right from the industrial setups, laboratory experimentations to the biological systems. Hence to say that there is no well defined temperature in nonequilibrium tantamounts to shun our minds from the stark realities.

6. Concluding remarks

From the above discussion we see that **q** cannot assume the role of the α variable in eq. (14) and hence s cannot have **q** as an independent variable. Thus we once more conclude that the physical fluxes such as **q** etc. or the physical forces ∇T etc. cannot serve as independent thermodynamic variables to construct an extended thermodynamic framework for describing certain irreversible processes which are (believed) not covered by the traditional Gibbs relation, namely,

$$\frac{\mathrm{d}s}{\mathrm{d}t} = \frac{1}{T}\frac{\mathrm{d}u}{\mathrm{d}t} + \frac{p}{T}\frac{\mathrm{d}v}{\mathrm{d}t} - \sum_k \frac{\mu_k}{T}\frac{\mathrm{d}c_k}{\mathrm{d}t}. \tag{34}$$

The additional thermodynamic variables, as said above in §3, must find their origin in the additional nonequilibrium interactions not related with the three fundamental interactions namely thermal, mechanical (which includes both the short and long range interactions) and which cause the changes in chemical composition. The same conclusion, that is the heat flux etc. are not suitable to act as additional independent thermodynamic variables, has been earlier arrived at by us [20] on considering the dictates of the Gibbs–Duhem equation corresponding to eq. (6), the extended Gibbs relation of GPITT and also on the basis of the requirements of the Pfaffian exact differential form for the entropy function and by García-Colín *et al* [23] on the basis of kinetic theory. However, if one uses **q** etc. as independent variables then it amounts to tampering with the concept of entropy based on thermodynamic laws. That is then one is not talking about the Clausius entropy and hence not working within the domain of thermodynamics.

Also we have seen above that an irreversible thermodynamic description contains in it the local thermometric temperature corresponding to a given nonequilibrium situation and none else. Of course, one is free to coincide it with the temperature on the Kelvin scale as one does in the case of equilibrium. The mechanism of registering temperatures involves the vanishing of the divergence of the heat flux within the tiny volume of the measuring device in contact with the local tiny pocket of the system and hence one measures the identically same entity as temperature in equilibrium as well as in nonequilibrium situations.

Acknowledgements

The authors are thankful to R M Velasco for reading the manuscript. One of the authors

[1] D Jou, J Casas-Vázquez and G Lebon, *Extended Irreversible Thermodynamics* (Springer-Verlag, Berlin, 1993; 1996)

[2] B C Eu, *Kinetic Theory and Irreversible Thermodynamics* (John Wiley, New York, 1992)

[3] P Salamon and S Sieniutycz (eds), *Extended Thermodynamic Systems* (Taylor and Francis, New York, 1992)

[4] I Müller and T Ruggeri, *Extended Thermodynamics* (Springer-Verlag, Berlin, 1993)

[5] L S García-Colín, *Rev. Fís. Mex.* **34**, 344 (1988)

[6] D Jou, J Casas-Vázquez and G Lebon, *Rep. Prog. Phys.* **51**, 1104 (1988)

[7] L S García-Colín and F Uribe, *J. Non-Equilib. Thermodyn.* **16**, 89 (1991)

[8] I Prigogine, *Introduction to Thermodynamics of Irreversible Processes* (Wiley-Interscience, New York, 1967)

[9] S R de Groot and P Mazur, *Non-Equilibrium Thermodynamics* (North-Holland, Amsterdam, 1962)

[10] R Haase, *Thermodynamics of Irreversible Processes* (Addison-Wesley, Reading, Ma., 1969)

[11] I Gyarmati, *Non-Equilibrium Thermodynamics* (Springer-Verlag, Berlin, 1970)

[12] D D Fitts, *Non-Equilibrium Thermodynamics* (McGraw-Hills, New York, 1962)

[13] K G Denbigh, *The Thermodynamics of the Steady State* (Wiley, New York, 1950)

[14] D D Joseph and L Preziosi, *Rev. Mod. Phys.* **61**, 41 (1989); **62**, 375 (1990)

[15] P W Bridgeman, *The Nature of Thermodynamics* (Peter Smith, Gloucester, Ma., 1969)

[16] E Kröner, *J. Non-Equilib. Thermodyn.* **11**, 277 (1986)

[17] J J Delgado Domingos, M N R Nina and J H Whitelaw (eds), *Foundations of Continuum Thermodynamics* (Macmillan, London, 1974)

[18] A A Bhalekar, *J. Math. Chem.* **5**, 187 (1990)

[19] A A Bhalekar, Proceedings of International Symposium ECOS'92, *Am. Soc. Mech. Eng.* 121 (1992)

[20] L S García-Colín and A A Bhalekar, Recent Trends in Irreversible Thermodynamics, *Proc. Pakistan Acad. Sci.* (in press)

[21] A A Bhalekar, Clausius' Inequality Basis of Generalized Phenomenological Irreversible Thermodynamic Theory (GPITT), *J. Non-Equilib. Thermodyn.* (submitted)

[22] A A Bhalekar, Does Clausius' Inequality Analogue Exists for Open System? *J. Non-Equilib. Thermodyn.* **21** 330 (1996)

[23] R M Velasco and L S García-Colín, *J. Stat. Phys.* **69**, 217 (1992)

[24] W Muschik, *Aspects of Non-Equilibrium Thermodynamics* (World Scientific, Singapore, 1990)

[25] J Kestin, *J. Non-Equilib. Thermodyn.* **15**, 193 (1990)

[26] W Muschik, *J. Non-Equilib. Thermodyn.* **4**, 277 (1979)

[27] W Muschik and G Brunk, *Int. J. Eng. Sci.* **15**, 377 (1977)

PRAMANA
—journal of
physics

© Printed in India

Vol. 50, No. 4,
April 1998
pp. 307–314

Schwarzschild black hole with global monopole charge

NARESH DADHICH, K NARAYAN* and U A YAJNIK*
Inter-University Centre for Astronomy and Astrophysics, Post Bag 4, Ganeshkhind, Pune 411 007, India
*Department of Physics, Indian Institute of Technology, Mumbai 400 076, India
E-mail: nkd@iucaa.ernet.in; narayan@tristan.TN.CORNELL.EDU;
yajnik@niharika.phy.iitb.ernet.in

MS received 2 September 1997

Abstract. We derive the metric for a Schwarzschild black hole with global monopole charge by relaxing asymptotic flatness of the Schwarzschild field. We then study the effect of global monopole charge on particle orbits and the Hawking radiation. It turns out that existence, boundedness and stability of circular orbits scale up by $(1-8\pi\eta^2)^{-1}$, and the perihelion shift and the light bending by $(1-8\pi\eta^2)^{-3/2}$, while the Hawking temperature scales down by $(1-8\pi\eta^2)^2$ the Schwarzschild values. Here η is the global charge.

Keywords. Black hole; Schwarzschild solution; global monopole; Hawking radiation; particle orbits; topological defect.

PACS Nos 04.20; 14.80; 04.50

1. Introduction

The Schwarzschild solution is the unique spherically symmetric solution of the vacuum Einstein equation. It represents a static black hole. It turns out [1] that a global monopole charge accompanies spontaneous breaking of global $0(3)$ symmetry into $U(1)$ in phase transitions in the Universe. Putting on global charge to the Schwarzschild black hole will amount to breaking the vacuum and asymptotic flatness of the Schwarzschild spacetime. It still represents a localized object with a horizon. Our main aim in this paper is to study the effect of global monopole charge on particle orbits and the Hawking radiation.

The spacetime of pure global monopole charge, when the Schwarzschild mass vanishes, can be regarded in some sense to be 'minimally' curved for gravitational charge density, $4\pi\rho_c = R_{ik}u^iu^k, u^iu_i = 1$, vanishes. That means the relativistic (active gravitational) mass is zero for the spacetime [2]. All radial trajectories will always remain parallel. Thus introduction of global monopole charge does not significantly alter the nature of the

2. The metric

Let us write the general spherically symmetric metric

$$ds^2 = B dt^2 - A dr^2 - r^2(d\theta^2 + \sin^2\theta d\varphi^2), \tag{2.1}$$

where A and B are functions of r and t.

Now the equations $R_{01} = 0$ and $R^0_0 = R^1_1$ will imply $B = A^{-1} = 1 + 2\phi$, where $\phi = \phi(r)$ [4]. Note that no boundary condition has been used. With this

$$R^0_0 = R^1_1 = -\nabla^2\phi \tag{2.2}$$

and

$$R^2_2 = R^3_3 = -\frac{2}{r^2}(r\phi)', \tag{2.3}$$

where a dash denotes derivative with respect to r. Then $R^0_0 = 0$ gives the good old Laplace equation which has the well-known general solution

$$\phi = k - \frac{M}{r}. \tag{2.4}$$

Now $R^2_2 = 0$ will determine $k = 0$ and we obtain the Schwarzschild solution. Retaining k will make $R^2_2 \neq 0$ and will give rise to stresses,

$$T^0_0 = T^1_1 = -\frac{k}{4\pi r^2}. \tag{2.5}$$

These are precisely the stresses at large r required for a global monopole as we shall see in the next section. Here k will be related to the global monopole charge which produces neither acceleration nor tidal acceleration for radially moving free particles. Note that the gravitational charge density, $4\pi\rho_c = R_{ik}u^i u^k$, continues to remain zero indicated by vanishing of R_{00}.

3. The gravitational field of a global monopole

Several authors [1, 5, 6, and the references therein] have discussed the gravitational field of a global monopole formed by spontaneous symmetry breaking of a triplet of scalar fields with a global symmetry group $O(3)$. The Lagrangian density of the isoscalar triplet ψ^a with $a = 1, 2, 3$ is

$$\mathcal{L} = \frac{1}{2}(\partial\psi^a)^2 - \frac{\lambda}{4}(\psi^a\psi^a - \eta^2)^2. \tag{3.1}$$

Topologically non-trivial self-supporting solutions to this system can be found. The ansatz describing a monopole is

$$\psi^a(\bar{\mathbf{x}}) = \eta f(r)\frac{x^a}{|\bar{\mathbf{x}}|}, \tag{3.2}$$

where

$$x^a x^a = r^2, \tag{3.3}$$

with x^a-meaning the corresponding cartesian component of $\bar{\mathbf{x}}$. Outside the monopole core we must have

$$f(r) \to 1 \text{ as } |\bar{\mathbf{x}}| \to \infty \tag{3.4}$$

for $V(\psi)$ to vanish asymptotically. The vanishing of energy density is however not fast enough because

$$|\nabla\psi|^2 \to \frac{\eta^2}{r^2}. \tag{3.5}$$

The stress tensor of the system outside the core can be approximated as

$$T_0^0 = T_1^1 = \frac{\eta^2}{r^2} \tag{3.6}$$

and the other components vanish. These are precisely the stresses generated (eq. (2.5)) by keeping k in (2.4).

Thus the most general metric for $T_0^0 = T_1^1 \neq 0$ and the remaining stress components being zero is

$$ds^2 = \left(1 + 2k - \frac{2M}{r}\right)dt^2 - \left(1 + 2k - \frac{2M}{r}\right)^{-1} dr^2 - r^2 d\theta^2 - r^2 \sin^2\theta d\phi^2, \tag{3.7}$$

with $k = -4\pi\eta^2$ and M having the usual meaning of mass of the central gravitating object [1]. Here then central mass is that of the monopole which is usually negligible. However if we consider the spherically symmetric gravitational collapse of the matter around such a monopole, we find that a black hole is formed. The parameter M then corresponds to the mass of the black hole.

Even when $M = 0$, this spacetime has non-zero curvature:

$$R_0^0 = R_1^1 = R_{01} = 0 \tag{3.8}$$

but

$$R_2^2 = \frac{8\pi\eta^2}{r^2}. \tag{3.9}$$

That the total energy of such solutions is divergent makes them unrealistic except perhaps as fleeting entities in the course of a cosmic phase transition [1]. The core mass M is nevertheless finite. It is interesting to note that retention of k in (2.4) amounts to giving up asymptotic flatness and that exactly generates the stresses of a global monopole.

A remarkable conclusion that follows from this is that a black hole can possess 'hair' in the form of topological charge. How will this charge be detected? Topologically nontrivial solutions are known to have the peculiar property that their symmetry generators are linear combinations of spacetime symmetries and internal symmetries. In the present case, it would mean that a motion on a sphere of constant radius r has to be

Similar conclusions should follow for topological sectors of higher winding number, except that the spacetime metric will not be in the simple form corresponding to spherical symmetry.

Another interesting manifestation of the topological charge can be obstruction to global definition of the wave function of certain particle species. For example, if the symmetry group is really the spin group $SU(2)$ instead of $O(3)$ (more generally, spin (N) instead of $O(N)$) then an isospinor species χ may exist. Now a 2π space rotation will induce a $2\pi O(3)$ rotation which will change the sign of the wave function which therefore cannot be globally defined.

Note that the fate of the global charge S_z of the $O(3)$ group will be the same as that of any other global charge such as the baryon number.

4. Particle orbits

In this section we wish to investigate the effect of global charge on the particle orbits; existence, boundedness and stability of circular orbits, light deflection and perihelion-shift.

4.1 *Circular orbits*

For the metric (3.7), we have

$$\Delta \dot{t} = E, \quad r^2 \dot{\varphi} = l, \tag{4.1}$$

where $\Delta = 1 + 2k - 2M/r$, $\dot{t} = \mathrm{d}t/\mathrm{d}s$; E and l are specific energy and angular momentum of a test particle. Substituting (4.1) in the metric (we have set $\theta = \pi/2$ as usual),

$$\dot{r}^2 = E^2 - \Delta\left(\frac{l^2}{r^2} + 1\right) = E^2 - V^2. \tag{4.2}$$

For existence of circular orbit, we should have both $\dot{r} = \ddot{r} = 0$. This will give the existence threshold

$$r_e \geq \frac{3M}{1 + 2k}, \tag{4.3}$$

where equality refers to the photon orbit. Of course $l \geq 2\sqrt{3}M/(1 + 2k)$. For boundedness, we should have $E^2 \geq (1 + 2k)$, which leads to

$$r_b \geq \frac{4M}{1 + 2k} \tag{4.4}$$

while stability of circular orbits will further require $V'' \geq 0$, giving

$$r_s \geq \frac{6M}{1 + 2k}. \tag{4.5}$$

Following the standard calculation [7], we write

$$\varphi(r) - \varphi(\infty) = \int_r^\infty \Delta^{-1/2}(r) \left[\left(\frac{r}{r_0}\right)^2 \frac{\Delta(r_0)}{\Delta(r)} - 1 \right]^{-1/2} \frac{\mathrm{d}r}{r}, \tag{4.6}$$

where r_0 is the radius vector of the closest approach to the gravitating body. The deflection angle will be given by

$$\delta\varphi = 2|\varphi(r_0) - \varphi(\infty)| - \frac{\pi}{\sqrt{1+2k}}. \tag{4.7}$$

Note that when $M = 0, \varphi$ has the period $2\pi/\sqrt{1+2k}$ and not 2π, there is a deficit angle similar to the case of cosmic string. From (4.6) and (4.7) we get

$$\delta\varphi = \frac{4M}{r_0(1+2k)^{3/2}} \approx \frac{4M}{r_0}(1 + 12\pi\eta^2). \tag{4.8}$$

4.3 *Perihelion-shift*

Here the corresponding relation [7] is

$$\varphi(r) - \varphi(r_-) = \int_{r_-}^{r} \left[\frac{r_-^2(\Delta^{-1}(r) - \Delta^{-1}(r_-)) - r_+^2(\Delta^{-1}(r) - \Delta^{-1}(r_+))}{r_+^2 r_-^2(\Delta^{-1}(r_+) - \Delta^{-1}(r_-))} - \frac{1}{r^2} \right]^{-1/2} \times \frac{\Delta^{-1/2}}{r^2} \mathrm{d}r, \tag{4.9}$$

where $r_\pm$ refer to aphelion and perihelion points. The perihelion shift is given by

$$\delta\varphi = 2|\varphi(r_+) - \varphi(r_-)| - \frac{2\pi}{\sqrt{1+2k}} \tag{4.10}$$

and we thus obtain

$$\delta\varphi = \frac{6\pi M}{L(1+2k)^3/2} \approx \frac{6\pi M}{L}(1 + 12\pi\eta^2), \tag{4.11}$$

where

$$L = \frac{1}{2}\left(\frac{1}{r_+} + \frac{1}{r_-}\right).$$

Thus effect of global charge is to scale the Schwarzschild values by $(1 - 8\pi\eta^2)^{-1}$ for existence, boundedness and stability thresholds of circular orbits and by $(1 - 8\pi\eta^2)^{-3/2}$ for light deflection and perihelion-shift. It means a slight enhancement in the Schwarzschild values.

5. Semiclassical effects

Next we investigate the question of Hawking radiation in this background metric. Since

Consider the equation satisfied by a massless scalar quantum field ψ

$$\Box\psi = 0. \tag{5.1}$$

The advanced and retarded coordinates for this spacetime are

$$v = t + r^*, \tag{5.2}$$

$$u = t - r^*, \tag{5.3}$$

where r^* is the tortoise coordinate defined in this case as

$$\mathrm{d}r^* = \frac{r\,\mathrm{d}r}{1 + 2k - (2M/r)}. \tag{5.4}$$

The wave equation can be separated in (t, r, θ, φ) coordinates. The mode functions relevant to this spacetime are of the form

$$\frac{R_{\omega l}(r)}{r} Y_{lm}(\theta, \varphi)\mathrm{e}^{-i\omega t}. \tag{5.5}$$

Y_{lm} is a spherical harmonic and $R_{\omega l}$ satisfies the equation

$$\frac{\mathrm{d}^2 R_{\omega l}}{\mathrm{d}r^{*2}} + (\omega^2 - [l(l+1)r^{-2} + 2Mr^{-3}][1 + 2k - 2Mr^{-1}])R_{\omega l} = 0. \tag{5.6}$$

Because of the 'potential' term in square brackets, the standard incoming waves will partially scatter back the gravitational field to become a superposition of incoming and outgoing waves. However, the effective potential vanishes as $r^* \rightarrow \pm\infty$ (i.e. for $r \rightarrow 2M, \infty$). Thus, in those regions the mode functions will be of the form

$$\left(\frac{1}{r}\,\mathrm{e}^{-i\omega u} Y_{lm}\right) \text{ and } \left(\frac{1}{r}\,\mathrm{e}^{-i\omega v} Y_{lm}\right). \tag{5.7}$$

The surface gravity of the black hole formed as a result of the gravitational collapse is

$$\kappa = \frac{(1 + 2k)^2}{4M} = \frac{(1 - 8\pi\eta^2)^2}{4M}. \tag{5.8}$$

This redefinition of the surface gravity reduces the calculation to that of the Schwarzschild case. With this redefinition, the Penrose diagram of the present system is identical to that of the Schwarzschild case.

As in the Schwarzschild case, assuming there are no bound states at late times, the ingoing and outgoing modes form a complete basis in terms of which the field at late times can be expanded. Then an outgoing mode of the form $r^{-1}\mathrm{e}^{-i\omega u} Y_{lm}$ at late times can be traced back to early times in the same fashion as in the Schwarzschild case. At early times, the ray, moving along constant phase v lines will have the form $\mathrm{e}^{-i\omega u}(v)$. The affine parameter on the past horizon can be chosen as

$$\lambda = -c\mathrm{e}^{-\kappa u}. \tag{5.9}$$

Then the function

$$u(v) = -\frac{1}{}\ln\left[\frac{v_0 - v}{}\right]. \tag{5.10}$$

$$N_\beta = \frac{1}{e^{2\pi\omega/\kappa} - 1} \tag{5.11}$$

$$= \left(e^{8\pi M\omega/(1+2k)^2} - 1\right)^{-1}. \tag{5.12}$$

Thus the thermal spectrum is recovered but the temperature is now $(1 - 8\pi\eta^2)^2/8\pi M$.

Consider next the quanta of the ψ field responsible for the monopole. The equations satisfied by

$$\tilde{\psi}^a = \psi^a - \psi^a_{bg} \tag{5.13}$$

are, after linearization,

$$\Box\tilde{\psi}^a + 2\lambda\eta^2\psi^a_{bg}\left(\sum_b \psi^b_{bg}\tilde{\psi}^b\right) = 0. \tag{5.14}$$

Asymptotically the equation becomes

$$\Box\tilde{\psi}^a + 2\lambda\eta^2\frac{x^a}{r^2}\left(\sum_b x^b\tilde{\psi}^b\right) = 0. \tag{5.15}$$

Consider the $a=3$ mode and the asymptotic z direction, the other two (x and y) remaining finite. Then the equations become

$$\Box\tilde{\psi}^3 + 2\lambda\eta^2\tilde{\psi}^3 = 0, \tag{5.16}$$

$$\Box\tilde{\psi}^1 = 0, \tag{5.17}$$

$$\Box\tilde{\psi}^2 = 0. \tag{5.18}$$

This corresponds to the radial mode being massive but the two transverse modes being massless. Thus the preceding analysis will apply to the two transverse modes as well. We see that an imprint of the topological charge of the black hole is left on the Hawking radiation as well, namely under angular displacement, different components of the ψ triplet will be detected.

Thus the fate of our black hole is similar to that of the magnetically charged black holes [8]. While the question of its ultimate fate cannot be settled within the semiclassical approximation, the answer will be the same as for a Schwarzschild black hole. If it can in fact evaporate completely, and does so, then it leaves behind a monopole identical to the original one before collapse.

In concluding this section, we note that the persistence of the thermal radiation is not surprising. It is known from the work in axiomatic field theory [9] that when horizons exist, a unique nontrivial automorphism exists for the ground state. The automorphism works out to be periodicity in time, leading to the Kubo–Martin–Schwinger boundary condition on the Green function. There has also been extensive work on thermodynamics

6. Discussion

The main purpose of this investigation was to study the effect of global monopole charge on particle orbits and the Hawking radiation. It turns out that existence, boundedness and stability threshold for circular orbits scale up by $(1 - 8\pi\eta^2)^{-1}$, perihelion shift and light bending by $(1 - 8\pi\eta^2)^{-3/2}$, while the Hawking temperature scales down by $(1 - 8\pi\eta^2)^2$ the Schwarzschild values. This is how the global monopole charge η affects the particle orbits and the Hawking radiation thermal spectrum. It may be noted that the event horizon is given by $r = 2M(1 - 8\pi\eta^2)^{-1}$, while the red-shifted proper acceleration remains unchanged as M/r^2. It is the scaling up of the horizon that leads to scaling down of the surface gravity (temperature) of the hole.

Acknowledgements

One of the authors (KN) thanks Jawaharlal Nehru Centre for Advanced Research, Bangalore for award of a summer fellowship and IUCAA for providing the facilities.

References

[1] M Barriola and A Vilenkin, *Phys. Rev. Lett.* **63**, 341 (1989)
[2] N Dadhich (1995) GR-14 abstracts, A. 98
[3] A Banerjee, S Chatterjee and A A Sen, *Class. Quantum Gravit.* **13**, 3141 (1996)
[4] N Dadhich, *On the Schwarzschild field*, gr-qc/9704068
[5] G W Gibbons, M E Ortiz, F Ruiz and T M Samols, *Nucl. Phys.* **B385**, 127 (1992)
[6] D Harari and C Lousto, *Phys. Rev.* **D42**, 2626 (1990)
[7] S Weinberg, *Gravitation and Cosmology* (John Wiley and Sons, New York, 1972) pp. 189–90, 194–96
[8] K Lee, V P Nair and E J Weinberg, *Gen. Relativ. Gravit.* **24**, 1203 (1992)
[9] J J Bisognano and E H Wichmann, *J. Math. Phys.* **16**, 985 (1975)
[10] Jiliang Jing, Hongwei Yu and Yongjiu Wang, *Phys. Lett.* **A178**, 59 (1993)
[11] B Jensen, *Nucl. Phys.* **B453**, 413 (1995)
[12] N Dadhich, A duality relation: global monopole and texture, gr-qc/9712021

Note added in the proof:

By resolving the Riemann curvature into electric and magnetic parts, it has now been shown [12] the Schwarzschild black hole with global monopole (3.7) is dual to the Schwarzschild black hole without global monopole. The solution (3.7) with $M = 0$ is dual to flat spacetime and hence it can justifiably be considered as "minimally" curved. By duality we mean the interchange between active and passive electric parts of the field.

Approximate fixed-ρ solution of 'sea-quark' evolution equation at small-x and HERA

A SAIKIA
Department of Physics, Arya Vidyapeeth College, Guwahati 781 016, India

MS received 24 April 1997; revised 18 March 1998

Abstract. We found an approximate simple solution of sea-quark evolution equation in terms of $\rho(=\sqrt{\ln(x_0/x)/\ln[\ln(Q^2/\Lambda^2)/\ln(Q_0^2/\Lambda^2)]})$ and $\zeta(\equiv \ln[\ln(Q^2\Lambda^2)/\ln(Q_0^2/\Lambda^2)])$ in the small-x region when ρ is fixed and compared with HERA data. Agreement with data is found for large Q^2 and small ρ. Comparison with double asymptotic scaling prediction is made. We found a critical value of ρ. More data are needed to confirm this point.

Keywords. DGLAP evolution equations; soft and hard pomeron.

PACS No. 12.35

In the small-x limit, the coupled DGLAP [1,2] sea-quark and gluon evolution equations for leading order can be written as sea-quark and gluon evolution equations in decoupled forms. The gluon evolution equation is of the form of wave equation in terms of the variables $\xi(\equiv \ln(x_0/x))$ and $\zeta(\equiv \ln[\ln(Q^2/\Lambda^2)/\ln(Q_0^2/\Lambda^2)])$ (x_0 and Q_0^2 being the starting scales of perturbative evolution) [3]. In the asymptotic limit of $\sigma(\equiv \sqrt{\xi\zeta})$, the solution of this wave equation gives rise to scaling in terms of σ and $\rho(\equiv \sqrt{\xi/\zeta})$, which is termed as 'double asymptotic scaling' (DAS) [3]. From the gluon momentum distribution function we can find the sea-quark momentum distribution function using DGLAP sea-quark evolution equation for small-x. Thus, we can obtain the structure function. The prediction for proton structure function from DAS, when compared with the data from HERA [7], has good agreement [3–5] for large values of σ and ρ. In the case of gluon, prediction from DAS agrees well with the fit obtained by Glück *et al* [6] above a certain value of $\rho(\equiv \delta/\gamma)$, which can be found analytically [8]. Hence, we found a simple solution [9] of gluon wave equation at fixed ρ which agrees well with the fit [6] below $\rho = \delta/\gamma$. Here, we extend the solution [9] in approximate form to proton structure function for large value of ζ (that is, Q^2) which can be used to analyse the data below the critical value of $\rho(\equiv \delta/\gamma)$, because, the complete expression for structure function from DAS has a discontinuity at $\rho = \delta/\gamma$ and is negative below this value. To compare our prediction with that from DAS, we separated the HERA data [11] into two sets one set having $\rho > \delta/\gamma$ and another one having $\rho < \delta/\gamma$. The DAS predictions, without inclusion of complete splitting kernel of the process $g \rightarrow q\bar{q}$, for proton structure function is found to be in good agreement with data, but our predictions fall far below the data for $\rho > \delta/\gamma$. But for $\rho < \delta/\gamma$ our

$$\left(\frac{\partial^2}{\partial\xi\partial\zeta}+\delta\frac{\partial}{\partial\xi}-\gamma^2\right)G(\xi,\zeta)=0 \tag{1}$$

where $G(\xi,\zeta)=xg(x,Q^2)$ is the gluon momentum distribution function, $\gamma=\sqrt{12/\beta_0}$, $\delta=(11+2n_f/27)/\beta_0$, $\beta_0=11-2n_f/3$, and n_f is number of flavours.

When ρ is fixed, the solution of (1) for large ζ is [9]

$$G(\zeta\rho^2,\zeta)\simeq A\exp[(-\delta+\sqrt{\delta^2+4\gamma^2\rho^2})\zeta/2]. \tag{2}$$

It is well known that, in the small-x limit, the contribution from gluon is very large compared to quark contribution. Hence the LO-DGLAP evolution equation for sea-quark can be approximated as

$$\frac{\partial\hat{q}(x,Q^2)}{\partial\ln Q^2}\simeq\frac{\alpha_s(Q^2)}{4\pi}\cdot 2n_fP_{qg}(x')\otimes G(x',Q^2)$$

or

$$\frac{\partial\hat{q}(\xi,\zeta)}{\partial\zeta}\simeq\frac{r^2}{3}n_fP_{qg}(\xi')\otimes G(\xi',\zeta) \tag{3}$$

where $\hat{q}(x,Q^2)$ is the quark momentum distribution function, P_{qg} is the leading order splitting kernel for $g\rightarrow q\bar{q}$ process and '$\otimes$' indicates convolution with respect to the variable x'. α_s is the strong coupling constant.

Since, in the LO

$$P_{qg}(z)=\tfrac{1}{2}[z^2+(1-z)^2] \tag{4}$$

hence, (3) can be written as

$$\frac{\partial\hat{q}}{\partial\zeta}(\xi,\zeta)=\frac{n_f\gamma^2}{6}\int_0^{\xi}d\xi'[2e^{2(\xi'-\xi)}+1-2e^{(\xi'-\xi)}]G(\xi',\zeta). \tag{5}$$

In the small-x limit, the proton structure function can be approximated as

$$F_2^p(\xi,\zeta)=\tfrac{5}{18}\hat{q}(\xi,\zeta) \tag{6}$$

Therefore, using (2) in (5), the expression for F_2^p can be written as

$$F_2^P=\frac{5A}{108}n_f\gamma^2\rho^2\left\{\frac{e^{(2\rho^2+a-2)\rho^2\zeta}}{(2\rho^2+a)(2\rho^2+a-2)}-\frac{e^{(\rho^2+a-1)\rho^2\zeta}}{(\rho^2+a)(\rho^2+a-1)}+\frac{e^{a\rho^2\zeta}}{2a^2\rho^2}\right.$$

$$+\frac{e^{-2\rho^2\zeta}}{(2\rho^2+a)2\rho^2}-\frac{e^{-\rho^2\zeta}}{\rho^2(\rho^2+a)}-\frac{1}{2a^2\rho^2}-\frac{\zeta}{2a}-\frac{1}{\rho^2(2\rho^2+a)(2\rho^2+a-2)}$$

$$2\rho^2(2\rho^2+a) \qquad \rho^2(\rho^2+a)(\rho^2+a-1) \qquad \rho^2(\rho^2+a) \Big\}$$

where $a = [(-\delta + \sqrt{\delta^2 + 4\gamma^2\rho^2})/2]$.

When $\rho \sim 1$

$$F_2^P(\zeta\rho^2, \zeta) = \frac{5A}{108} n_f \gamma^2, \left\{ \frac{e^{a\zeta}}{a(a+2)} - \frac{e^{a\zeta}}{a(a+1)} + \frac{e^{a\zeta}}{2a^2} + \frac{e^{-2\zeta}}{2(a+2)} - \frac{e^{-\zeta}}{(1+a)} \right.$$
$$\left. - \frac{1}{2a^2} - \frac{\zeta}{2a} - \frac{1}{a(a+2)} - \frac{1}{2(a+2)} + \frac{1}{a(1+a)} + \frac{1}{1+a} \right\}.$$

If ζ is large,

$$F_2^P(\zeta\rho^2, \zeta) = \frac{5A}{108} n_f \gamma^2 e^{a\zeta} \left[\frac{1}{a(a+2)} - \frac{1}{a(1+a)} + \frac{1}{2a^2} \right]$$
$$= \frac{5A}{108} n_f \gamma^2 \frac{e^{a\zeta}}{a} \left[\frac{a^2+a+2}{2a(a+1)(a+2)} \right].$$

For fixed ρ, a is fixed and hence

$$F_2^P = N\gamma^2 \, \frac{e^{a\zeta}}{a} \tag{7}$$

where

$$N = \frac{5A}{108} n_f \left[\frac{a^2+a+2}{2a(a+1)(a+2)} \right].$$

The normalising factor N has a dependency on ρ. But, it has no singularity for all $\rho > 0$, which is the advantage over the DAS result [3].

From (7) we can have

$$F_2^P \sim N \frac{\gamma}{\rho} e^{\gamma,\sigma} \tag{8}$$

the approximate double scaling, when ρ is large, which is a consequence of double log approximation [10] (it is due to gluon density). For fixed ρ, the slope of the curve, ln F_2^P vs. σ, is half to that predicted by DAS. It shows that for approximate double scaling of F_2^P it is not necessary to use DAS form of splitting kernel for the evolution of sea-quark. In both the cases subasymptotic contribution from quark (P_{qq}) is neglected.

To compare with HERA data [11], we use (7). In deriving the expression for proton structure function, our approximation is such that it is applicable for large ζ, that is, large Q^2..

It has been observed in gluon that [8], there is a lower bound on ρ, below which the prediction from DAS differs from fit obtained by Glück *et al* [6]. To find a similar behaviour in proton structure function, we use the complete form of F_2^P, that is

C is a constant, $y = \gamma/\rho$, $G(\sigma, \rho) = \sigma^{1/2}\exp\left(2\gamma\sigma - \delta\frac{\sigma}{\rho}\right)$,

$$f_g(y) \simeq \left(1 - \beta x_e \frac{y}{1+y}\right), \quad f_q(y) = \left(1 - \frac{\delta}{\gamma^2}y\right)^{-1} \frac{3(4+3y+y^2)}{2(1+y)(2+y)(3+y)}$$

and the limiting form of (9) (when $y \to 0$),

$$F_2^p(\sigma, \rho) \simeq C\,\frac{\gamma}{\rho}\sigma^{1/2}\exp\left(2\gamma\sigma - \delta\frac{\sigma}{\rho}\right), \tag{10}$$

σ, ρ, ξ and ζ are evaluated using $x_0 = 0.1, Q_0^2 = 1\ \mathrm{GeV}^2$ $\Lambda = 0.23$ GeV. F_2^p is evaluated using $n_f = 4$ and $\beta = 5$.

It can be observed (figure 1) that eq. (9) has a singularity at $\rho = \delta/\gamma (\simeq 1.13)$ due to $f_q(y)$ and uncertainty of this function is much greater than $f_g(y)$ near the 'singularity' and hence its effect cannot be neglected. It is easy to find that F_2^p is negative according to eq. (9) for $\rho < \delta/\gamma$. The prediction for F_2^p from DAS in the region $\rho \leq \delta/\gamma$ contradicts QCD as in the case of gluon [8]. So, $\rho = \delta/\gamma$ is being termed as 'critical point'.

Next, we separated the HERA data [11] into two sets (figures 2 and 3). One set is for $\rho < 1.13$ (indicated by traingles) and another one for $\rho > 1.13$ (indicated by circles). The shaded regions (with dots) indicate the average error in experimental data. In figure 2 the dotted-dashed line indicates the prediction from DAS for $\rho = 2$ (using (10)) and the solid line is the prediction from (7) for the same value of ρ. For the predictions, we put $A = 1.4763$ and $C = 0.1245$. The prediction from DAS agrees with data. But, the

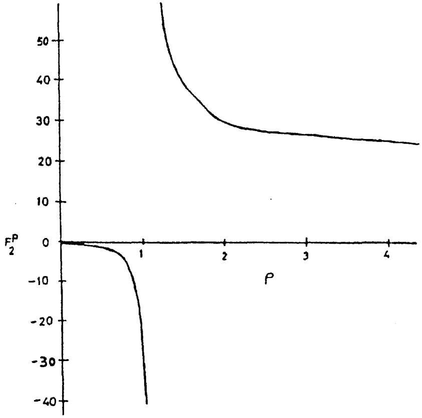

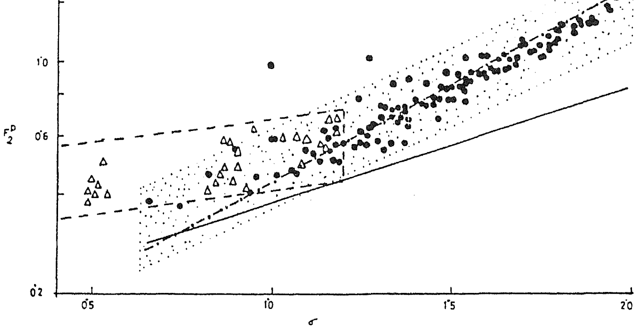

Figure 2. In F_2^p plotted against σ using eq. (10) (the dotted dashed line) and eq. (7) (the solid line) for $\rho = 2$. The black circles indicate experimental data points having $\rho > 1.13$ and the triangles indicate data points having $\rho < 1.13$. The region shaded with dots indicates average uncertainty in experimental HERA data.

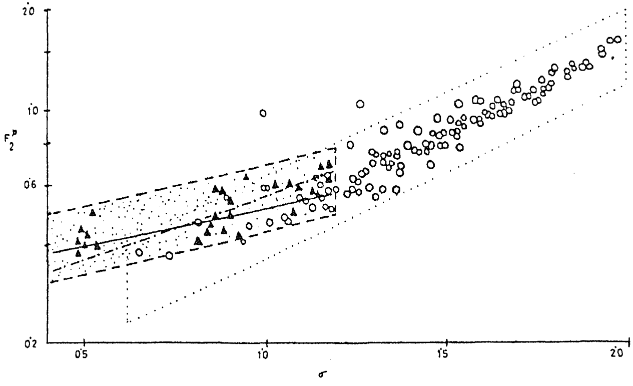

Figure 3. In F_2^p plotted against σ using eq. (7) (the solid line) and eq. (10) (the dotted dashed line) for $\rho = 1$. The black triangles indicate experimental data points having $\rho < 1.13$ and circles indicate data points having $\rho > 1.13$. The region shaded with dots indicates average uncertainty in experimental data.

found that for $\rho \leq 1.13, f_q(y) \neq 1$ and so, use of (10) in this region is questionable.

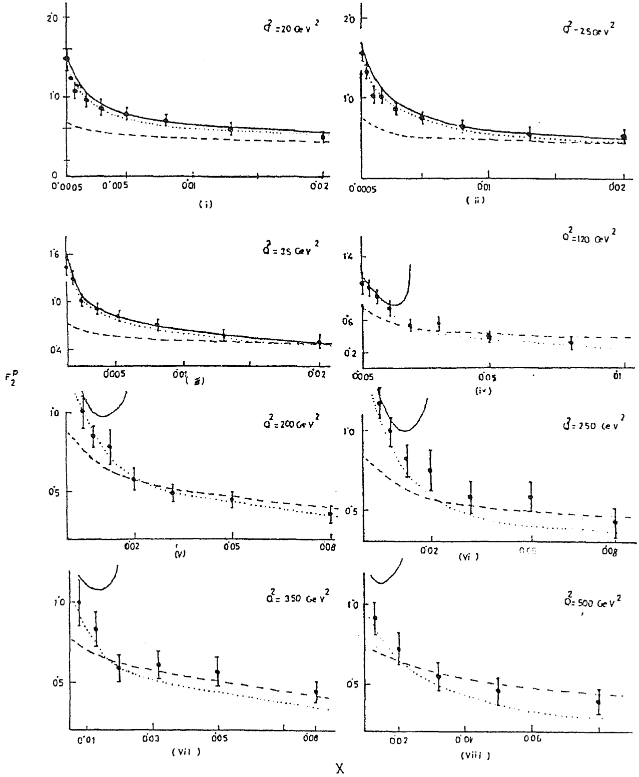

Figure 4. F_2^p vs. x for $Q^2 = 20, 25, 35, 120, 200, 250, 350$ and 500 GeV^2. The predictions from eq. (9) (the solid lines), eq. (10) (the dotted lines) and eq. (7) (the dashed lines). Data points with error bars are from HERA [11].

such that variation of ρ is very small, which may be considered as fixed. Under this consideration (7) can be used for conventional plot of x vs. F_2^p at fixed, but large Q^2. In figure 4, we plot x vs. F_2^p from (7) (dashed line), (9) (solid line) and (10) (dotted line) for $Q^2 = 20, 25, 35, 120, 200, 250, 350$ and 500 GeV^2. Equation (9) agrees well with data for $Q^2 = 20, 25$ and 35 GeV^2 (figure 4 (i,ii,iii)). But for large $Q^2 (Q^2 \geq 120$ GeV^2) it does not agree with data for comparatively large values of x (figure 4 (iv,v,vi,vii,viii)). Agreement with data is found for 56 data points out of 169. Equation (10) agrees well with data for all the Q^2 and nearly all x (agreement is found for 115 points out of 169). Equation (7) is found to be valid for $Q^2 = 120, 200, 250, 350$ and 500 GeV^2 and $x \geq 0.02$ (figure 4 (iv,v,vi,vii,viii)) (agreement is found for 45 points out of 169). Keeping $\rho \sim 1$ as we go on increasing Q^2, x can be decreased and (7) can be used to smaller values of x.

Thus, we have shown that DAS is not the only one solution to explore the physics at HERA. There is a critical value of ρ below which application of DAS is questionable. The difference in slope of the curve $\ln F_2^p$vs.σ for data having $\rho < \delta/\gamma$ with the data having $\rho > \delta/\gamma$ indicates a change in physics of low-x, that is, a change from hard pomeron to soft pomeron [9]. More data below and above the critical value of ρ will properly indicate the change.

Acknowledgement

The author is grateful to D K Choudhury, R Deka and A Das for supplying the necessary materials.

References

[1] V N Gribov and L N Lipatov, *Sov. J. Nucl. Phys.* **15**, 438 (1972)
L N Lipatov, *Sov. J. Nucl. Phys.* **20**, 94 (1974)
G Altarelli and G Parisi, *Nucl. Phys.* **B126**, 298 (1977)
[2] Y L Dokshitzer, *Sov. Phys. JETP* **46**, 641 (1977)
[3] R D Ball and S Forte, *Phys. Lett.* **B335**, 77 (1994)
[4] R D Ball and S Forte, *Phys. Lett.* **B336**, 77 (1994)
[5] J R Forshaw and R G Roberts, *Phys. Lett.* **B351**, 308 (1995)
[6] M Glück, E Reya and A Vogt, *Z. Phys.* **C53**, 127 (1992)
[7] Hl Collaboration, *Nucl. Phys.* **B407**, 515 (1993)
[8] A Saikia, *Pramana – J. Phys.* **47**, 393 (1996)
[9] A Saikia, *Pramana – J. Phys.* **48**, 1015 (1997)
[10] L N Gribov, E M Levin and M G Ryskin, *Phys. Rep.* **C100**, 1 (1983)
[11] Hl Collaboration, DESY preprint 96-036 (1996)

Weak radiative decay $\Lambda_b \to \Lambda\gamma$ in the heavy quark effective theory

A K GIRI* and R MOHANTA
Department of Physics, Utkal University, Bhubaneswar 751 004, India
*Physics Department, Punjab University, Chandigarh 160 014, India
Email: nanda@iopb.ernet.in

MS received 15 March 1997; revised 4 December 1997

Abstract. The weak radiative decay $\Lambda_b \to \Lambda\gamma$ is studied in the heavy quark effective theory treating s-quark as heavy. This rare decay is induced by the short distance electromagnetic penguins. Including corrections of the order of $(1/m_Q)$, we obtain the transition matrix element and the corresponding decay width. The Isgur–Wise function is evaluated in the large N_c limit and the branching ratio obtained is 1.48×10^{-5}.

Keywords. Heavy quark effective theory; $1/m_Q$ corrections; Isgur–Wise function.

PACS Nos 11.30; 13.40; 14.20

1. Introduction

The weak radiative decays (flavor changing radiative decays) of hyperons have proven to be a challenge to both theorists and experimentalists. Experimental difficulties result from small branching ratios of these decays and their copious photon background. These transitions require the joint occurence of weak and electromagnetic interactions. Their theoretical treatment requires the inclusion of separate short distance (SD) and long distance (LD) contributions [1, 2]. The relative size of the two types of processes is an issue to be determined for every specific process. At the quark level there are three types of processes which contribute to the weak radiative decays of baryons classified as single, two and three quark transitions. The two quark transition corresponds to W exchange with the photon radiated by the participating quarks. The three quark transition, where the quark not participating in W exchange, radiates the photon, which is strongly suppressed. The single quark transition involves a (SD) contribution due to electromagnetic penguin diagrams [2, 3]. The weak radiative decay $\Lambda_b \to \Lambda\gamma$ is described by the single quark transition and is dominated by the short distance electromagnetic penguin transition $b \to s\gamma$. The recent measurement by CLEO of $B \to K^*\gamma$ [4] and $B \to X\gamma$ [5] processes confirm that this mode is indeed dominated by the electromagnetic penguins.

After knowing the fact that the decay process $\Lambda_b \to \Lambda\gamma$ is dominated by the short distance electromagnetic penguin, we use heavy quark effective theory to study this decay process. Important progress in the theoretical description of hadrons containing one particles involved, and is normalized at the point of zero recoil. Similarly in case of weak decays of heavy baryons one can also write the form factors in terms of another Isgur–Wise function [8, 10].

The idea of heavy quark symmetry is considered to be effective only for heavy quarks whose masses m_Q are significantly larger than the QCD scale Λ_{QCD} ($\approx 200\,\mathrm{MeV}$). Thus, the hadrons including c/b quarks are reasonable laboratory to test the heavy quark effective theory. The s quark is not heavy but not light as the u and d quarks. In many cases the light flavor $SU(3)$ symmetry is successful for s quark system after nondegeneracy of s-quark mass is taken into account as symmetry breaking. However some features of s quark physics are understood if the s quark is treated as heavy. A notable example is the Okubo–Zweig–Iizuka suppression of the decay $\phi \rightarrow \pi\pi\pi$, which is a direct consequence of the fact that the s quark mass or twice the s quark mass is heavier than the QCD scale. The s-quark seems to be marginal in both heavy quark symmetry and light flavor one. Therefore it is interesting to examine the applicability of the heavy flavor symmetry with corrections, for the s-quark system even if s-quark mass is not large enough compared to Λ_{QCD}. Although this assumption might be too optimistic the previous challenging studies [11–14] suggest that heavy quark effective theory is still effective for s-quark system if the constituent quark mass is employed for m_s and $1/m_s$ corrections are taken into account properly. The $1/m_Q$ corrections in the HQET is formulated by putting the heavy quark Q almost on on-shell and expanding in powers of the residual momentum k which is generally written as Λ_{QCD}/m_Q. Then with $\Lambda_{QCD} = 200\,\mathrm{MeV}$ and $m_s = 550\,\mathrm{MeV}$, a measure for $1/m_s$ correction becomes $\Lambda_{QCD}/m_s \simeq 0.36$, which is expected to keep the perturbation meaningful. Treating the s quark as heavy Ali *et al* [13] have studied the radiative rare decays $B \rightarrow K^*\gamma$. Ahmady and Liu [14] estimated the $B \rightarrow K\Psi$ decay rates and obtained quite good results. However in a recent letter Chakraverty *et al* [15] have shown that the application of heavy quark symmetry is not reliable for s-quark system. On the other hand applying HQET to $B \rightarrow K^{(*)}$ transitions, Roberts and Ledroit [16] have suggested that the heavy s-limit may give an acceptable description of unpolarized data, but does not give reliable results when applied to polarization observables.

In this work we intend to test the applicability of heavy quark effective theory to the weak radiative decay $\Lambda_b \rightarrow \Lambda\gamma$ including corrections of the order $1/m_Q$. In the HQET there are two types of $1/m_Q$ corrections to the hadronic form factors: one from $1/m_Q$ corrections to the current operators and the other from the presence of higher dimensional operators in the effective Lagrangian [9, 17]. The latter amounts to the hadronic wave function modification. As shown in [17] all the form factors at $1/m_Q$ order are still expressible in terms of a single function and one dimensional constant. Thus including $1/m_Q$ corrections arising from both the sources, we calculate the branching ratio for the decay process. The Isgur–Wise function is evaluated in the large N_c limit [18]. This decay is also studied in [19] in the effective Lagrangian approach, where they have incorporated two ideas – the heavy quark symmetry scheme with both b and s treated as heavy and the MIT bag model. However, regarding the $1/m_Q$ corrections, they have included the corrections of order our predicted result should be much more reliable than that of theirs.

The paper is organized as follows. In § 2 we present the general framework for the study of the radiative rare decays. The Isgur–Wise function is evaluated in the large N_c limit in § 3. Section 4 contains results and discussion.

2. General framework

The short distance electromagnetic penguin process is governed by the electromagnetic penguins operators. At the weak scale $\mu = m_b$, the transition $b \to s\gamma$ is mediated by the effective Hamiltonian [20]

$$\mathcal{H}_{\text{eff}} = -\frac{4G_{\text{F}}}{\sqrt{2}} V_{tb}V_{ts}^* C_7(m_b)\mathbf{O}_7(m_b), \tag{1}$$

where the operator $\mathbf{O}_7(m_b)$ is given by

$$\mathbf{O}_7(m_b) = \frac{e}{32\pi^2} F_{\mu\nu}[m_b\, \bar{s}\sigma^{\mu\nu}(1+\gamma_5)b + m_s\bar{s}\sigma^{\mu\nu}(1-\gamma_5)b] \tag{2}$$

and the Wilson coefficient $C_7(m_b)$ is

$$C_7(m_b) = \eta^{-16/23}[C_7(M_W) + \tfrac{58}{135}(\eta^{10/23} - 1) + \tfrac{29}{189}(\eta^{28/23} - 1)] \tag{3}$$

with $\eta = \alpha_s(m_b)/\alpha_s(M_W)$ and

$$C_7(M_W) = \frac{x}{2}\left(\frac{8x^3 + 5x - 7}{12(x-1)^3} - \frac{3x^2 - 2x}{2(x-1)^4}\ln x\right); \quad x = \frac{m_t^2}{M_W^2}. \tag{4}$$

The value of $C_7(m_b)$ is taken as $C_7(m_b) = 0.31$ [21]. The transition amplitude for the decay process $\Lambda_b \to \Lambda\gamma$ is given as

$$\mathcal{M}(\Lambda_b \to \Lambda\gamma) = \langle\Lambda\gamma|\mathcal{H}_{\text{eff}}|\Lambda_b\rangle = -\frac{4G_{\text{F}}}{\sqrt{2}} V_{tb}V_{ts}^* C_7(m_b)\langle\Lambda\gamma|\mathbf{O}_7|\Lambda_b\rangle. \tag{5}$$

We shall use HQET to compute this matrix element. In the HQET the heavy Λ_{Q} baryons are described as the bound state of the heavy quark field and the light diquark field. In terms of the interpolating fields it is given as [22]

$$\Lambda_{\text{Q}}(v,s) = \bar{u}_{\Lambda_{\text{Q}}}(v,s)\phi_v h_v, \tag{6}$$

where ϕ_v represents the light diquark field and h_v is the heavy quark field. $u_{\Lambda_{\text{Q}}}(v,s)$ is the usual Dirac spinor, which obeys the constraint relation

$$\not{v}u(v,s) = u(v,s). \tag{7}$$

The heavy quark field in the effective theory $h_{\text{Q}}(v,x)$ is related to the quark field $\text{Q}(x)$ of the QCD Lagrangian by

$$h_{\text{Q}}(v,x) = e^{im_{\text{Q}}v\cdot x}\left(\frac{1+\not{v}}{2}\right)\text{Q}(x). \tag{8}$$

$$\bar{Q}'\Gamma Q = \bar{h}'\Gamma h + \frac{1}{2m_Q}\,\bar{h}'\Gamma(i\overrightarrow{\not D})h + \frac{1}{2m_{Q'}}\bar{h}'(-i\overleftarrow{\not D})\Gamma h, \tag{9}$$

where h and h' are the heavy quark field operators in the effective theory for the quarks Q and Q′. In the effective theory the matrix elements of the operators on the right hand side of (9) between the Λ_Q-baryon states are given as [23]

$$\langle \Lambda_{Q'}(v',s')|\bar{h}'\Gamma h|\Lambda_Q(v,s)\rangle = \zeta(v\cdot v')\bar{u}_{\Lambda_{Q'}}(v',s')\Gamma u_{\Lambda_Q}(v,s), \tag{10}$$

$$\langle \Lambda_{Q'}(v',s')|\bar{h}'\Gamma(i\overrightarrow{\not D})h|\Lambda_Q(v,s)\rangle = \zeta_\alpha(v,v')\bar{u}_{\Lambda_{Q'}}(v',s')\Gamma\gamma_\alpha u_{\Lambda_Q}(v,s), \tag{11}$$

$$\langle \Lambda_{Q'}(v',s')|\bar{h}'(-i\overleftarrow{\not D})\Gamma h|\Lambda_Q(v,s)\rangle = \zeta_\alpha(v',v)\bar{u}_{\Lambda_{Q'}}(v',s')\gamma_\alpha\Gamma u_{\Lambda_Q}(v,s). \tag{12}$$

The most general decomposition of ζ_α involves two scalar functions defined by

$$\zeta_\alpha(v,v') = \zeta_+(w)(v+v')_\alpha + \zeta_-(w)(v-v')_\alpha, \tag{13}$$

where $w = v\cdot v'$, $\zeta_\pm(w)$ are given as [23]

$$\zeta_+(w) = \frac{\bar{\Lambda}}{2}\left(\frac{w-1}{w+1}\right)\zeta(w), \tag{14}$$

$$\zeta_-(w) = \frac{\bar{\Lambda}}{2}\zeta(w). \tag{15}$$

The parameter $\bar{\Lambda}$ is the scale of light degrees of freedom given as $\bar{\Lambda} = m_{\Lambda_Q} - m_Q \approx 700\,\text{MeV}$. Now at $1/m_Q$ order arising from the current operator modification, the matrix element of the operator $\mathbf{O}_7$ between the Λ_b baryon in the initial state and a photon with Λ baryon in the final state may be written as

$$\langle \Lambda(v',s'),\gamma(k,\epsilon)|\mathbf{O}_7|\Lambda_b(v,s)\rangle = \frac{-ie}{16\pi^2}\,\epsilon_\mu k_\nu\langle\Lambda(v',s')|\Omega^{\mu\nu}|\Lambda_b(v,s)\rangle, \tag{16}$$

where

$$\Omega^{\mu\nu} = \bar{h}_{v'}^{(s)}\left[m_b\left\{\sigma^{\mu\nu}(1+\gamma_5) + \frac{1}{2m_b}\,\sigma^{\mu\nu}(1+\gamma_5)(i\overrightarrow{\not D}) + \frac{1}{2m_s}(-i\overleftarrow{\not D})\sigma^{\mu\nu}(1+\gamma_5)\right\}\right.$$
$$\left. + m_s\left\{\sigma^{\mu\nu}(1-\gamma_5) + \frac{1}{2m_b}\,\sigma^{\mu\nu}(1-\gamma_5)(i\overrightarrow{\not D}) + \frac{1}{2m_s}(-i\overleftarrow{\not D})\sigma^{\mu\nu}(1-\gamma_5)\right\}\right]h_v^{(b)} \tag{17}$$

and ϵ_μ is the polarization vector of the emitted photon. Using eqs (10–17) one can obtain

$$\langle\Lambda(v',s')\gamma(k,\epsilon)|\mathbf{O}_7|\Lambda_b(v,s)\rangle = \frac{-ie}{16\pi^2}\epsilon_\mu k_\nu\zeta(w)\bar{u}_\Lambda(v',s')$$
$$\times\left[m_b\left\{\sigma^{\mu\nu}(1+\gamma_5) + \frac{\bar{\Lambda}}{2m_b}\left(\frac{w}{w+1}v_\alpha - \frac{1}{w+1}v'_\alpha\right)\sigma^{\mu\nu}(1+\gamma_5)\gamma_\alpha\right.\right.$$

$$+m_s\left\{\sigma^{\mu\nu}(1-\gamma_5)+\frac{\bar{\Lambda}}{2m_b}\left(\frac{w}{w+1}v_\alpha-\frac{1}{w+1}v'_\alpha\right)\sigma^{\mu\nu}(1-\gamma_5)\gamma^\alpha\right.$$
$$\left.\left.+\frac{\bar{\Lambda}}{2m_s}\left(\frac{w}{w+1}v'_\alpha-\frac{1}{w+1}v_\alpha\right)\gamma^\alpha\sigma^{\mu\nu}(1-\gamma_5)\right\}\right]u_{\Lambda_b}(v,s). \tag{18}$$

As for the corrections arising from the hadronic states, we must also include $1/m_{\mathrm{Q}}$ corrections to the effective Lagrangian, i.e.,

$$\mathcal{L}_{\mathrm{eff}}=\sum_{\mathrm{Q}}\left[h_v^{(\mathrm{Q})}iv\cdot Dh_v^{(\mathrm{Q})}+\frac{\mathcal{L}_I}{2m_{\mathrm{Q}}}\right], \tag{19}$$

where

$$\mathcal{L}_I=\bar{h}_v^{\mathrm{Q}}\left[(iD)^2+\frac{g}{2}\sigma_{\mu\nu}G^{\mu\nu}\right]h_v^{\mathrm{Q}}=\mathcal{O}_1+\mathcal{O}_2. \tag{20}$$

Now inserting the higher order term of the effective Lagrangian ($\mathcal{L}_{\mathrm{I}}$) into the matrix elements of the lowest order current $J=\bar{h}'\Gamma h$, we obtain [23]

$$\langle\Lambda(v',s')|iT\int \mathrm{d}x\{J(0),\mathcal{O}_1(x)\}|\Lambda(v,s)\rangle=\bar{\Lambda}\chi(w)\bar{u}_\Lambda(v',s')\Gamma u_{\Lambda_b}(v,s). \tag{21}$$

Insertion of the kinetic operator $\mathcal{O}_1$ preserves the Dirac structure of the current and transforms trivially under the spin symmetry, contributing to the form factors in the same proportion as the leading order term (10) and hence effectively correcting the Isgur–Wise function [9, 17, 23]. The contributions from the chromomagnetic operator $\mathcal{O}_2$ vanishes by Lorentz invariance. For the subleading form factor, vector current conservation implies

$$\chi(1)=0. \tag{22}$$

Since $\chi(w)$ only corrects the Isgur–Wise function, we assume a simple form being consistent with the constraint (22) as done in [12] for the mesonic case

$$\chi(w)=(w-1)\zeta(w). \tag{23}$$

Thus with eqs (5, 18–23) we obtain the transition amplitude for the weak radiative decay $\Lambda_b\to\Lambda\gamma$, including corrections of order $(1/m_{\mathrm{Q}})$ as

$$\mathcal{M}(\Lambda_b(v',s')\to\Lambda(v,s)\gamma(k))=i\bar{u}_\Lambda(v',s')(A+B\gamma_5)\sigma_{\mu\nu}\epsilon^\mu k^\nu u_{\Lambda_b}(v,s), \tag{24}$$

where A and B are given as

$$A=\frac{G_{\mathrm{F}}}{\sqrt{2}}\frac{e}{4\pi^2}V_{tb}V_{ts}^*C_7(m_b)\zeta(w)(m_s+m_b)\left[1+(w+2)\left(\frac{w-1}{w+1}\right)\left(\frac{\bar{\Lambda}}{2m_b}+\frac{\bar{\Lambda}}{2m_s}\right)\right] \tag{25}$$

and

$$\Gamma(\Lambda_b(v,s) \to \Lambda(v',s')\gamma(k)) = \frac{1}{\pi}|k|^3(|A|^2+|B|^2), \tag{27}$$

where k is the c.o.m. momentum of the emitted photon.

Since it is not possible to find out the Isgur–Wise function in HQET, we will evaluate the same using some model. Recently a breakthrough has been achieved to evaluate the IW function for baryons i.e., the bound state soliton picture in the large N_c limit [18].

3. Evaluation of the Isgur–Wise function

Here we have presented the evaluation of the Isgur-Wise function in the same manner as suggested in [18]. In the large N_c limit the light baryons n, p, Δ etc. can be viewed as solitons in the chiral Lagrangian for pion self interaction [24]. The baryons containing a single heavy strange (or bottom) quark are bound states of these solitons with K and K^* (or B and B^*) mesons [25–29]. In this paper we use the bound state soliton picture to estimate the value of the baryonic Isgur–Wise function. In the ground state of Λ_Q baryons, the light quarks are in the spin 0 state [22]. Hence in the bound state soliton picture, Λ_Q-type bound state arise when the spin of the light degrees of freedom of the heavy meson and the spin of the nucleon are combined into a spin zero configuration where as the isospin of the heavy meson and that of the nucleon are combined into an isospin zero state. Other baryons (e.g., the Δ) only contribute to the bound states with higher isospin.

Let the light degrees of freedom of the heavy baryon be denoted by $|I,I_3;s_l,m_l\rangle$, where I and s_l denote their isospin and spin quantum numbers while I_3 and m_l are their three components respectively. Hence the light degrees of freedom of Λ_Q baryon is denoted by $|0,0;0,0\rangle$. The chiral soliton is denoted by $|R,b;R,n)$, where $R=1/2$ for the nucleon. On the other hand the light degrees of freedom of the heavy meson is given as $|1/2,c;1/2,p\}$.

In the large N_c limit, the binding potential between the chiral soliton and heavy meson is independent of both the isospin and spin of the particles. Hence for the light degrees of freedom of Λ_Q baryon, we have the decomposition as

$$\begin{aligned}|0,0;0,0(v)\rangle = \int d^3\mathbf{q}\Phi(\mathbf{q})(1/2,b;1/2,c|0,0)(1/2,n;1/2,p|0,0)\\ \times|1/2,b;1/2,n(-\mathbf{q}+M_B\mathbf{v}))|1/2,c;1/2,p(\mathbf{q}+M_H\mathbf{v})\},\end{aligned} \tag{28}$$

where $(j_1,m_1;j_2,m_2|J,M)$'s are the Clebsch–Gordan coefficients. $\Phi(\mathbf{q})$ is the ground state wave function and M_B and M_H are the masses of the chiral soliton and heavy meson respectively.

The spin-1/2 Λ_Q baryon is composed of a spin-1/2 heavy quark and spin-0 light degrees of freedom. Hence the matrix element of the current $\bar{h}^{(s)}(v')\Gamma h^{(b)}(v)$ between Λ_b and Λ baryons is given as

$$\langle\Lambda(v',s')|\bar{h}^{(s)}_{v'}\Gamma h^{(b)}_{v}|\Lambda_b(v,s)\rangle = \langle 0,0;0,0\ (v')|0,0;0,0\ (v)\rangle\bar{u}_\Lambda(v',s')\Gamma u_{\Lambda_b}(v,s).$$

$$\begin{aligned}\zeta(v\cdot v') &= \langle 0,0;0,0\ (v')|0,0;0,0(v)\rangle \\ &= \int \mathrm{d}^3\mathbf{q}'\mathrm{d}^3\mathbf{q}\Phi^*(\mathbf{q}')\Phi(\mathbf{q})(1/2,b';1/2,c'|0,0)^* \\ &\quad\times(1/2,n';1/2,p'|0,0)^*(1/2,b;1/2,c|0,0)(1/2,n;1/2,p|0,0) \\ &\quad\times(1/2,b';1/2,n'(-\mathbf{q}'+M_B\mathbf{v}')|1/2,b;1/2,n(-\mathbf{q}+M_B\mathbf{v})) \\ &\quad\times\{1/2,c';1/2,p'(\mathbf{q}'+M_H\mathbf{v}')|1/2,c;1/2,p(\mathbf{q}+M_H\mathbf{v})\}. \end{aligned} \tag{30}$$

Using the normalization conditions for the chiral soliton and heavy meson states, all the Clebsch–Gordan coefficients in (30) turn out to be unity and the Isgur–Wise function is given as

$$\zeta(v\cdot v') = \int \mathrm{d}^3\mathbf{q}\Phi^*(\mathbf{q})\Phi(\mathbf{q}+M_B(\mathbf{v}-\mathbf{v}')). \tag{31}$$

It is noted from eq. (31) that the IW function depends on the spatial wave function $\Phi(\mathbf{q})$ of the Λ_Q baryon. In the large N_c limit, the binding potential between the heavy meson and the chiral soliton is simple harmonic [29], and hence the wave function is taken as

$$\Phi(\mathbf{q}) = \frac{1}{(\pi^2 M_B\kappa)^{3/8}}\exp\left(-\frac{\mathbf{q}^2}{2\sqrt{M_B\kappa}}\right), \tag{32}$$

κ is the spring constant and its value is taken to be $(440\,\mathrm{MeV})^3$ [30]. In the rest frame of the initial state, $v=(1,\vec{0})$ and $\mathbf{v}'$ directed along z-axis we obtain the Isgur–Wise function (31) using (32) for non-relativistic recoils i.e., $|\mathbf{v}'|^2 \approx 2(v\cdot v'-1)$, as

$$\zeta(v\cdot v') = \exp\left(-\frac{(v\cdot v'-1)}{2}\sqrt{\frac{M_B^3}{\kappa}}\right). \tag{33}$$

The product $(v\cdot v')$ is determined by considering the kinematics of the system. Since we are dealing with the two body decays $\Lambda_b(v)\to\Lambda(v')\gamma(k)$, momemtum conservation implies

$$M_{\Lambda_b}v^\mu = M_\Lambda v'^\mu + k^\mu, \tag{34}$$

which gives

$$v\cdot v' = \frac{M_{\Lambda_b}^2+M_\Lambda^2}{2M_{\Lambda_b}M_\Lambda}. \tag{35}$$

With eqs (33) and (35), the value of the Isgur–Wise function is extracted as

$$\zeta(v\cdot v') = 0.0794. \tag{36}$$

4. Results and discussion

To estimate the numerical result we have used the following values. The values of the

$$\mathcal{B}(\Lambda_b \to \Lambda\gamma) = 1.48 \times 10^{-5}. \tag{37}$$

In this paper treating s-quark as heavy an attempt is made to study the rare radiative decay $\Lambda_b \to \Lambda\gamma$ in the heavy quark effective theory. The decay is described by the single quark transition and is dominated by the short distance electromagnetic penguins. In the effective theory this decay matrix element can be written by an expression involving the Isgur–Wise function. Since the quark masses are not infinitely heavy, we have considered $1/m_{\mathrm{Q}}(\mathrm{Q} = b, s)$ corrections arising from the modification of current as well as the hadronic states. As suggested in [17] all the hadronic form factors at order $(1/m_{\mathrm{Q}})$ are expressed in terms of a single function, the Isgur–Wise function. Since HQET does not predict the shape of the IW function, it makes sense to extract the same using a model. Here we have evaluated the same using the bound state soliton picture, in the large N_c limit [18] and obtained the branching ratio for the decay $\Lambda_b \to \Lambda\gamma$. The present status of the subject, in particular the still unavailable data, do not allow for a more complete theoretical approach, however we are hopeful that future experiments will lead to more theoretical understanding. The predicted branching ratio for this decay is $(1 \pm 0.5) \times 10^{-5}$ [32]. In an earlier investigation Cheng *et al* [19] obtained this branching ratio using heavy quark symmetry, MIT bag model and $1/m_s$ correction only to the current operator, to be $(0.8–1.5) \times 10^{-5}$. Additional experimental data would greatly help for a better understanding of the weak radiative decays of heavy hyperons, which can serve as a signal for new physics beyond the standard model. Our result indicates that heavy quark symmetry does work in the first approximation to calculate the exclusive decays involving $b \to s$ transitions.

Acknowledgements

We are very much thankful to Prof. B B Deo, Prof. N Barik and Dr L Maharana for useful discussions. RM would like to thank CSIR, Government of India for financial assistance.

References

[1] P Singer, *Phys. Rev.* **D42**, 3255 (1990)
[2] M A Shifman, A I Vainstein and V I Zakharov, *Phys. Rev.* **D18**, 2853 (1978)
[3] A Buras, M Misiak, M Munz and S Pokorski, *Nucl. Phys.* **B424**, 374 (1994)
[4] R Ammer *et al*, *Phys. Rev. Lett.* **71**, 674 (1993)
[5] M S Alam *et al*, *Phys. Rev. Lett.* **74**, 2885 (1995)
[6] N Isgur and M B Wise, *Phys. Lett.* **B232**, 113 (1989); *Phys. Lett.* **B237**, 527 (1990)
[7] A F Falk, H Georgi, B Grinstein and M B Wise, *Nucl. Phys.* **B343**, 1 (1990)
[8] N Isgur and M B Wise, *Nucl. Phys.* **B348**, 276 (1991)
[9] M Neubert, *Phys. Rep.* **245**, 259 (1994)
[10] H Georgi, *Phys. Lett.* **B240**, 447 (1990); *Nucl. Phys.* **B348**, 293 (1991)
[11] A Ali and T Mannel, *Phys. Lett.* **B264**, 447 (1991)
[12] T Ito, T Morii and M Tanimoto, *Phys. Lett.* **B274**, 449 (1992); *Prog. Theor. Phys.* **88**, 561 (1992)
[13] A Ali, T Ohl and T Mannel, *Phys. Lett.* **B298**, 195 (1993)

[15] D Chakraverty, T De, B Dutta-Roy and A Kundu, *Int. J. Mod. Phys.* **A12**, 2763 (1997)
[16] W Roberts and F Ledroit, *Phys. Rev.* **D53**, 3643 (1996)
[17] H Georgi, B Grinstein and M B Wise, *Phys. Lett.* **B252**, 456 (1990)
B Grinstein, *Ann. Rev. Nucl. Part. Sci.* **42**, 101 (1992)
[18] C K Chow, *Phys. Rev.* **D51**, 1224 (1995)
[19] H Y Cheng, C-Y Cheung, G-Lin Lin, Y C Lin, T M Yan and H-L Yu, *Phys. Rev.* **D51**, 1199 (1995)
[20] S Bartolini, F Borzumati and A Mariero, *Phys. Rev. Lett.* **59**, 180 (1987)
R Grigjanis, P J O'Donnell, M Sutherland and H Navelet, *Phys. Lett.* **B213**, 355 (1988)
B Grinstein, M J Savage and M Wise, *Nucl. Phys.* **B319**, 217 (1990)
B Grinstein, R Springer and M Wise, *Nucl. Phys.* **B339**, 269 (1990)
G Cella, G Curci, G Ricciardi and A Vicere, *Phys. Lett.* **B248**, 181 (1990)
M Misiak *et al*, *Phys. Lett.* **B269**, 161 (1991)
[21] M Ciucini *et al*, *Phys. Lett.* **B316**, 127 (1993); *Nucl. Phys.* **B415**, 403 (1993)
G Cella, G Curci, G Ricciardi and A Vicere, *Nucl. Phys.* **B431**, 417 (1994)
M Misiak and M Munz, *Phys. Lett.* **B344**, 308 (1994)
[22] T M Yan, H Y Cheng, C-Y Cheung, G-L Lin, Y C Lin and H-L Yu, *Phys. Rev.* **D46**, 1148 (1992)
[23] A F Falk and M Neubert, *Phys. Rev.* **D47**, 2982 (1994)
[24] E Witten, *Nucl. Phys.* **B223**, 433 (1983)
G S Adkins, C R Nappi and E Witten, *Nucl. Phys.* **228**, 552 (1985)
[25] C G Callan and I Klebanov, *Nucl. Phys.* **B262**, 365 (1985); *Phys. Lett.* **B202**, 269 (1988)
[26] M Rho, D O Riska and N N Scoccola, *Phys. Lett.* **B251**, 597 (1990)
D O Riska and N N Scoccola, *Phys. Lett.* **B265**, 188 (1991)
[27] E Jenkins, A Manohar and M B Wise, *Nucl. Phys.* **B396**, 27 (1993)
[28] Z Guralnik, M Luke and A Maohar, *Nucl. Phys.* **B390**, 474 (1993)
[29] E Jenkins and A Manohar, *Phys. Lett.* **B294**, 273 (1992)
[30] C K Chow and M B Wise, *Phys. Rev.* **D50**, 2135 (1994)
[31] Particle Data Group, Review of Particle Properties, *Phys. Rev.* **D54**, part I (1996)
[32] P Singer, *Nucl. Phys.* **B50**, 202 (1996) (Proc. Suppl.)

Frictional trajectories near a barrier: A dissipationless Newtonian approach

V J MENON, N CHANANA and Y SINGH
Department of Physics, Banaras Hindu University, Varanasi 221 005, India
Email: vjmenon@banaras.ernet.in

MS received 15 March 1997; revised 15 April 1998

Abstract. We address the problem of classical frictional motion under a potential *V* possessing a barrier, apart from other possible confining and nonstationary terms. It is pointed out that the Green's solution of the exact equation of motion can be reduced (under suitable conditions) either to an improved Rayleigh form or a non-Rayleigh form, the latter being outside the scope of the standard large-friction treatment of the Fokker–Planck equation. The resulting dissipationless dynamics involves an appropriately scaled potential which may have promising applications to quantum stochastic phenomena. Genuine dissipative corrections in regions far away from the barrier can be accounted for by the higher-order terms in our asymptotic expansions.

Keywords. Friction; barrier; Rayleigh; Green's solution; dissipationless.

PACS Nos 03.20; 34.10

1. Introduction

The properties of *single-particle*, nonconservative, frictional motion in classical [1], quantum [2], stochastic [3] and statistical [4] mechanics are very important conceptually and quite interesting application-wise. Damping effects on classical trajectories are theoretically introduced via a linear-velocity term [1a] in an extension of Newton's law or a quadratic dissipation function [1b] in a generalization of Lagrange's equations or an explicitly time-dependent factor [1c] in the Bateman–Caldirola–kanai (BCK) Hamiltonian. Numerous applications of frictional trajectories include the calculation of deterministic collision [1d] of nuclear heavy ions and probabilistic description of phenomena-like Brownian movement [3a] of the harmonic oscillator, signal-to-noise ratio for stochastic resonance [3b] in a double well etc. It may be noted that the problems tackled in refs, [1d] and [3b] involve a potential energy which has a pronounced barrier (see figure 1) apart from other possible nonlinear/nonstationary terms.

In the above context, previous workers have employed two different types of theoretical modelling, viz., *the standard frictional equation* and its *overdamped Rayleigh version.* We review their salient features in § 2 and point out that generally these equations have been solved [1d, 3b] by numerical computation/analog simulation and their associated Lagrangians are inconvenient to use in practice. In § 3 we carefully set up the formal Green's solution of the exact equation of motion and show analytically that the

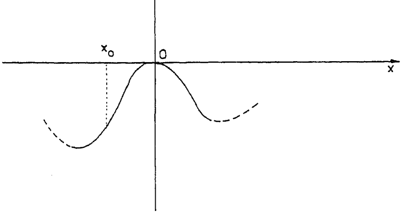

Figure 1. Schematic plot of the potential energy as a function of position (at a specific time). The barrier is explicitly shown. The dashed portions represent other confining and nonstationary parts of the potential.

non-Newtonian dissipational trajectory near the barrier approximately coincides with a Newtonian dissipationless trajectory provided the applied potential is scaled by a suitable factor. Our concluding remarks appear in § 4 where it is emphasized that a Lagrangian employing such a scaled potential can be useful both for path-integral based quantization and for the treatment of quantum stochastic resonance. The algebraic details of our formulation are relegated to the Appendix for convenience.

2. Review of existing models

Consider a test particle moving in an environment and let the symbols

$$m, t, x, v = \mathrm{d}x/\mathrm{d}t, V, F = -\partial V/\partial x, \gamma \tag{1a}$$

respectively denote the mass, time, position, velocity, external potential, applied force and the coefficient of friction. This V may contain possible nonlinear terms in position and/or nonstationary terms in time. The symbols

$$V_I = V_I(x); \quad F_I = -\partial V_I(x)/\partial x \tag{1b}$$

will refer to the particular situation when the potential and force do not contain the time explicitly.

2.1 *Standard frictional equation*

The basic equation of motion for the unknown trajectory $x(t)$ valid for arbitrary damping, reads

$$\mathrm{d}v/\mathrm{d}t + \gamma V = F/m \tag{2a}$$

subject to the initial conditions

Item	Standard frictional model
Motivation	Dissipative force proportional to velocity is motivated experimentally
Parameters	The barrier frequency Ω and the coefficient of friction γ are arbitrary
Estimated velocity	For general potentials with a barrier v is obtained by numerical computation/analog simulation
Effective acceleration	$\frac{\mathrm{d}v}{\mathrm{d}t} = -\gamma v + \frac{F}{m}$
Branch of motion	Both types of branches are present depending on whether the particle is sliding down (Rayleigh-like branch) or climbing up (non-Rayleigh-like branch) the barrier
Lagrangian	$L = \mathrm{e}^{\gamma t}(mv^2 - V)$ due to Bateman–Caldirola–Kanai which is explicitly time-dependent
Mechanical energy	$E_I = mv^2/2 + V_I$ $\mathrm{d}E_I/\mathrm{d}t = -m\gamma v^2 < 0$

As far as x as a function of t is concerned, eq. (2a) is a second-order differential equation of the deterministic (stochastic) type according as the temporal of the force F is definite (random). Equation (2a) is equivalent to the *formal* expression

$$v = v_0\,\mathrm{e}^{-\gamma t} + \mathrm{e}^{-\gamma t}\int_0^t \mathrm{d}t'\,\mathrm{e}^{\gamma t'} F'/m, \tag{2c}$$

where $F' = F(x(t'), t')$ is the force at the integration time t' when the position becomes $x(t')$. Other known features of the standard frictional equation are summarized in table 1. It is seen that irreversible dissipation of the mechanical energy $E_I = mv^2/2 + V_I$ is an inherent property of the model so that a dissipationless approximation to the motion is never attempted. Furthermore, since the underlying BCK [1c, 2a] Lagrangian $L = (mv^2/2 - V)\,\mathrm{e}^{\gamma t}$ is explicitly time-dependent, its path integration in general, would require complicated numerical matrix multiplication [5a].

2.2 *Overdamped Rayleigh equation*

If the coefficient of friction is large enough, the right-hand-side of eq. (2c) can be evaluated by repeated partial integration to yield

$$v \approx F/m\gamma - \dot{F}/m\gamma^2 + \cdots; \quad \gamma t \gg 1 \tag{3a}$$

where $\dot{F} = \mathrm{d}F/\mathrm{d}t$. On the so-called Rayleigh branch of motion (labelled by the superscript R), the leading term of eq. (3a) is picked up, giving a velocity parallel to the applied force,

$$v^{(R)} = F/m\gamma. \tag{3b}$$

As regards the trajectory $x^{(R)}$ as a function of t, this is a first-order differential equation of the deterministic (stochastic) variety depending on whether F has a definite (random)

Item	Conventional Rayleigh model (label R)
Motivation	The frictional force balances the applied force
Parameter	γ large, $\gamma t \gg 1$
Estimated velocity	$v^{(R)} = \dfrac{F}{m\gamma}$
Effective acceleration	$\dfrac{\mathrm{d}v^{(R)}}{\mathrm{d}t} \approx -\gamma v^{(R)} + \dfrac{F}{m} \approx 0$
Branch of motion	Emphasis is on those branches where v and F are almost parallel as happens when the particle is sliding down the barrier in figure 1
Lagrangian	$L^{(R)}$ does not exist because the acceleration has become trivial
Potential energy	$V_I^{(R)}(x)$ such that $\mathrm{d}V_I^{(R)}/\mathrm{d}t = -m\gamma v^{(R)^2} < 0$

equation. It is observed that there is no recipe available to handle the so-called non-Rayleigh branch on which the velocity would be antiparallel to the external force. Furthermore, eq. (3b) being of the first order can not follow from a usual Lagrangian in which $x^{(R)}$ is the only degree of freedom.

3. The dissipationless Newtonian model

3.1 *Preliminaries*

In view of what has been said above it is worth examining (for finite γ) questions such as the possibility of a dissipationless picture, existence of a non-Rayleigh branch, construction of a convenient Lagrangian, etc. This task will be accomplished analytically for those problems [1d, 3b] in which the input potential includes a parabolic barrier. Then the full external force on the particle can be decomposed as

$$F = F_{\mathrm{B}} + F_{\mathrm{p}} = m\Omega^2 x + F_{\mathrm{p}}(x, t) \tag{4}$$

where F_{B} is the linear force due to the barrier, Ω the corresponding angular frequency and all the remaining contributions are lumped together in the perturbation force F_{p} which is supposed to be confining at large distances. In the sequel we shall also need the useful symbols

$$\bar{\Omega} = (\Omega^2 + \gamma^2/4)^{1/2}; \quad \Omega_{\pm} = \bar{\Omega} \pm \gamma/2. \tag{5}$$

3.2 *Formulation*

The standard frictional equation (2a) is rewritten as

$$\left[\frac{\mathrm{d}^2}{\mathrm{d}t^2} + (\Omega_+ - \Omega_-)\frac{\mathrm{d}}{\mathrm{d}t} - \Omega^2\right] x = \frac{F_{\mathrm{p}}}{m}. \tag{6}$$

$t \to \infty$. This leads to a pair of exact, formal relations involving integrals (see Appendix, eqs (A8), (A9a, b) between v, x and F_{p}, which can be suitably approximated depending upon the mechanical branch of interest.

3.3 *The 'improved' Rayleigh branch*

Suppose the particle is sliding down the potential hill of figure 1 so that its velocity is essentially parallel to the applied force. The particle then takes relatively less time to cover a given distance down the hill. After the system has relaxed with respect to the time scale Ω_+^{-1} one employs the asymptotic expansion (All) and finds for the velocity

$$v^{(R)^*} = F/m\Omega_+ - \cdots; \quad \Omega_+ t \gg 1. \tag{7a}$$

Here the dots ... stand for nonleading terms of order $\dot{F}_{\mathrm{p}}/m\Omega_+^2$ and the superscript $(R)^*$ labels the Rayleigh branch as improved by our analysis. Of course, in the limit $\gamma/\Omega \gg 1$ the above result coincides with the usual Rayleigh estimate $F/m\gamma$. The improved expression for the acceleration is given by

$$\frac{\mathrm{d}v^{(R)^*}}{\mathrm{d}t} = -\gamma v^{(R)^*} + \frac{F}{m} = q^{(R)^*}\frac{F}{m}; \quad q^{(R)^*} = \frac{\Omega_-}{\Omega+} \tag{7b}$$

which indeed has the appearance of a dissipationless Newtonian equation under a force that has been scaled down by a factor $q^{(R)^*} < 1$. Finally, the improved equation of motion (7b) does follow conveniently from a Lagrangian

$$L^{(R)^*} = mv^2/2 - V^{(R)^*} \quad \text{where } V^{(R)^*} = q^{(R)^*}V, \tag{7c}$$

in sharp contrast to the customary Rayleigh model. Clearly, if V does not contain t explicitly the improved energy $E_I^{(R)^*} = mv^2/2 + V_I^{(R)^*}$ is approximately conserved, unless one goes far from the barrier.

3.4 *The non-Rayleigh branch*

Next, we turn to the very interesting case of the particle climbing up the potential hill in figure 1, so that the velocity is essentially antiparallel to the applied force. The particle then takes a relatively long time to cover a given distance up the hill. For times large compared to $1/\Omega_-$ employing the asymtotic expansion (A12) we obtain for the velocity

$$v^{(N)^*} = -F/m\Omega_- - \cdots; \quad \Omega_- t \gg 1. \tag{8a}$$

Here the dots ... represent nonleading terms of order $\dot{F}_{\mathrm{p}}/m\Omega_-^2$ and the superscript $(N)^*$ labels the non-Rayleigh branch under consideration. The corresponding acceleration is deduced from

$$\frac{\mathrm{d}v^{(N)^*}}{\mathrm{d}t} = -\gamma v^{(N)^*} + \frac{F}{m} = q^{(N)^*}\frac{F}{m}; \quad q^{(R)^*} = \frac{\Omega_+}{\Omega_-} \tag{8b}$$

which will not depend on t explicitly if V does not, in sharp contrast to the BCK [1c, 2a] model. The corresponding energy $E_l^{(N)^*} = mv^2/2 + V_l^{(N)^*}$ becomes an approximate constant of motion unless we go far from the barrier.

3.5 *Physical interpretation and numerical estimates*

From the conceptual viewpoint we can say that the effect of the $-\gamma v$ term in the exact frictional equation for dv/dt is roughly simulated by altering the force in the dissipationless formulation. The scale factor $q^{(N)^*}$ in eq. (8b) is greater than unity and is an increasing function of γ. This physically implies that as the coefficient of friction increases, the effective potential hill $V^{(N)^*}$ to be surmounted by the particle becomes higher and the deceleration grows. Let us estimate a typical numerical range for the ratio γ/Ω for which the asymptotic expansion (8a) on the non-Rayleigh branch holds. Suppose $\Omega + t \approx 100$, implying that the particle has completely relaxed with respect to the time scale Ω_+^{-1}. Relaxation with respect to the other time scale, viz. Ω_+^{-1}, would also have been achieved during this time provided $\Omega_- t > 1$, i.e.,

$$\Omega_-/\Omega_+ > 1/100, \quad \text{i.e. } 0 \leq \gamma/\Omega < 10. \tag{9}$$

In other words the analysis based on eqs (8a–c) remains valid over a fairly wide range of underdamped as well as overdamped motions, because $\gamma/\Omega = 0$ means no-damping and $\gamma/\Omega = 10$ implies very heavy damping.

3.6 *Comparison with statistical large-friction expansion*

When the input force includes a random component we must examine any possible link between our theory and the 'large γ expansions' in statistical mechanics, especially in the context of the Fokker–Planck [4a, b] equation. It is well known [4a] that the kramers distribution function $P(x, v, t)$ in phase space can be systematically represented by a series in inverse powers of γ (for very large values of γ) as

$$P = P^{(0)} + r^{-1}P^{(1)} + O(r^{-2}). \tag{10}$$

The first two terms of this expansion, after integration over the velocity, lead directly to the Smoluchowski distribution function $W(x, t)$ in configuration space. Reverting to the trajectory language one may say that the asymptotic reduction from Kramers to Smoluchowski distribution is equivalent to the asymptotic reduction from the underlying Langevin [4b] (cf. eqs ((2a), (b)) to the overdamped Rayleigh [4b] (cf. eqs (3b), 7(a)) stochastic differential equation (provided the noise is white Gaussian). In this context, the main results of our theory (cf. eqs (8), (9)) are entirely new because they pertain to the non-Rayleigh branch of motion, the large parameters involved are $\Omega_\pm$, and the domain of validity extends even to the extreme underdamped limit.

All our important results are collected in table 3 which should be compared against the entries of tables 1 and 2. Some additional points which deserve mention are as follows:

(a) *Limited equivalence:* We do not claim perfect equivalence between the actual frictional eq. (2a) and its proposed dissipationless versions viz. eqs (7b, 8b). As a matter of fact, for *time-independent* static potentials the exact x trajectories would eventually come to rest at a potential minimum whereas our $x^{(N)^*}$ trajectories would go on oscillating between static confining walls. However, our approximation (8b) is most effective when the particle is climbing up the hill in figure 1, and hence it can be profitably employed to calculate the first transit time from the bottom to the top of the barrier. Far away from the barrier, i.e., in the region of the confining wells, the one-term approximations (7b, 8b) may become poor. In these regions nontrivial corrections due to dissipation may be systematically made by including the $\dot{F}_{\mathrm{P}}$ terms of the asymptotic expansions (All, 12).

(b) *Time-dependent situations*: Of greater physical interest is the case when the perturbation force F_{p} contains *explicit time-dependence* due to applied modulation, white noise, etc. It is known that at times large compared to Ω^{-1} the frictional energy loss suffered by the actual x trajectories tends to be compensated by the energy gain from the time-dependent perturbation so that the particle tends to follow the profile of F_{p} (see Appendix, eq. (A8)). Obviously, in the absence of net loss our dissipationless formulation based on the $x^{(N)^*}$ trajectories should also become equally valid.

Table 3. Salient features of the dissipationless Newtonian model (cf. eqs (7), (8)). Useful abbreviations are $\bar{\Omega} = (\Omega^2 + \gamma^2/4)^{1/2}$, $\Omega_+ = \bar{\Omega} + \gamma/2$, $\Omega_- = \bar{\Omega} - \gamma/2$, $q^{(R)^*} = \Omega_-/\Omega_+$ and $q^{(N)^*} = \Omega_+/\Omega_-$.

Item	Dissipationless Newtonian model
Motivation	The effect of deleting the $-\gamma v$ term in the exact equation of motion is sought to be partially restored by suitably scaling the external force
Parameters	$(R)^*$ branch: Ω_+large, i.e. $\Omega_+ t \gg 1$ $(N)^*$ branch: Ω_-large, i.e $\Omega_- t \gg 1$. Even the limit of zero friction is included in these inequalities
Estimated velocity	$v^{(R)^*} = F/m\Omega_+$, $v^{(N)^*} = -F/m\Omega_-$
Effective acceleration	$\mathrm{d}v^{(R)^*}/\mathrm{d}t = q^{(R)^*}F$, $\mathrm{d}v^{(N)^*}/\mathrm{d}t = q^{(N)^*}F$
Branch of motion	On the improved Rayleigh branch v and f are essentially parallel as happens while sliding down the barrier. On the non-Rayleigh branch reverse is the case
Lagrangian	$(L)^{(R)^*} = mv^2/2 - q^{(R)^*}V$, $(L)^{(N)^*} = mv^2/2 - q^{(N)^*}V$
Mechanical energy	$(E)_I^{(R)^*} = mv^2/2 + q^{(R)^*}V_I$, $(E)_I^{(N)^*} = mv^2/2 + q^{(N)^*}V_I$ which are approximately conserved in regions not too far from the barrier (i.e., not inside the confining wells)

The superscript $(R)^*$ labels the improved Rayleigh branch and $(N)^*$ labels the non-Rayleigh quantum wave packet near the barrier, our dissipationless Lagrangian $L^{(N)^*}$ (see eq. (8c)) may have bright applicational prospects. Indeed, if the input V represents time-independent mean field, the path integral corresponding to the scaled-potential $V^{(N)^*}$ can be readily computed via the short-time propagator method [5b] of Sethia *et al.* Next, if V includes time-dependent random components, the ensuing dynamics based on $V^{(N)^*}$ can be treated using the recently developed concept [6] of quantum dissipationless random motion. Finally, a detailed application of these ideas to study the quantum stochastic resonance phenomenon [7] in a double well potential under the simultaneous influence of thermal temperature, linear friction, external noise and sinusoidal modulation is in progress and the results will be reported elsewhere.

Appendix:

Solution of eq. (6)

(i) *Green's function.* Given the initial condition x_0 and v_0 we wish to solve eq. (6) written in the form

$$\left[\left(\frac{\mathrm{d}}{\mathrm{d}t}+\Omega_+\right)\left(\frac{\mathrm{d}}{\mathrm{d}t}-\Omega_-\right)\right]x=\frac{F_\mathrm{p}}{m}, \tag{A1}$$

where $\bar{\Omega}$, Ω_+ and Ω_- are given by eqs (5). The differential operator within square brackets has the causal Green's function

$$G(t,t')=\frac{-\theta(t-t')}{2\bar{\Omega}}\left[\mathrm{e}^{-\Omega_+(t-t')}-\mathrm{e}^{\Omega_-(t-t')}\right], \tag{A2}$$

where $\theta(t-t')$ is the unit step function.

(ii) *Formal solution.* If the perturbative force F_p were absent, the trajectory x_B in presence of the barrier alone would have been

$$x_B=\frac{1}{2\bar{\Omega}}\left[\mathrm{e}^{-\Omega_+t}(\Omega_-x_0-v_0)+\mathrm{e}^{\Omega_-t}(\Omega_+x_0+v_0)\right]. \tag{A3}$$

When F_p is also present the use of eqs (A2, 3) permits us to convert eq. (A1) into the integral equation

$$\begin{aligned} x&=x_B+\int_0^\infty \mathrm{d}t'G(t,t')F'_\mathrm{p}/m \\ &=x_B-\frac{1}{2m\bar{\Omega}}\left\{\mathrm{e}^{-\Omega_+t}\int_0^t \mathrm{d}t'\mathrm{e}^{\Omega_+t'}F'_\mathrm{p}-\mathrm{e}^{\Omega_-t}\left[\int_0^\infty+\int_t^\infty\right]\mathrm{d}t'\mathrm{e}^{-\Omega_-t'}F'_\mathrm{p}\right\}, \end{aligned} \tag{A4}$$

where $F'_\mathrm{p}=F_\mathrm{p}(x(t'),\ t')$ is the perturbative force at the integration time t' when the position becomes $x(t')$.

$$\lambda_{\mathrm{p}} = \mathrm{e}^{\Omega_- t} \cdot \int_t \mathrm{d}t' \mathrm{e}^{-\Omega_- t'} F'_{\mathrm{p}}. \tag{A5}$$

Then the formal solution (A4) may be recast into the compact form

$$x = \frac{1}{2\bar{\Omega}} \left\{ \left[K\mathrm{e}^{-\Omega_+ t} - \frac{\xi_{\mathrm{p}}}{m} \right] + \left[N\mathrm{e}^{\Omega_- t} - \frac{\lambda_{\mathrm{p}}}{m} \right] \right\} \tag{A6}$$

(iii) *Asymptotic condition.* We shall suppose that the static part of the applied force is confining at large distances as happens, for instance, in the case of a double-well potential. Then, as $t \to \infty$ the position x can not blow up exponentially, implying that the coefficient of $\mathrm{e}^{\Omega_- t}$ in eq. (A6) should vanish, i.e.,

$$N = 0; \quad v_0 = \Omega_+ x_0 + v_0 - \rho_{\mathrm{p}}/m. \tag{A7}$$

(iv) *Final expressions.* Inserting the conditions (A7) into eq. (A6) we get the following exact, general expression for the position:

$$x = x_0 \mathrm{e}^{-\Omega_+ t} - [\xi_{\mathrm{p}} - \rho_{\mathrm{p}} \mathrm{e}^{-\Omega_+ t} + \lambda_{\mathrm{p}}]/2m\bar{\Omega}. \tag{A8}$$

Differentiation with respect to t yields two mutually equivalent representations for the velocity, viz.,

$$v = \Omega_- x - 2\bar{\Omega} x_0 \mathrm{e}^{-\Omega_+ t} + [\xi_{\mathrm{p}} - \rho_{\mathrm{p}} \mathrm{e}^{-\Omega_+ t}]/m \tag{A9a}$$

$$= -\Omega_+ x - \lambda_{\mathrm{p}}/m. \tag{A9b}$$

It is not difficult to verify explicitly that this v satisfies the standard frictional equation (2a) of the text along with the specified initial conditions (2b).

(v) *Existence.* At this stage some comments on the mathematical validity of the above analysis are in order. Although the adjective 'perturbative' was used to describe F'_{p}, our eqs (A8), (9) are exact because no assumption apart from confinement has been made as regards the shape and strength of F_{P}. Also, the functions ξ_{p}, ρ_{p} and λ_{p} in eq. (A5) exist throughout the interval $0 \leq t \leq \infty$ provided the integrand $\mathrm{e}^{-\Omega_- t'} F'_{\mathrm{p}}$ remains bounded at all finite t' and drops faster than $1/t'$ as $t' \to \infty$. Finally, although the top of the barrier in figure 1 corresponds to a point of unstable equilibrium, our solutions (A8, 9) are quite stable with respect to choice of the initial location x_0 because of the important identity (A7) satisfied by v_0.

(vi) *Lowest order estimates.* We shall now evaluate the integrals appearing in eq. (A5) approximately without employing any specific model for F_{p}, but making a few reasonable assumptions. Suppose that $F_{\mathrm{p}}(x, t)$ is a slowly varying function of space and time so that its derivatives may be neglected – a situation which is somewhat reminiscent of the potential smoothness assumption in the quantum WKB method. Also, suppose that the particle has relaxed with respect to the time-scale Ω_-^{-1} implying that $\Omega_\pm t \gg 1$. Then, partial integration in eq. (A5) yields

$$\xi_{\mathrm{p}} \approx \dot{F}_{\mathrm{p}}/\Omega_+; \quad \lambda_{\mathrm{p}} \approx F_{\mathrm{p}} + \dot{F}_{\mathrm{p}}/\Omega_-, \tag{A10}$$

where terms of order $\dot{F}_{\mathrm{p}}/\Omega_\pm^2$ have been dropped. With the help of these estimates we can describe motion on two different types of branches as explained below.

(vii) *The improved Rayleigh branch.* If the particle starts sliding down the barrier in figure 1 its speed may be relatively substantial. Relaxation with respect to the time scale Ω_+^{-1} happens soon so that one can take $\Omega_+ t \gg 1$. Neglecting the $\mathrm{e}^{-\Omega_+ t}$ terms in the first representation (cf. eq. (A9a)) for the velocity and using the estimate (A10) one obtains

$$v^{(R)^*} \approx \Omega_- x + \frac{\xi_{\mathrm{p}}}{m} \approx \frac{F}{m\omega_+} - \frac{\dot{F}_{\mathrm{p}}}{m\Omega_+^2}, \tag{A11}$$

where the superscript $(R)^*$ labels the 'improved' Rayleigh branch and $F = m\Omega^2 x + F_{\mathrm{p}}$ is the full external force. Note that the customary Rayleigh velocity is just $F/m\gamma$ instead (cf. eq. (3b)). Other dynamical functions of interest, viz., the effective acceleration, Lagrangian and conserved energy associated with $v^{(R)^*}$ are reported explicitly in table 3.

(viii) *The non-Rayleigh branch.* If the particle starts climbing up the hill in figure 1 its speed may get reduced substantially. Since the particle will take a relatively long time to cover a given distance, relaxation with respect to the time scale Ω_-^{-1} may occur so that we can take $\Omega_t \gg 1$. From the second representation (cf. eq. (A9b)) of the velocity we obtain the asymptotic expansion

$$v^{(N)^*} = -\Omega_+ x - \frac{\lambda_{\mathrm{p}}}{m} \approx \frac{-F}{m\Omega_-} - \frac{\dot{F}_{\mathrm{p}}}{m\Omega_-^2}, \tag{A12}$$

where use has been made of the estimate (A10), and the superscript $(N)^*$ labels the non-Rayleigh branch. Note that $v^{(N)^*}$ is outside the scope of the conventional Rayleigh velocity. The relevant acceleration, Lagrangian and conserved energy are again displayed explicitly in table 3.

Acknowledgement

The author (VJM) thanks the UGC for financial support.

References

[1] Classical single-particle frictional motion is treated in, e.g.
(a) R R Long, *Engineering Science and Mechanics* (Prentice Hall, New Jersey, 1963) p. 251
(b) H Goldstein, *Classical Mechanics* (Addison Wesley/Narosa, New Delhi, 1985) p. 24

(b) H Dekker, *Phys. Rep.* **80**, 1 (1981)
R W Hasse, *Rep. Prog. Phys.* **41**, 1027 (1978)
S N Mukherjee and L N Pandey, *Phys. Rev.* **C28**, 1104 (1983)

[3] The role of frictional trajectories in Brownian movement and stochastic resonance has been discussed e.g. by
(a) S Chandrasekhar, *Rev. Mod. Phys.* **15**, 1 (1943)
F Reif, *Fundamentals of statistical and Thermal Physics* (McGraw Hill, Singapore, (1985) p. 560
(b) B McNamara, K Wiesenfeld and R Roy, *Phys. Rev.* **A39**, 4854 (1989)
L Gammaitoni, E Menichella-Saetta, S Santucci, F Marchesoni and C Presilla, *Phys. Rev.* **A40**, 2114 (1989)
P Jung, G Gray and R Roy, *Phys. Rev. Lett.* **65**, 1873 (1990)
S Fauve and F Heslot, *Phys. Lett.* **A97**, 5 (1983)
B McNamara, K Wiesenfeld and R Roy, *Phys. Rev. Lett.* **60**, 2626 (1988)
L Gammaitoni, F Marchesoni, E Menichella-Saetta and S Santucci, *Phys. Rev. Lett.* **62**, 349 (1989)

[4] For the properties of statistical mechanical distribution functions with friction see, e.g.,
(a) N G Van Kampen, *Stochastic processes in physics and chemistry* (North Holland, Amsterdam, 1990) p. 233
(b) H Risken, *The Fokker-Planck equation* (Springer Verlag, Berlin, 1984) pp. 7, 257

[5] Computation of path integrals via numerical matrix multiplication and short-time propagator has been described e.g. by
(a) D Thirumalai and B J Berne, *J. Chem. Phys.* **81**, 2512 (1984)
(b) A Sethia, S Sanyal and Y Singh, *J. Chem. Phys.* **93**, 7268 (1990)

[6] A formulation of quantum dissipationless random motion has been given by
N Chanana, V J Menon and Y Singh, *Indian. J. Phys.* **B71**, 147 (1997)

[7] V J Menon, N Chanana and Y Singh, *Single-particle treatment of quantum stochastic resonance* (unpublished)

Orthogonal interaction of Bernstein mode with ion-acoustic wave through plasma maser effect

P N DEKA*
Center of Plasma Physics, Saptaswahid Path, Dispur Guwahati 781 006, India
*Permanent Address: Department of Mathematics, Dibrugarh University, Dibrugarh 786 004, India
Email: root@univdib.nic.aren.in.

MS received 20 November 1996; revised 3 March 1998

Abstract. Interaction of Bernstein mode wave with ion-acoustic turbulence is treated as the plasma maser effect. Ion-acoustic turbulence is considered as resonant mode, propagating orthogonal to the test Bernstein mode. The external magnetic field, in the direction of ion-acoustic turbulence, is playing key role in transferring energy in upconversion process from resonant low frequency wave to the high frequency wave through modulated electric field. It is shown that the direct coupling term and the associated reverse absorbtion effect do not contribute individually to the growth or damping to the Bernstein mode. Only the polarization coupling term is found to be effective in the energy upconversion process as the external magnetic field is providing momentum in the direction of propogation of Bernstein mode. The polarization coupling term is identified to be the dominant upconversion factor in the plasma maser effect.

Keywords. Weak turbulence theory; resonant and nonresonant waves; linear response theory; growth rate.

PACS No. 52.20

1. Introduction

Anomalous radiation phenomenon in the presence of enhanced low frequency fluctuation is often observed in laboratory and space plasma. Such radiation phenomena of high frequency wave may be interpreted as an energy upconversion process. The possibility of growth of high frequency wave from low frequency fluctuation was indicated by Roses [1]. The theory of Plasma maser effect as an effective upconversion process, was put forward independently by Nambu [2] and Tsytovich [3]. Plasma maser effect is a mode-mode coupling process in which turbulent energy from low frequency wave is transferred to the high frequency wave. Since most of turbulent energy in astrophysical plasma is contained in low frequency fluctuations, many energy upconversion processes in it can be interpreted through plasma maser effect [4]. Recent numerical simulation [5] shows that the accelerated electrons by the electrostatic lower hybrid wave effectively generates the electromagnetic radiation at the electron gyrofrequency; this suggests that the theory of plasma maser effect can be effective for the interpretation of many radiation phenomena

Plasma maser effect occurs when resonant as well as nonresonant waves are present in the system. The resonant waves are those for which the Cherenkov resonant condition is satisfied: $\vec{v}\cdot\vec{k}-\omega=0$; whereas the nonresonant waves are those for which both the Cherenkov resonance condition and the nonlinear scattering conditions are not satisfied i.e. $\Omega-\vec{K}\cdot\vec{v}\neq 0$ and $(\vec{K}-\vec{k})\cdot\vec{v}-(\Omega-\omega)\neq 0$. Here, ω and Ω are frequencies of the resonant and nonresonant waves respectively, and $\vec{k}$ and $\vec{K}$ are the corresponding wave numbers. According to the recent weak turbulence theory, the standard mode coupling process consists of three parts, (a) the three wave resonance, (b) the nonlinear Landau resonance and (c) the plasma maser effect. Plasma maser effect co-exists with the reverse absorption effect due to slow change in distribution function. It is effective in strongly magnetised plasma where a free source of energy for the particles is available. For unmagnetised plasma, plasma maser effect vanishes [6]; in fact it exactly cancels the reversed absorption effect. In this paper we consider ion-acoustic wave fluctuation be present in the system and consider its interaction with high frequency Bernstein mode when they are propagating in direction orthogonal to each other. Thus we observe growth of nonresonant Bernstein mode through plasma maser effect. In this orthogonal interaction the transfer of wave energy is possible due to the presence of magnetic field.

2. Formulations

We consider a homogeneous plasma imbedded in an external uniform magnetic field $\vec{B}_0$ along z axis. The interaction of high frequency Bernstein mode with ion-acoustic turbulence is studied using the Vlasov Poisson equations

$$\left[\frac{\partial}{\partial t}+\vec{v}\cdot\frac{\partial}{\partial\vec{r}}-\frac{e}{m}\left(\vec{E}+\frac{\vec{v}\times\vec{B}}{c}\right)\cdot\frac{\partial}{\partial\vec{v}}\right]f_e(\vec{r},\vec{v},t)=0 \tag{1}$$

$$\vec{\nabla}\cdot\vec{E}=-4\pi n_e e\int f_e(\vec{r},\vec{v},t)\,\mathrm{d}\vec{v}. \tag{2}$$

We consider the Maxwellian distribution for both the background and beam electrons given by

$$\begin{aligned}f_{0e}(\vec{v}) ={}&(1-\delta)\left(\frac{m}{2\pi T_b}\right)^{3/2}\exp\left[-\frac{m}{2T_b}(v_\perp^2+v_\parallel^2)\right]\\&+\delta\left(\frac{m}{2\pi T}\right)^{3/2}\exp\left[-\left(\frac{m}{2T}\right)[v_\perp^2+(v_\parallel-v_0)^2]\right],\end{aligned} \tag{3}$$

where T_b, T are temperatures of the background and beam plasma, $\delta=n_b/n_0$ $(\delta\ll 1)$ is the ratio of the beam electron density n_b to the background plasma density n_0, v_0 is the beam electron velocity, $(2T/m)^{1/2}$ is the thermal velocity $(v_0\gg(2T/m)^{1/2})$ and the subscripts $\perp$ and $\parallel$ denote components perpendicular and parallel to the external magnetic field.

According to the linear-response theory of a turbulent plasma [7], the unperturbed

$$\left[\frac{\partial}{\partial t}+\vec{v}\cdot\frac{\partial}{\partial\vec{r}}-\left(\frac{e}{m}\right)\frac{\vec{v}\times\vec{B}_0}{c}\cdot\frac{\partial}{\partial\vec{v}}\right]f_{1e}=\left(\frac{e}{m}\right)\vec{E}_l\cdot\frac{\partial}{\partial\vec{v}}f_{0e}. \tag{6}$$

Using Fourier transforms

$$A(\vec{r},\vec{v},t)=\sum_{\vec{k},\omega}A(\vec{k},\omega,\vec{v})\exp\{i(\vec{k}\cdot\vec{r}-\omega t)\}, \tag{7}$$

the Fourier component of $f_{1e}(k,\omega)$ from (6) will be

$$f_{1e}(k,\omega)=\left(\frac{ie}{m}\right)\frac{\partial/\partial v_{\parallel}f_{0e}}{\omega-k_{\parallel}v_{\parallel}+i0^{+}}, \tag{8}$$

where $i0^{+}$ represents small imaginary part of the frequency ω, and $\vec{k}$ is the wave number of ion-acoustic wave fields.

To this quasisteady state, we apply perturbation $\mu\delta\vec{E}_h$ of test high frequency electrostatic Bernstein mode wave ($\mu\ll\epsilon$) such that the total perturbed electromagnetic fields and the distribution function are given as

$$\delta\vec{E}=\mu\delta\vec{E}_h+\mu\epsilon\delta\vec{E}_{lh}+\mu\epsilon^2\Delta\vec{E},$$

$$\delta\vec{B}=0$$

and

$$\delta f=\mu\delta f_h+\mu\epsilon\delta f_{lh}+\mu\epsilon^2\Delta f$$

where $\delta\vec{E}_{lh}$, $\Delta\vec{E}$ are the modulation electric fields and δf_{lh}, Δf are electron distribution function corresponding to modulation fields.

Rewriting the Vlasov equation (1),

$$\left[\frac{\partial}{\partial t}+\vec{v}\cdot\frac{\partial}{\partial\vec{r}}-\frac{e}{m}\left\{(\epsilon\vec{E}_l+\epsilon^2\vec{E}_2)+\frac{\vec{v}\times\vec{B}_0}{c}\right\}\cdot\frac{\partial}{\partial\vec{v}}\right]\delta f(\vec{r},\vec{v},t)$$
$$=\frac{e}{m}\delta E(\vec{r},t)\cdot\frac{\partial}{\partial\vec{v}}\left(f_{0e}+\epsilon f_{1e}+\epsilon^2 f_{2e}\right).$$

We collect the terms of order μ, $\mu\epsilon$ and $\mu\epsilon^2$. These respectively are

$$P\delta f_h=\frac{e}{m}\delta\vec{E}_h\cdot\frac{\partial}{\partial\vec{v}}f_{0e}, \tag{9}$$

$$P\delta f_{lh}=\frac{e}{m}\vec{E}_l\cdot\frac{\partial}{\partial\vec{v}}\delta f_h+\frac{e}{m}\delta\vec{E}_h\cdot\frac{\partial}{\partial\vec{v}}f_{1e}+\frac{e}{m}\delta\vec{E}_{lh}\cdot\frac{\partial}{\partial\vec{v}}f_{0e} \tag{10}$$

$$P\Delta f_h = \frac{e}{m}\,\vec{E}_2 \cdot \frac{\partial}{\partial \vec{v}}\,\delta f_h + \frac{e}{m}\,\vec{E}_l \cdot \frac{\partial}{\partial \vec{v}}\,\delta f_{lh} + \frac{e}{m}\,\delta\vec{E}_h \cdot \frac{\partial}{\partial \vec{v}}\,f_{2e} + \frac{e}{m}\,\delta\vec{E}_{lh} \cdot \frac{\partial}{\partial \vec{v}}\,f_{1e} + \frac{e}{m}\,\Delta\vec{E} \cdot \frac{\partial}{\partial \vec{v}}\,f_{0e}; \tag{11}$$

where

$$P = \frac{\partial}{\partial t} + \vec{v} \cdot \frac{\partial}{\partial \vec{r}} - \frac{e}{mc}\vec{v} \times \vec{B}_0 \cdot \frac{\partial}{\partial \vec{v}}$$

We obtain δf_h, δf_{lh} and Δf by integrating along the unperturbed orbits [8], using cylindrical co-ordinate system to the velocity space, as follows.

From (9) we have

$$\delta f_h(\vec{K}, \Omega) = \frac{ie}{m}\,\delta E_h \sum_a \sum_b \frac{J_b(\alpha)\frac{J_{a+1}(\alpha)+J_{a-1}(\alpha)}{2}\exp\{i(b-a)\theta\}}{\Omega - a\Omega_e}\,\frac{\partial}{\partial v_\perp}\,f_{0e}(v_\perp). \tag{12}$$

where $\alpha = K_\perp v_\perp / \Omega_e$. From (10) we have

$$\delta f_{lh}(\vec{K}-\vec{k}, \Omega-\omega) = \frac{ie}{m} \sum_a \sum_b \frac{J_a(\alpha)J_b(\alpha)\exp\{i(b-a)\theta\}}{\Omega - \omega + k_\| v_\| - a\Omega_e} \left[E_\|(k',\omega')\frac{\partial}{\partial v_\|}\delta f_h(\vec{K},\Omega) + \delta E_{lh}\left\{ \frac{K_\perp}{|\vec{K}-\vec{k}|}\frac{a\Omega_e}{K_\perp v_\perp}\frac{\partial}{\partial v_\perp} - \frac{k_\|}{|\vec{K}-\vec{k}|}\frac{\partial}{\partial v_\|} \right\} f_{0e}(\vec{v}) + \delta E_h \frac{a\Omega_e}{K_\perp v_\perp}\frac{\partial}{\partial v_\perp} f_{1e}(k') \right]. \tag{13}$$

From (11) we obtain

$$\Delta f(\vec{K}, \Omega) = \frac{ie}{m} \sum_{a,b} \frac{J_a(\alpha)J_b(\alpha)\exp\{i(b-a)\theta\}}{\Omega - a\omega_e} \left[E_{l\|}(k'')\frac{\partial}{\partial v_\|}\{f_{lh}(\vec{K}-\vec{k}'')\} + \delta E_{lh}\left\{ \frac{K_\perp}{|\vec{K}-\vec{k}|}\frac{a\Omega_e}{K_\perp v_\perp}\frac{\partial}{\partial v_\perp} - \frac{k_\|}{|\vec{K}-\vec{k}|}\frac{\partial}{\partial v_\|} \right\} f_{1e}(k'') \right]. \tag{14}$$

The Poisson equation gives the modulated field as

$$\vec{\nabla} \cdot \delta\vec{E}_{lh} = -4\pi n_e e \int f_{lh}(\vec{K}-\vec{k})d\vec{v}$$

so that

$$\delta E_{lh}(\vec{K}-\vec{k}) = -\frac{\omega_{pe}^2}{(\vec{K}-\vec{k})M(\vec{K}-\vec{k})} \int \left[\sum_{a,b} \frac{J_a(\alpha)J_b(\alpha)\exp\{i(b-a)\theta\}}{\Omega - \omega + k_\| v_\| - a\Omega_e} \times \left(E_{l\|}\frac{\partial}{\partial}\delta f_h + \frac{a\Omega_e}{\vec{K}}\frac{\partial}{\partial}\,f_{1e}(k') \right) \right] \mathrm{d}\vec{v}; \tag{15}$$

$$M(\vec{K}-\vec{k}) = 1 + \frac{{\omega_{pe}}^2}{|\vec{K}-\vec{k}|^2}\int \sum_{a,b} \frac{J_a(\alpha)J_b(\alpha)\exp\{i(b-a)\theta\}}{\Omega-\omega+k_\|v_\| - a\Omega_e} \times \left[\frac{a\Omega_e}{v_\perp}\frac{\partial}{\partial v_\perp} - k_\| \frac{\partial}{\partial v_\|}\right] f_{0e}(\vec{v})\mathrm{d}\vec{v}. \qquad (1$$

Now we obtain dielectric response function for high frequency Bernstein mode wav from Poisson equation:

$$\vec{\nabla}\cdot\delta\vec{E}_h = -4\pi e n_e \int [\delta f_h + \Delta f]\mathrm{d}\vec{v},$$

where the integration is taken over the entire velocity space, which takes the form

$$\delta E_h \epsilon_h(\vec{K},\Omega) = 0.$$

The dispersion relation $\epsilon_h(\vec{K},\Omega)$ can be written as

$$\epsilon_h(\vec{K},\Omega) = \epsilon_0(\vec{K},\Omega) + \epsilon_d(\vec{K},\Omega) + \epsilon_p(\vec{K},\Omega)$$

where $\epsilon_0(\vec{K},\Omega)$ is the linear part, and is given by

$$\epsilon_0(\vec{K},\Omega) = 1 + \frac{\omega_{pe}}{K_\perp}\int \sum_{a,b} \frac{(J_a+J_b)/2J_b\exp\{i(b-a)\theta\}}{\Omega - a\Omega_e}\frac{\partial}{\partial v_\perp} f_{0e}(\vec{v})\mathrm{d}\vec{v}. \qquad (1$$

$\epsilon_d(\vec{K},\Omega)$ is the direct coupling part given by

$$\begin{aligned}\epsilon_d(\vec{K},\Omega) = &-\frac{{\omega_{pe}}^2}{K_\perp}\left(\frac{e}{m}\right)^2 \sum_k |E_{l\|}|^2 \int \frac{J_aJ_b\exp\{i(b-a)\theta\}}{\Omega - a\Omega_e}\frac{\partial}{\partial v_\|} \\ &\times \left\{ \sum_{s,t} \frac{J_sJ_t\exp\{i(t-s)\theta\}}{\Omega-\omega+k_\|v_\| - a\Omega_e}\frac{\partial}{\partial v_\|} \right. \\ &\times \left(\sum_{p,q} \frac{J_q(J_{p+1}+J_{p-1})/2\exp\{i(q-p)\theta\}}{\Omega - p\Omega_e} f_{0e}(\vec{v}) \right) \\ &+ \sum_{s,t} \frac{J_t(J_{s+1}+J_{s-1})/2\exp\{i(t-s)\theta\}}{\Omega-\omega+k_\|v_\| - a\Omega_e}\frac{\partial}{\partial v_\perp} \\ &\left. \times \left(\frac{\partial/\partial v_\| f_{0e}}{-\omega + k_\|v_\| + i0^+} \right) \right\} \mathrm{d}\vec{v} \qquad (1\end{aligned}$$

and $\epsilon_p(\vec{K},\Omega)$ is the polarization coupling given by

$$\epsilon_p(\vec{K},\Omega) = \frac{\omega_{pe}^4}{\;}\sum \frac{|E_{l\|}(\vec{k},\omega)|^2}{\;}\left(\frac{e}{\;}\right)^2 (A+B)(C+D) \qquad ($$

$$A = \int \frac{\exp\{i(b-a)\theta\}}{\Omega - a\Omega_e} J_b J_a \frac{\partial}{\partial v_\parallel} \left\{ \sum \frac{\exp\{i(t-s)\theta\}}{\Omega - s\Omega_e - \omega + k_\parallel v_\parallel} J_s J_t \right.$$
$$\left. \times \left\{ \frac{s\Omega_e}{K_\perp v_\perp} K_\perp \frac{\partial}{\partial v_\perp} - k_\parallel \frac{\partial}{\partial v_\parallel} \right\} f_{0e}(\vec{v}) \right\} \mathrm{d}\vec{v}$$
$$B = \int \frac{\exp\{i(b-a)\theta\}}{\Omega - a\Omega_e} \left[K_\perp \left(\frac{a\Omega_e}{K_\perp v_\perp} \right) J_a J_b \frac{\partial}{\partial v_\perp} - k_\parallel J_a J_b \frac{\partial}{\partial v_\parallel} \right]$$
$$\times \left(\frac{\partial/\partial v_\parallel f_{0e}(\vec{v})}{\omega - k_\parallel v_\parallel + i0^+} \right) \mathrm{d}\vec{v}$$
$$C = \int \frac{\exp\{i(b-a)\theta\}}{\Omega - \omega + k_\parallel v_\parallel - a\Omega_e} J_a J_b \frac{\partial}{\partial v_\parallel} \left\{ \sum \frac{\exp\{i(b-a)\theta\}}{\Omega - a\Omega_e} J_t \frac{s\Omega_e}{v_\perp} \frac{\partial}{\partial v_\perp} f_{0e}(\vec{v}) \mathrm{d}\vec{v} \right\}$$
$$D = \int \frac{\exp\{i(b-a)\theta\}}{\Omega - \omega + k_\parallel v_\parallel - a\Omega_e} J_b J_b \frac{a\Omega_e}{v_\perp} \frac{\partial}{\partial v_\perp} \left(\frac{\partial/\partial v_\parallel f_{0e}(\vec{v})}{-\omega + k_\parallel v_\parallel + i0^+} \right) \mathrm{d}\vec{v}$$

Intregrating (17) by parts we have,

$$\begin{aligned} \epsilon_0(\vec{K}, \Omega) &= 1 + \frac{\omega_{pe}^2}{K_\perp} \int_0^\infty \sum_{a,b} \frac{J_a^2}{\Omega - a\Omega_e} \left(\frac{a\Omega_e}{k_\perp v_\perp} \right) \frac{\partial}{\partial v_\perp} f_{0e}(v_\perp) 2\pi v_\perp \mathrm{d}v_\perp \\ &\quad \times \int_{-\infty}^\infty f_{0e}(v_\parallel) \mathrm{d}v_\parallel \\ &= 1 - \frac{\omega_{pe}^2}{K_\perp} \sum_{a=1}^\infty \left[\left(\int_0^\infty J_a^2 f_{0e}(v_\perp) 2\pi v_\perp \mathrm{d}v_\perp \right) \frac{2a^2\Omega_e^2}{\Omega^2 - a^2\Omega_e^2} \left(\frac{1}{K_\perp} \right) \frac{m}{T_e} \right] \\ &= 1 - \left(\frac{\omega_{pe}}{K_\perp} \right)^2 \left(\Omega_e^2 \frac{m}{T_e} \right) \frac{2}{\Omega_e^2 - \Omega_e^2} \left[\sum_{a=1}^\infty 2a^2 I_a \left(\frac{K_\perp^2 T_e}{m\Omega_e^2} \right) \exp\left(- \frac{K_\perp^2 T_e}{m\Omega_e^2} \right) \right] \end{aligned} \tag{20}$$

where I_a denotes the modified Bessel function. While integrating (18) by parts we have assumed

$$\epsilon_d(\vec{K}, \Omega) = 0$$

Since A and C are real and $B \propto D^*$ (* denotes complex conjugate) we have

$$\operatorname{Im} \epsilon_p(\vec{K}, \Omega) = \frac{\omega_{pe}^4}{K_\perp^2} \frac{|E_{l\parallel}(\vec{k}, \omega)|^2}{|\vec{K} - \vec{k}|^2 M(\vec{K} - \vec{k})} \left(\frac{e}{m} \right)^2 \operatorname{Im}(A \times D + B \times C). \tag{21}$$

Here Im is used to denote imaginary part.

After partial integration, we obtain

$$A = 0$$

$$\operatorname{Im} B = \int_0^\infty \sum \frac{J_a^2 \Omega_e a / K_\perp v_\perp}{\Omega - a\Omega_e} 2\pi v_\perp \frac{\partial}{\partial v_\perp} f_{0e}(v_\perp) \mathrm{d}v_\perp$$

$$\times \operatorname{Im}\left(\int_{-\infty}^{\infty} \frac{\partial/\partial v_{\|}\, f_{0e}(v_{\|})}{\omega - k_{\|} v_{\|} + i0^{+}} \mathrm{d}v_{\|}\right)$$
$$= \sum_{a=1}\left(\frac{2\Omega_e^2}{\Omega^2 - a^2\Omega_e^2}\right)\frac{2\sqrt{\pi}}{v_e^2|k_{\|}|}\left[\frac{\omega/k_{\|} - v_0}{v_e}\right]\exp\left[-\frac{\left(\omega/k_{\|} - v_0\right)^2}{v_e^2}\right]\Lambda_1$$

where

$$\Lambda_1 = \sum_{a=1}\int_0^{\infty} J_a^2\, 2\pi \frac{\partial}{\partial v_{\perp}} f_{0e}(v_{\perp})\mathrm{d}v_{\perp}$$
$$= -\left(\frac{m}{T_e}\right) I_1\left(\frac{K_{\perp}^2 T_e}{\Omega_e^2 m}\right)\exp\left(\frac{K_{\perp}^2 T_e}{\Omega_e^2 m}\right)$$

in obtaining

$$\operatorname{Im}\int_{\infty}^{\infty} \frac{\partial/\partial v_{\|}\, f_{0e}(v_{\|})}{\omega - k_{\|} v_{\|} + i0^{+}} \mathrm{d}v_{\|}$$

we have used the relation

$$\operatorname{Im}\frac{1}{kv - \omega + i0} = -\pi i \delta(\omega - kv)$$

and

$$\int_{\infty}^{\infty} G(v)\delta(\omega - kv)\mathrm{d}v = \left(\frac{1}{|k|} G\left(\frac{\omega}{k}\right)\right)$$

Next considering the fact that for Bernstein mode, the most dominant contribution to th Bessel's sums comes from the terms $a = s = 1$, we estimate

$$C = \frac{k_{\|}}{K_{\perp}}\frac{4\Omega_e^2(\Omega^2 + \Omega_e^3)}{(\Omega^2 - \Omega_e^2)^2}\Lambda_2$$

where Λ_2 is given by

$$\Lambda_2 = \int_0^{\infty} J_1(\alpha)^4 2\pi \frac{\partial}{\partial v_{\perp}} f_{0e}(v_{\perp})\mathrm{d}v_{\perp}$$
$$= \frac{\Omega_e^4}{16K_{\perp}^4}\int_0^{\infty} \frac{\partial}{\partial v_{\perp}} f_{0e}(v_{\perp}) 2\pi v_{\perp}^4 .$$

The expression for Im ϵ_p (Eq. (19)) now becomes

$$\operatorname{Im}\epsilon_p(\vec{K}, \Omega) = \frac{\omega_{pe}^4}{K_{\perp}^2}\frac{|E_{l\|}(\vec{k}, \omega)|^2}{M(\vec{K} - \vec{k}, \Omega - \omega)|\vec{K} - \vec{k}|^2}\left(\frac{e}{m}\right)^2$$

$$M(K-k,\Omega-\omega)|K-k| \qquad k_{\|}$$

3. Instabilities

We calculate the growth rate using the formula

$$\frac{\gamma_h}{\Omega} = -\left.\frac{[\operatorname{Im}\epsilon_h + \partial^2\epsilon_0/\partial\Omega\partial t]}{\Omega\partial\epsilon_0/\partial\Omega}\right|_{\Omega_r};$$

where Ω_r denotes the real part of Ω. The second part is due to revesre absorption effect, which in our case is

$$\frac{\partial^2\epsilon_0(K,\Omega)}{\partial\Omega\partial t} = \frac{\omega_{pe}^2}{K_\perp}\sum_{a=1}^{\infty}\frac{2\Omega a^2 I_n(K_\perp^2 k_e^2)\exp(-K_\perp^2 k_e^2)}{(\Omega^2 - a^2\Omega_e^2)k_e^2}\int_{-\infty}^{\infty}\frac{\partial f_{0e}(v_\|)}{\partial t}\mathrm{d}v_\|; \tag{23}$$

where

$$\int_{-\infty}^{\infty}\frac{\partial f_{0e}(v_\|)}{\partial t}\mathrm{d}v_\| = \left(\frac{e}{m}\right)^2\int_{-\infty}^{\infty}\frac{\partial}{\partial v_\|}\left\{\sum_{k,\omega}|E_{l\|}(\vec{k},\omega)|^2\pi\delta(\omega - k_\| v_\|)\frac{\partial}{v_\|}f_{0e}(v_\|)\right\}\mathrm{d}v_\|.$$

After partial integration this contribution due to the reverse absorption effect becomes zero.

The growth rate due to polarization coupling term is found to be

$$\frac{\gamma_p}{\Omega} = \frac{\delta\sqrt{\pi}}{4}\sum_{\vec{k},w} W_T(\vec{k},\omega)\left(\frac{\omega_{pe}^2(\Omega^2+\Omega_e^2)}{(\Omega^2-\Omega_e^2)^2}\right)\left(\frac{v_e^4 K_\perp^4}{\Omega^2\Omega_e^2}\right)\left(\frac{v_0 - \omega/k_\|}{v_e}\right)\left(\frac{k_\|}{|k_\||}\right)$$
$$\times\exp\left\{-\frac{(\omega/k_\| - v_0)^2}{v_e^2}\right\}. \tag{24}$$

where

$$W_T(\vec{k}) = \sum_{\vec{k}}\left(\frac{E_{l\|}(\vec{k})}{4\pi N T_e}\right)\left(\frac{k_e}{k_\|}\right)^2,$$

is the ion-acoustic turbulence wave energy. Here N denotes electron number density and T_e denotes electron temperature. This growth rate is $+ve$ for $v_0 > \omega/k_\|$, therefore only the beam plasma is taking part in this process.

4. Discussions

Plasma maser effect which comes from the imaginary part of the nonlinear dispersion relation, $\operatorname{Im}\epsilon_h(\vec{K},\Omega)$, is accompanied by absorption effect $\partial^2\epsilon_0(\vec{K},\Omega,f_{0e}(t))/2\partial\Omega\partial t$

condition i.e., $k_{\|}v_{\|} - \omega = 0$. In the absence of magnetic field or in a closed system where external source of momentum and particle are not available there is exact cancellation between plasma maser effect and the reverse absorption effect i.e., $\mathrm{Im}\epsilon_h(\vec{K},\Omega) + (1/2)\ \partial^2\epsilon_0(\vec{K},\Omega)/\partial\Omega\partial t = 0$. However for a open system with energy and particle supply, the cancellation does not occur and plasma maser interaction is effective.

In the present case the contribution to $\mathrm{Im}\,\epsilon_h$ due to the direct coupling part is found to be identically zero. As the resonant ion-acoustic wave is propagating orthogonally there is no direct transfer of momentum to the Bernstein mode from ion-acoustic turbulence and the direct coupling term will not contribute in the upconversion process. For the same reason the contribution due to reverse absorption effect is again found to be zero in this particular problem. However, in the presence of the external magnetic field, the system is equivalent to externally driven rotation and we have non-zero contribution from polarization coupling part to the imaginary part of nonlinear dispersion relation $\mathrm{Im}\,\epsilon_h$.

In the expresion for growth rate (eq. 24), we have only surviving +ve contribution due to the polarization coupling term for $v_0 > \omega/k_{\|}$. Here, the ambient magnetic field carries momentum in the perpendicular to its direction, i.e., towards the propagation of non-resonant Bernstein mode in the system. From (eq. 22), for the external magnetic field $\vec{B} \rightarrow 0$ which gives $\Omega_e \rightarrow 0$ we have $\mathrm{Im}\,\epsilon_p \rightarrow 0$ and the plasma maser effect becomes ineffective. This clarifies the role of external magnetic field in this energy upconversion process.

In earlier studies [9] on plasma maser effect where interaction of two electrostatic waves is considered, both the direct coupling part and the polarization coupling part of the nonlinear dispersion relation contributed to the growth rate. In that, the interacting waves viz. the resonant ion-acoustic turbulence wave and the nonresonant Langmuir wave had common component of their propagation vector in the z-axis so that there is direct exchange of momentum among these waves.

The electron cyclotron maser mechanism [10, 11] is driven by a loss cone type of anisotropy. The cyclotron maser mechanism would work if the relativistic electron satisfy $\Omega K_{\|}v_{\|} - \Omega_e/\gamma = 0$ where $K_{\|}$ is parallel component of high frequency electromagnetic radiation and $\gamma = (1 - v^2/c^2)^{-1/2}$. The relativistic correction term provides a mechanism which couples the perpendicular motion $v_{\perp}^2$ with waves and allows the free energy perpendicular to the magnetic field to be transferred to electromagnetic radiation. Again the standard cyclotron maser mechanism predicts that the radiation mechanism is effective only at frequencies just above the cutoff frequency of high frequency electromagnetic wave which is very close to electron cyclotron frequency Ω_e. However the nonrelativistic theory of cyclotron maser theory proposed by Sagdeev and Sharfranov [12] states that cylotron maser instability can develop in nonrelativistic magnetised plasma with anisotropic distribution function. The cyclotron maser instability cannot developie [13] in tenuous plasma $N \approx 1$, (N is refractive index) for the longitudinal propagation. Further it has been established with the relativistic consideration [14] that cyclotron maser instability can developie at $N > 1$ if only the distribution function is anisotropic. The instability disappears when $N \rightarrow 1$, and the negative aborption is exponentially small at $N^2 - 1 \ll 1$.

On the other hand in plasma maser effect, the free energy to be transferred to the high nonrelativistic electrons. It does not require any frequency matching condition among the interacting waves; so for the case of electromagnetic radition [15] in the presence of low frequency turbulence field the plasma maser is effective well above the local electron gyrofrequency. On the other hand the standard cyclotron maser mechanism [10, 11] predicts that the generation is effective only at frequencies just above the cutoff frequency of electromagnetic radiation which is very close to Ω_e. In plasma maser effect the accompanying reverse absorption effect competes with the direct coupling part of the dispersion relation. The dominant part in plasma maser effect comes from polarization coupling part. The plasma maser instability becomes ineffective as the strength of the external magnetic field decreases.

References

[1] D W Ross, *Phys. Fluids* **12**, 613 (1969)

[2] M Nambu, *Laser and particle beams* **1**, 427 (1983)

[3] V N Tsytovich, *Sov. Phys.–JETP* **62**, 483 (1985)

[4] M Nambu, *Space Sci. Rev.* **44**, 357 (1986)

[5] K G McClements, R Bingham, J J Su, J M Dawson and D S Spicer, *Astrophys. J.* **409**, 465 (1993)

[6] M Nambu, T Hada, S N Sarma and S Bujarbarua, *J. Phys. Soc. Jap.* **60**, 3004 (1991)

[7] M Nambu, *Phys. Fluids* **19**, 412 (1976)

[8] N A Krall and A W Trivelpiece, *Principles of Plasma Physics* (McGraw-Hill, New York, 1973)

[9] M Nambu, S Bujarbarua and S N Sarma, *Phys. Rev.* **A35**, 2 (1987)

[10] R Q Twiss, *Aust. J. Phys.* **11**, 564 (1958)

[11] L C Lee, J R Kan and C S Wu, *Planet. Space Sci.* **28**, 703 (1980)

[12] R Z Sagdeev and V D Shafranov, *JEPT* **39**, 189 (1960)

[13] V G Bezchastnov and G G Pavlov, *Astrophys. Space Sci.* **148**, 257 (1988)

[14] V G Bezehastnov and G G Pavlov, *Proceeding of the Joint Varenna-Abastumani-ESA-Nagoya-Potsdam Workshop on 'Plasma Astrophysics'*, **ESA SP 311**, 153 (1990)

[15] S N Sarma and M Nambu, *Phys. Rev. Lett.* **74**, 94 (1995)

Pramana journal of physics Vol. 50 (No. 4), April 1998

Contents

Correlation between zeroes and poles of S matrix for complex potentials . . . . *I Jamir, E F P Lyngdoh and C S Shastry* 271

Universal inaccessibility principle . . . . *Anil A Bhalekar* 281

On the construction of an extended thermodynamic framework for ireversible processes . . . . *Anil A Bhalekar and Leopoldo S García-Colín* 295

Schwarzschild black hole with global monopole charge. . . . . *Naresh Dadhich, K Narayan and U A Yajnik* 307

Approximate fixed-ρ solution of 'sea-quark' evolution equation at small-x and HERA . . . . *A Saikia* 315

Weak radiative decay $\Lambda_b \rightarrow \Lambda\gamma$ in the heavy quark effective theory . . . . *A K Giri and R Mohanta* 323

Frictional trajectories near a barrier: A dissipationless Newtonian approach. . . . . *V J Menon, N Chanana and Y Singh* 333

Orthogonal interaction of Bernstein mode with ion-acoustic wave through plasma maser effect . . . . *P N Deka* 345

Indexed in CURRENT CONTENTS

ISSN 0304–428

PRAMANA

journal o
physic

Vol. 50 No.
April 19

INDIAN ACADEMY OF SCIENCES
Indian National Science Academy
Indian Physics Association